Small multi-target compounds for the treatment of neurodegenerative pathologies like Alzheimer's disease and glioblastoma

Dissertation

zur Erlangung des Grades
des Doktors der Naturwissenschaften
der Naturwissenschaftlich-Technischen Fakultät
der Universität des Saarlandes
von

Dipl.-Pharm. Marica Mariano

Saarbrücken
2016

Tag des Kolloquiums: 19.05.2017

Dekan:	Univ.-Prof. Dr. rer. Nat. Guido Kickelbick
Vorsitz:	Prof. Dr. Gerhard Wenz
Berichterstatter:	Prof. Dr. Rolf W. Hartmann
	Prof. Dr. Claus Jacob
Akad. Mitarbeiter:	Dr. Matthias Engel

Die vorliegende Arbeit wurde von August 2011 bis Juli 2014 unter Anleitung von Herrn Univ.-Prof. Dr. Rolf W. Hartmann in der Fachrichtung 8.2 Pharmazeutische und Medizinische Chemie der Naturwissenschaftlich-Technischen Fakultät III der Universität des Saarlandes angefertigt.

A mio nonno Carlo

“L'Alzheimer non fa sconti, ti mette a nudo l'anima,
e spogliandoti di tutto sveste anche il cuore”
(Lorenzo Licalzi)

SUMMARY

Neurodegenerative pathologies like Alzheimer's disease (AD), Down syndrome (DS) and glioblastoma are the main targets of the presented work. This project brought to the creation of a small library of selective inhibitors which interfere with the principal pathways involved in the development and progression of the above-mentioned pathologies. In particular, some of the primary goals achieved are: the development of selective compounds towards the kinase Dyrk1A, the discovery of dual-inhibitor compounds for the potential treatment of AD, and the development of multi-target molecules towards glioblastoma. Because of the complexity of the treated diseases, the multi-target approach was fundamental in order to avoid drug resistance, attack the pathologies by interfering with different pathways, and increase the chances to stop their progression. During this research project, we were able to test our compounds activities using a newly developed cellular kinase inhibitory assay acquiring further information on the behavior of our active compounds in a cellular environment.

ZUSAMMENFASSUNG

Die vorliegende Arbeit beschäftigt sich insbesondere mit neurodegenerativen Erkrankungen wie Alzheimer, Down-Syndrom und Glioblastom. Hierbei wurde eine kleine Bibliothek von selektiven Inhibitoren entwickelt, die in die Entstehung und das Fortschreiten der besagten Erkrankungen eingreifen. Insbesondere wurden folgende Hauptziele erreicht: die Entwicklung selektiver Inhibitoren der DyrK1A-Kinase, die Entdeckung dualer Inhibitoren zur möglichen Behandlung von Alzheimer und die Entwicklung von Wirkstoffen mit multiplen Angriffspunkten gegen das Glioblastom. Aufgrund der Komplexität der zu behandelnden Krankheiten war ein Multi-Target-Ansatz fundamental wichtig: um Arzneimittelresistenzen zu vermeiden, die Erkrankungen durch Angriff an verschiedenen Stellen der Signalwege zu bekämpfen, und die Chancen zu erhöhen, das Fortschreiten der Erkrankungen zu stoppen. Während des Forschungsprojektes konnten wir die Aktivität unserer Verbindungen in einem neu entwickelten zellbasierten Kinase-Hemmassay testen, wobei weitere Informationen über das Verhalten unserer Wirkstoffe in zellulärer Umgebung erhalten wurden.

PAPERS INCLUDED IN THIS THESIS

This thesis is divided into two publications, which are referred to in the text by their letter.

A **First selective dual inhibitors of tau phosphorylation and beta-amyloid aggregation, two major pathogenic mechanisms in Alzheimer's disease**

Marica Mariano, Christian Schmitt, Parisa Miralinaghi, Marco Catto, Rolf W. Hartmann, Angelo Carotti, Matthias Engel

ACS Chem. Neurosci. 2014, 5, 1198−1202; dx.doi.org/10.1021/cn5001815

B **Systematic diversification of benzylidene heterocycles yields novel inhibitor scaffolds selective for Dyrk1A, Clk1 and CK2**

Marica Mariano, Rolf W. Hartmann, Matthias Engel

European Journal of Medicinal Chemistry 2016 vol: 112 pp: 209-216; http://dx.doi.org/10.1016/j.ejmech.2016.02.017

Other publications as co-author:

1. **Design and Synthesis of a Library of Lead-Like 2,4-Bisheterocyclic Substituted Thiophenes as Selective Dyrk/Clk Inhibitors**

   Schmitt C, Kail D, Mariano M, Empting M, Weber N, Paul, T., Hartmann R. W., Engel, M.

   PLoS One 2014, 9 (3), e87851.

2. **Hydroxybenzothiophene ketones are efficient pre-mRNA splicing modulators due to dual inhibition of Dyrk1A and Clk1/4**

   Schmitt, Christian; Miralinaghi, Parisa Sadat; Mariano, Marica; Hartmann, Rolf; Engel, Matthias

   (2014) ACS Medicinal Chemistry Letters

CONTRIBUTION REPORT

The author would like to declare her contributions to the papers A-B included in this thesis.

A The author developed and performed the cellular tau phosphorylation experiment and repeated kinase inhibition assays. She contributed to composition of manuscript.

B The author synthesized the compounds and tested them both in the cell-free kinase assay and in HEK293-tau-Dyrk1A cell assay. She contributed to the metabolic stability tests in rat plasma. She contributed to composition of manuscript.

Table of contents

1. Introduction

1.1. The CMGC group

This thesis focuses on kinases of the GMGC subfamily of the human kinome. The CMGC group takes its name from the initials of some of its members: cyclin-dependent kinases (CDKs), mitogen-activated protein kinases (MAP kinases), glycogen synthase kinases (GSK) and CDK-like kinases.

They represent an important and large group of kinases distributed in all eukaryotic cells (Figure 1). They are involved in several different processes such as cell progression and proliferation. They are, therefore, essential for cell survival and they represent an ideal target for the treatment of different types of pathologies including cancer and neurodegenerative disorders.

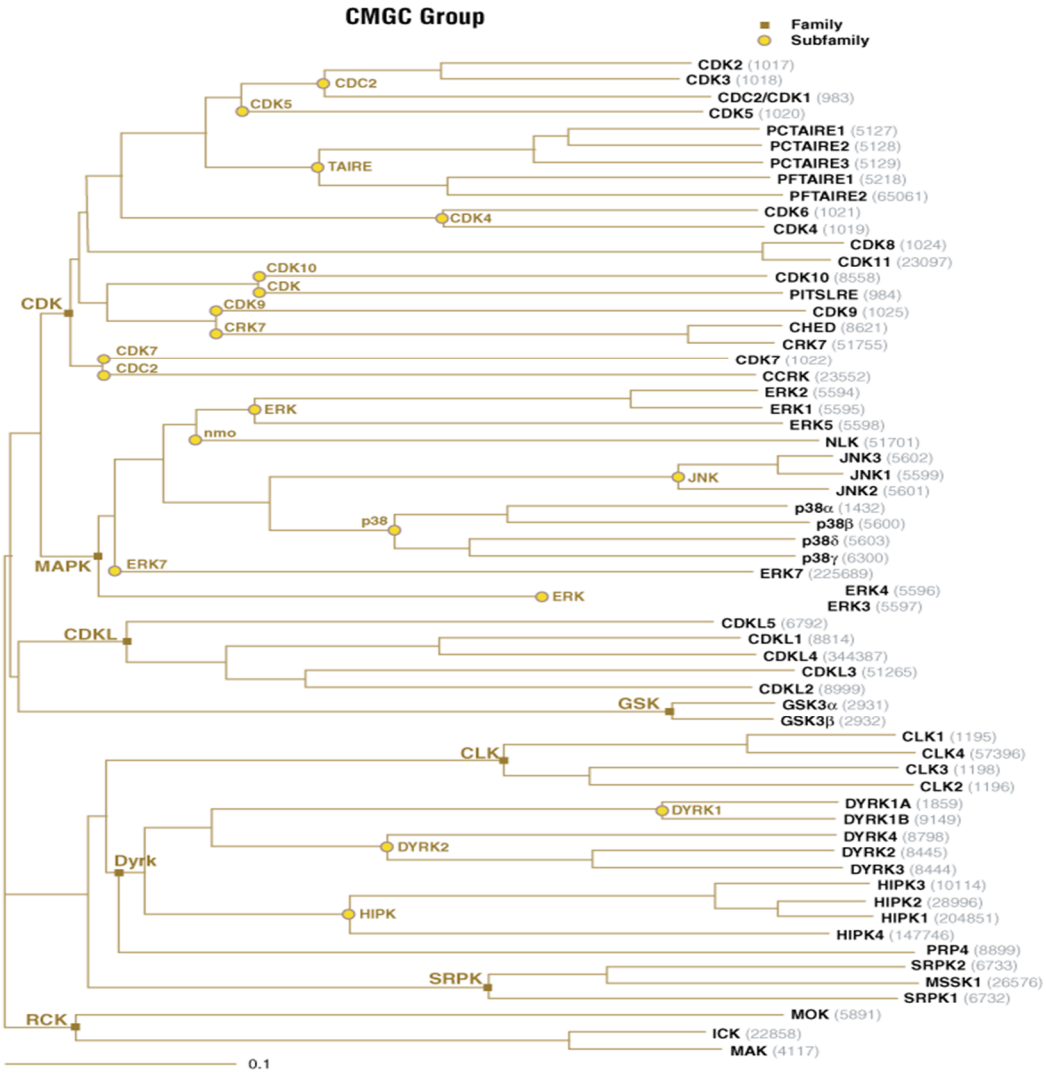

Figure 1. CMGC families and subfamilies. Picture from www.cellsignal.com

1.1.1. DYRK family

Dual tYrosine phospo-Regulated Kinases (DYRKs) belong to the CMGC group and they are divided into 5 sub-types: DYRK1A, DYRK1B, DYRK2, DYRK3 and DYRK4.

DYRK 1A and 1B belong to Class I, while DYRK 2, 3 and 4 to Class II. These 2 classes can be distinguished by the presence of some specific motifs (Figure 2).

- Class I DYRK proteins are formed by a nuclear localization signal (NLS) area and a DYRK homology box (DH) in the N-terminal region and by a motif rich in proline and glutamic acid (PEST motif), serine and threonine in the C-terminal region.
- Class II DYRKs are characterized by N-terminal autophosphorylation accessory regions (N1 and N2) and a DYRK homology box (DH) in the N-terminal part, while there is no known protein domain in the C-terminal side of the protein.

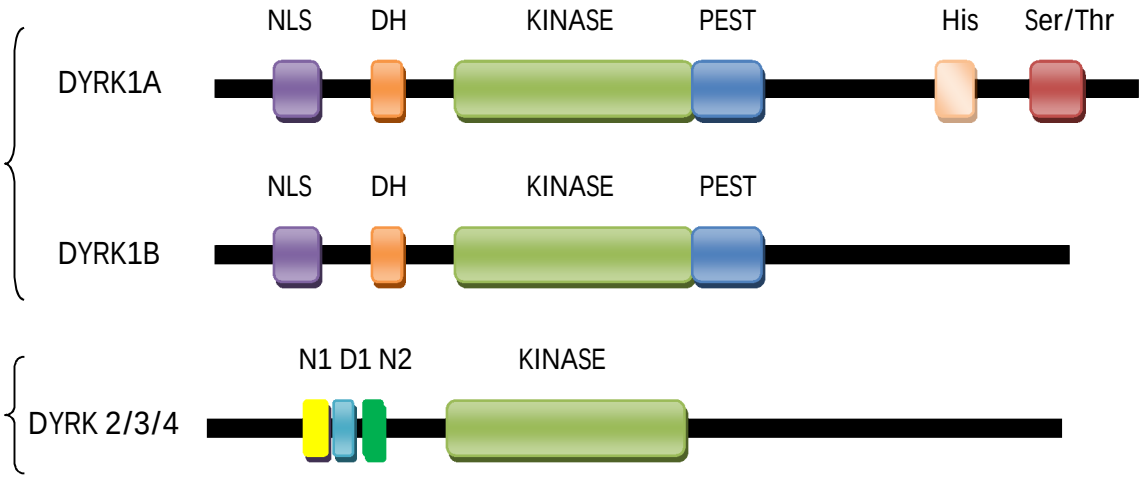

Figure 2. Schematic representation of the DYRKs structure.

1.1.1.1. DYRK1A

The Dyrk1A isoform is ubiquitously expressed and its localization inside the cell is nuclear and/or cytoplasmic. Its gene was found to be present in the Drosophila Melanogaster[1] genome and it produces 3 alternative transcripts, expressed at different stages of the embryonal development and at the adult stage. In the human genome, alternative splicing in the N-terminal domain generates 2 protein isoforms that are different by the presence or absence of a 9 amino acids portion.

As a member of the DYRK family, this isoform has the property of self-activating via autophosphorylation on the tyrosine residues and it subsequently phosphorylates serine/threonine moieties situated on its target proteins.

DYRK1A presents a highly conserved structure and it is formed by 763 amino acids with a molecular mass of 85.6 KDa. It has a high homology among the rat, mouse and human sequences with an identity of 99%. DYRK1A has a typical kinase structure, formed by three regions: the N-terminal, the C-terminal and the central domain.

The DYRK1A gene is located on chromosome 21, in the so called Down Syndrome Critical Region (DSCR) and it plays an important role in several cellular mechanisms joining different signal pathways. Because of its multiple functions exerted by its target proteins, DYRK1A is associated, directly or indirectly, to a high number of physiological and pathological functions such as:

- Phosphorylation of transcription factors like NFAT, CREB, FKHR playing an important role in the regulation of these gene transcription;
- Regulation of cellular proliferation, differentiation and growth by phophorylating proteins which control the cell cycle, apoptosis activation mechanisms and cellular survival like caspase 9 and p53;
- Control of endocytosis, synaptic vescicles fusion and neurotransmitters release in the synaptic space by phosphorylating the synaptic proteins involved in the regulation of synaptical plasticity;
- Determination of brain volume and cellular density, formation of neurons and glial cells and placement of neuritis;
- Phosphorylation of some of the proteins involved in alternative splicing mechanisms such as ASF and Cyclin 2.

Due to its multiple functions, DYRK1A is considered a suitable target for the treatment of some disorders connected with the pathways described above, including Alzheimer's disease and many types of tumor.

1.1.1.2. DYRK1B

Dyrk1B is the closest related kinase to Dyrk1A as it shares 85% homology and it differs from one amino acid in the ATP binding site (a methionine in Dyrk1A , a leucine in Dyrk1B). It is mainly expressed in testes and muscle tissue and it plays an important role in tumors as an anti-apoptotic agent in different types of cancer, including pancreatic cancer[2]. Dyrk1B blocks the cellular cycle in

the quiescent state G0[3], via phosphorylation of the cellular cycle regulator cyclin D1[4–6]. While in healthy cells the quiescent state G0 protects them from metabolic stress, in tumor cells it helps them to survive to chemiotherapic treatments or radiations. Furthermore, Dyrk1B increases the expression of some antioxidant genes, scavenging reactive oxygen species (ROS) and promoting cell survival[7].

1.1.1.3. DYRK2

Dyrk2 belongs to Class II Dyrks, it is mainly present in the nucleus and it plays different roles in the survival of cells. It is demonstrated that Dyrk2 phosphorylates the tumor suppressor p53 on Ser46 in response to DNA damage[8], therefore it is considered important as apoptosis enhancer and tumor growth suppressor. A later study has found that Dyrk2 is involved in the regulation of cell cycle progression in tumor cells. In normal cells, during the late G1 phase, Dyrk2 phosporylates c-Jun and c-Myc, which are then ready to be phosphorylated by GSK3β. In this way, these proteins are recognized and then degradated by ubiquitin. In tumor cells Dyrk2 is down-regulated, thus avoiding the previous mentioned pathway and ultimately c-Jun and c-Myc degradation, shortening the G1 phase and increasing cell proliferation[9].

1.1.1.4. DYRK 3 and 4

The role of DYRK3 and DYRK4 is still not very clear. Some researchers have found an overexpression of mDYRK3 in testes and erythroid cells, therefore it is supposed to play an important role in erythropoiesis as a regulator of red cells development[10] by phosphorylating some histones in the nucleus, thus controlling cell cycle progression.

Apart from some studies about alternative splicing which generates different DYRK4 isoforms[11], there is not so much known about this kinase.

1.1.2. Clk family

1.1.2.1. Clk1

Clk1 phosphorylates Serine-Arginine Rich proteins (SR proteins), which are involved in RNA splicing[12]. When phosphorylated, SR proteins translocate out of the nuclear speckle and become associate with RNA polymerase II for co-transcription splicing[13]. Alternative splicing is essential in the regulation of inclusion or exclusion of exons leading to different protein isoforms, thus it is

involved in the development of several diseases, like neurodegenerative diseases and cancer[14–16]. Therefore, different Clk1 inhibitors has been developed with the idea of blocking the aberrant splicing event, typically found in these diseases.

1.1.3. Ck family

1.1.3.1. Ck2

Casein kinase II (CK2) is a highly conserved serine/threonine kinase which has a tetrameric structure formed by two alpha subunits and two beta subunits. It is ubiquitously expressed in eukaryotic cells and it has an important role in many cellular functions such as cell cycle control, DNA repair and cell cycle progression. It is upregulated in several human cancers like in mammary gland tumor cells[17] and it has been found to be essential in the cell survival. Its mechanism of action remains still unclear because it phosphorylates a high amount of critical substrates in the cell. Therefore it is a promising target for the treatment of several pathologies, such as neurodegenerative diseases, virus infections and glioblastoma[18–20].

1.2. PI3k family

Phosphatidylinositol-3-phosphates (PI3K) belong to another important family of kinases: the lipid kinase family of enzymes which phosphorylate the hydroxyl moiety on position 3 of the inositol ring present in the phosphatidylinositol molecule. They are involved in many cellular mechanisms including cell proliferation and differentiation, therefore they play an important role in cancer progression. In particular, the PI3K/AKT pathway is an essential step in the development of glioblastoma, one of the most malignant brain tumor, as we will discuss further.

PI3Ks are divided into 3 classes depending on their structure and substrate characteristics (reviewed in [21]). In mammals class I kinases are further divided into class IA and class IB kinases[22].

Class IA enzymes are heterodimers formed by a p110 catalytic subunit and a p85 regulatory subunit. In mammals there are three p110 isoforms: p110α, p110β and p110δ. The first two isoforms are ubiquitously expressed, while the latter one is mainly expressed in leukocites[22,23]. The regulatory subunit recruits the p110 catalytic subunit to tyrosine phosphorylated proteins at the plasma membrane, where the p110 phosphorylates its lipid substrates. Furthermore, the

interaction between p85 and p110 down-regulates p110 activity. However this inhibition is removed when p85 binds to the tyrosine phosphorylated peptides. The activation of receptor tyrosine kinases by the growth factor, recruits PI3K to the membrane via interaction of its p85 subunit to tyrosine phosphate motifs on activated receptors directly (e.g. PDGFR) or to other proteins associated with the receptors (e.g. insulin receptor substrate 1, IRS1). The activated p110 catalytic subunit phosphorylates phosphatidylinositol-4,5-diphosphate (PIP2) to phosphatidylinositol-3,4,5-triphosphate (PIP3), which in turn activates multiple signaling pathways.

Class IB PI3K is a heterodimer composed by a catalytic subunit p110γ and a regulatory subunit p101[24]. p110γ is activated directly by G protein–coupled receptors (GPCRs) and, in particular, by its free Gβγ subunit by a mechanism that is stimulated by the regulatory subunit p101[25]. p110γ is present only in mammals and it is mainly expressed in leukocytes but is also found in the heart, pancreas, liver and skeletal muscles.

Class II PI3Ks are larger proteins consisting of a single catalytic subunit, which prefers PI or PI(4)P as substrates[26,27]. Nevertheless, in some specific conditions, they also phosphorylate PIP2. There are three isoforms: PI3KC2α, PI3KC2β and PI3KC2γ, activated by receptor tyrosine kinases, cytokine receptors, and integrins[28–32]. PI3KC2α and PI3KC2β are expressed in all tissues, whereas PI3KC2γ is predominantly expressed in liver. It has been recently found that class II PI3Ks are involved in tumour angiogenesis and in the regulation of hepatitis C virus replication[33,34].

1.3. Therapeutic implications of kinase inhibitors

1.3.1. Neurodegenerative diseases

Neurodegenerative diseases are pathologies which involve the central nervous system (CNS) and are characterized by a chronic and selective process of neuronal cell death. The etiology of this pathological process is still unknown, nevertheless some genetic and environmental factors seem to play an important role. The brain damage is irreversible and it exhibits cognitive deficits, dementia, motor alteration, behavioral and psychological disorders.

Some excitatory amino acid brain transmitters, such as glutamate, are known to be toxic for neuronal cells as they could over-activate excitatory amino acid receptors. In some acute situations, this toxicity is responsible of the damage of brain cells, thence development of selective antagonists was considered one of the major chance of treatment[35].

Oxidative stress is shown to be another possible cause of neurodegenerative disease, especially those related with age-increasing[36–38]. Furthermore glutamate toxicity and oxidative stress were demonstrated to be linked by a common path[39,40].

The most common neurodegenerative diseases are: Amyotrophic Lateral Sclerosis (ALS), Progressive Supranuclear Palsy (PSP), Frontotemporal Dementia (FTD), Lewy Body Dementia (LBD), Alzheimer's Disease (AD), Parkinson's Disease (PD), Huntington's Disease (HD). In this work, we will focus on the description of Alzheimer's Disease as it represents the principal target of our project.

1.3.1.1. Alzheimer's disease

In 1901 the German psychiatrist Alois Alzheimer identified for the first time the symptoms of a particular dementia, which will be named after him. Thereafter many scientists studied (and are currently studying) the causes of this disease, in order to be able to cure it. Alzheimer's disease (AD) is a multifactorial disorder and it is one of the most invalidating and costly pathology in the industrial world. AD represents the 50-80% of all dementias and it is often considered "the elderly disease", even though in some cases it affects people at an earlier age. Alzheimer's disease is the sixth cause of death in USA[41] and the number of people affected by this disease is going to increase as the percentage of population age over65 is going to grow.

The principal symptoms of Alzheimer's are:

- Memory loss, important in ordinary life;
- Difficulties in planning and problem solving;
- Efforts to accomplish some goals at home, at work or during free time;
- Confusion with "when" and "where";
- Problems in understanding some images or some spatial connections;
- Difficulties with spoken and written words;
- Less judgment capacities;
- Mood swings.

Unfortunately, some of these factors are not easy to recognize, therefore the diagnosis is revealed when the pathology is already at an advanced stage.

Many studies where addressed on understanding the causes of this important pathology. AD is a neurodegenerative disease and it is irreversible. All the therapies are oriented on decelerate more than on arresting the pathological development.

There are some interesting studies on the discovery of a genetic cause of AD (reviewed in [42]). During this research, some genes where identified to be causative of the onset (early or late) and development of AD, such as the gene STM/PS-2 (presenilin 2) on chromosome 1[43], the S182iPS-1 (presenilin 1) gene on chromosome 14[44], the apolipoprotein E (ApoE) gene on chromosome 19[45,46] and the amyloid precursor protein (APP) on chromosome 21[47].

Alzheimer's disease's multiple factors are a combination of brain changes, which may begin several years before symptoms appear. Some of the brain changes which are contributing to the development of AD are the formation of beta-amyloid plaques and of the tau tangles. The diagnosis of AD is confirmed by the post-mortem analysis. The presence in the brain of high percentage of neurofibrillary tangles (NFTs) and amyloid plaques are considered a further evidence of AD. Aβ plaques accumulate outside the neurons and they interfere with neurons' communication, while NFTs are mostly stored inside the neurons and they impede the transport of essential substances inside the cells. They both contribute to neuronal cell death and they represent the principal hallmarks of Alzheimer's disease.

The amyloid precursor protein (APP) is proteolysed by α-, β- and γ-secretase to oligomers of beta-amyloid (Aβ)[48]. In a pathological state, there is a prevalence of Aβ terminating at the aminoacid 42 ($A\beta_{42}$), which is the form more prone to oligomerization and fibril formation[49].

Targeting one of these effects failed in the past, therefore there is no successful treatment against AD known so far, as it is not possible to stop or slow down the neuronal cell death process.

1.3.1.2. Down syndrome

Down syndrome (DS) is a congenital chromosomal disease caused by the presence of an extra chromosome 21, that is why it is also called "Trisomy 21". It represents the first genetic abnormality described and identified on humans and the first pathology on which the relation between the genotype and the phenotype has been shown. There are three forms of trisomy 21, but the majority of patients presents a free trisomy form, which is caused by the presence of a full extra chromosome, in 95% of the cases of maternal origin[50,51]. Another form of trisomy is the one for robertsonian translocation of parental origin. There is a fusion of two chromosomes by the translocation on chromosome 14 or 21[52]. Finally, 2% of the cases present cellular mosaics. Two types of cells are observed: one has the right number of chromosomes, the other one has three chromosomes 21. This kind of trisomies are of mitotic origin and they appear during the embryogenesis[51].

This pathology has a strong connection with the associated phenotype of patients. Each individual affected by DS presents a combination of unique phenotypical characteristics[53]. Apart from the physical malformations, DS patients have a mental retardation more or less pronounced, depending on each single individual. Furthermore, people affected by DS show strong linguistic difficulties.

The principal cause of dementia, and in particular of Alzheimer's disease in DS patients, is the presence of the gene encoding amyloid precursor protein (APP) located on chromosome 21. Its overexpression produces an increase of β-amyloid 42 concentration in the brain of individuals with DS younger than 40 years of age.

1.3.2. Glioma

Glioma represents the most malignant brain tumor with a life expectation of 2 year survival in 58% of the cases in USA[54]. Glioblastoma multiforme (GBM) is the most aggressive type of glioma, classified as grade IV from the World Health Organization (WHO), which represents the maximum hazardous level, also known as high-grade glioma (HGG).

Some of the symptoms of GBM are headache, nausea and symptoms similar to stroke which become worse with the passing of time, leading to a state of unconsciousness[55]. The causes include genetic factors, such as chromosomic alterations[56]. Some of the pathways (Figure 3) have been identified in the past few years, which have brought to the development of new drugs with the purpose of blocking some of the aberrant cellular mechanisms involved in abnormal cell proliferation and tumor progression[57]. Nevertheless, treatments result unsuccessful because of the resistance of the tumor to most of the tested drugs[58].

Surgery followed by chemo- and radio-therapy is the most frequent method for the treatment of glioblastoma. Also immunotherapy showed promising results[59,60].

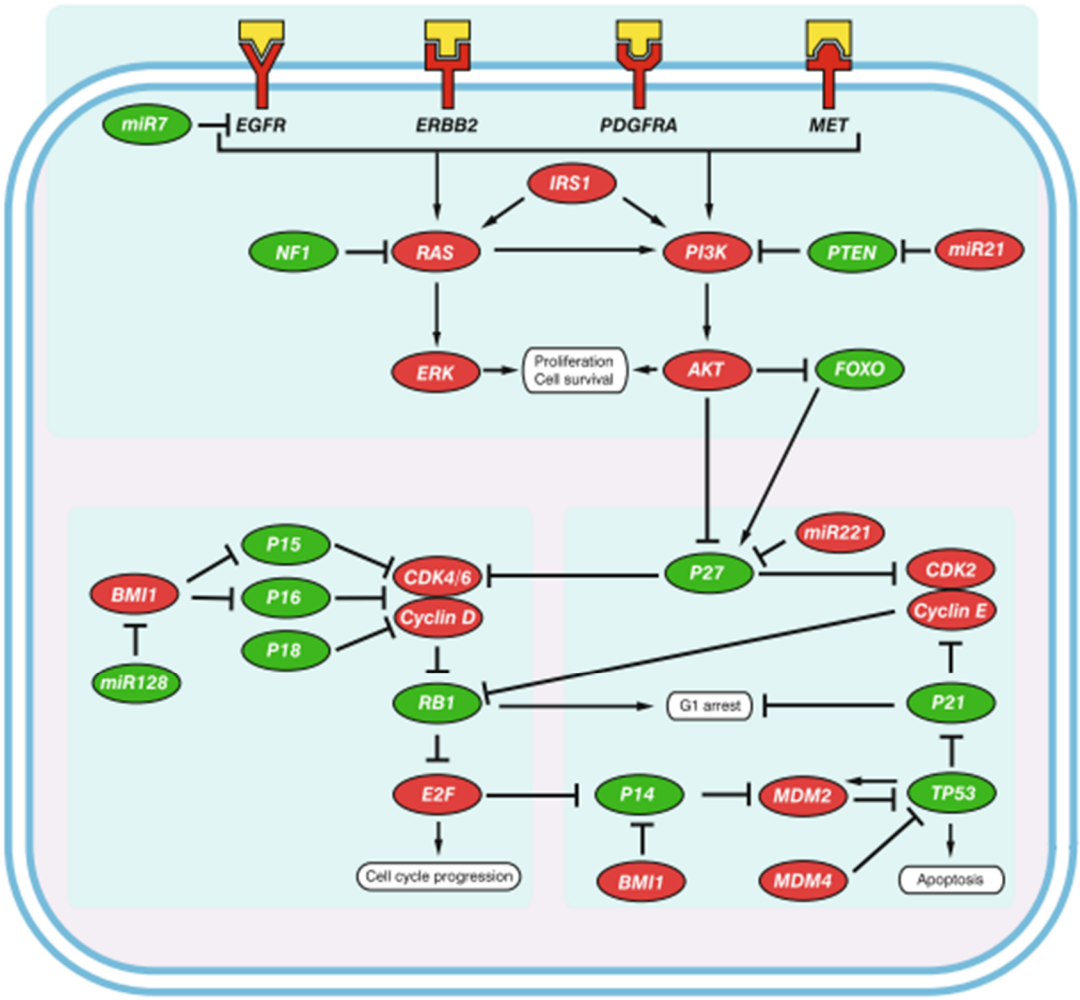

Figure 3. (from [56]). Some of the pathways involved in GBM progression.

2. Aims of the thesis

This thesis focused on the development of a new series of small compounds which were quite selective towards the principal targets of different CNS pathologies also including "multi-" or "group-"selective inhibitors. Our main goals were:

1) development of new selective Dyrk1A inhibitors;
2) development of potential anti-Alzheimer agents with dual mode of action;
3) development of multi-kinase targeting compounds for the treatment of glioblastoma.

Ad 1) An important requirement for the treatment of chronic diseases like neurodegeneration is selectivity. A long-term therapy must achieve the best results by minimizing any possible side effect for having a good compliance from the patient. At the beginning of this project, no selective Dyrk1A inhibitor was known so far. Also the most potent inhibitor discovered until that time, harmine, a beta-carboline alkaloid, was showing a moderate selectivity towards other members of Dyrk family but a strong MAO-A inhibition[61], which led to several neuronal side effects. Our primary goal was, therefore, to develop selective Dyrk1A inhibitors for the treatment of Alzheimer's disease and Down syndrome, where this kinase is overexpressed. For this purpose, our project was considering the possibility to evaluate the inhibitory activities of our molecules in a cellular in vitro assay. Therefore we elaborated a new cell assay for demonstrating the specific activity of Dyrk1A inhibitors in intact cells. This goal was very challenging because of the high homology between Dyrk1A and Dyrk1B (one amino acid difference, a methionine in Dyrk1A and a leucine in Dyrk1B, which, however, expose only the peptide backbone to the ATP-binding pocket).

Ad 2) Another important goal was to develop dual inhibitors with the intention of addressing two important cellular mechanisms involved in the development of Alzheimer's disease: tau phosphorylation and beta-amyloid aggregation. Considering the idea that a simultaneous and specific inhibition of these two important pathogenic processes could increase the efficacy, we decided to focus on this polypharmacological approach. Other studies[62–65] were based on the combination of A-beta peptide and acetylcholinesterase inhibitors. Nevertheless this approach was unsuccessful as the anticolinergic activity was not decreasing the progression of the disease as expected. The most important advantage of our strategy was to selectively address our dual inhibitors to the main pathways of the target pathologies, without inhibiting other targets.

Ad 3) Furthermore, we explored additional functions directing also other relevant non-kinase targets in order to boost the inhibitory activity. Single-target drugs may not always induce the

desired effect and/or may not prevent cell compensatory reactions. The pathologies object of our study are very complex and they involve many cellular pathways, hence it is necessary to address different targets. Therefore we tried to hit more than one cellular mechanism using the so called "multi-target" approach, without increasing side effects. An immediate example is the lacking of effective therapeutics for the treatment of malignant brain cancer. The percentage of survival patients affected by glioblastoma multiforme is very low and the most used pharmacological treatment with temozolomide gives a high probability of drug-resistance. It is then believed that multi-targeting kinase inhibitors could be more effective in combating this disease.

Muti-targeted inhibitory activity is an established concept in the treatment of cancer. The well characterized drug Imatinib is an inhibitor of three tyrosine kinases, BCR-Abl (main target), PDGF receptor kinase and c-kit. This multi-targeted activity is believed to be beneficial in some cases of chronic myeloid leukemia (CML), which may also be caused by dysregulated PDGFR signaling[66,67]. Intriguingly, several second generation BCR-Abl inhibitors, which are effective in cases of Imatinib-resistant CML, such as Bosutinib, Dasatinib and Ponatinib are not more but even less selective than Imatinib[68].

Finally, as all the target pathologies of this thesis are involving the central nervous system, it is very important to design compounds able to permeate through the brain blood barrier in order to easily reach the target. Having this purpose in mind, we planned the synthesis of compounds with such specific properties. In particular, our set of compounds is composed by molecules with a very low molecular weight and maximum one H-bond donor.

3. Results

3.1. Publication A: First selective dual inhibitors of tau phosphorylation and beta-amyloid aggregation, two major pathogenic mechanisms in Alzheimer's disease

Marica Mariano, Christian Schmitt, Parisa Miralinaghi, Marco Catto, Rolf W. Hartmann, Angelo Carotti, Matthias Engel

ACS Chem. Neurosci. 2014, 5, 1198−1202; dx.doi.org/10.1021/cn5001815

ACS Chemical Neuroscience

Letter

pubs.acs.org/chemneuro

First Selective Dual Inhibitors of Tau Phosphorylation and Beta-Amyloid Aggregation, Two Major Pathogenic Mechanisms in Alzheimer's Disease

Marica Mariano,[†] Christian Schmitt,[†] Parisa Miralinaghi,[†] Marco Catto,[‡] Rolf W. Hartmann,[†] Angelo Carotti,[‡] and Matthias Engel*[,†]

[†]Department of Pharmaceutical and Medicinal Chemistry, Saarland University, Saarbrücken 66123, Germany

[‡]Dipartimento di Farmacia-Scienze del Farmaco, Università degli Studi di Bari "Aldo Moro", via Orabona 4, 70125 Bari, Italy

Supporting Information

ABSTRACT: In Alzheimer's disease (AD), multiple factors account for the accumulation of neurocellular changes, which may begin several years before symptoms appear. The most important pathogenic brain changes that are contributing to the development of AD are the formation of the cytotoxic β-amyloid aggregates and of the neurofibrillary tangles, which originate from amyloid-β peptides and hyperphosphorylated tau protein, respectively. New therapeutic agents that target both major pathogenic mechanisms may be particularly efficient. In this study, we introduce bis(hydroxyphenyl)-substituted thiophenes as a novel class of selective, dual inhibitors of the tau kinase Dyrk1A and of the amyloid-β aggregation.

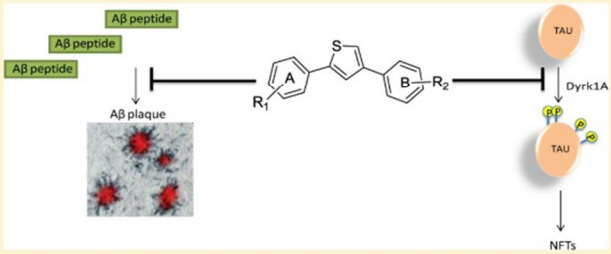

KEYWORDS: *Alzheimer's disease, β-amyloid, tau protein, Dyrk1A, dual inhibitors*

Alzheimer's disease (AD) is the sixth leading cause of death in the United States[1] with an increasing incidence as the percentage of population aged over 65 is steadily growing. AD, as other chronic diseases, is a result of multiple factors rather than a single cause. Two of the most prominent pathological events in the appearance and development of Alzheimer's disease are the formation of insoluble amyloid plaques and neurofibrillary tangles.[2] The amyloid plaques are extracellular deposit of amyloid β (Aβ) fibrils, which are aggregates derived from oligomeric Aβ peptides, and thought to trigger the disease, probably in concert with neurofibrillary tangles (NFT).[2,3] NFT are insoluble aggregates of the microtubule-associated tau protein, which were also shown to promote neurodegeneration.[2] The formation of NFT is caused by hyperphosphorylation of the tau protein, for which several protein kinases are discussed to play major roles, including GSK3β, PKA, CDK5, and Dyrk1A.[4]

In people affected by Down syndrome (DS), AD occurs at a substantially earlier age of about 40 years.[5] The early amyloidosis-β in these patients was mainly attributed to an overexpression of the amyloid precursor protein (APP) due to the location of the APP gene in the so-called "Down syndrome critical region" (DSCR) on chromosome 21, of which three copies are present in all DS cases.[6] However, with respect to the early neurofibrillary degeneration, one of the major responsible factors was shown to be the dual specificity tyrosine phospho-regulated kinase 1A (Dyrk1A), which is encoded by another gene in the DSCR and therefore about 1.5-fold overexpressed in DS patients.[6−9] It has been demonstrated that Dyrk1A is involved in the premature development of AD in DS[8,9] because it phosphorylates several crucial substrates, such as the tau protein and α-synuclein (reviewed in ref 10). Phosphorylation of α-synuclein enhances the formation of neurotoxic intracellular inclusions, the so-called Lewy bodies, which are present in about 30−40% of the AD cases. It is assumed that in AD, Aβ, tau, and α-synuclein can promote each other's aggregation.[11] Dyrk1A is the major tau kinase in DS/AD patients, but it was also shown to be overexpressed in sporadic AD cases and may act as a priming kinase by creating the recognition sites for GSK3β, for example, via tau phosphorylation at Thr212.[12]

The production of Aβ peptides requires proteolysis of the APP by α-, β-, and γ-secretase. Of note, Dyrk1A was shown to phosphorylate APP and presenilin-1, a key component of the γ-secretase complex, thereby accelerating the formation of Aβ peptides.[10] In a pathological state, different Aβ peptides ranging from 39 to 42 amino acid residues are formed, with the prevalence of Aβ terminating at the amino acid 42 (Aβ_{42}), which is the form more prone to oligomerization and fibril formation.[13] In the brains of Down syndrome patients, Aβ_{42} can form numerous diffuse plaques already at the age of 12 years, whereas Aβ_{40} occurs first in plaques almost 20 years later.[14]

Not surprisingly, both these major neurotoxic processes, the formation of NFT and Aβ plaques, were proposed independently as pivotal targets for pharmacological inter-

Published: September 23, 2014

   dx.doi.org/10.1021/cn5001815 | ACS Chem. Neurosci. 2014, 5, 1198−1202

vention. However, attempts to inhibit either of these pathogenic mechanisms alone have so far been disappointing. Although the reasons for this are not fully clear, it can be hypothesized that a higher efficacy may arise from the simultaneous, specific inhibition of both major pathogenic processes, in line with the view that complex diseases may require polypharmacology approaches.[15] Only few examples of such dual inhibitors were hitherto described, and they were mainly restricted to approaches combining the inhibition of Aβ peptide aggregation with the inhibition of acetylcholinesterase (AChE).[16−19] These prototype inhibitors were believed to be superior to existing single-target agents; however, the AChE inhibitory activity aimed at treatment of the symptoms by amplification of the cholinergic neurotransmission, rather than at stopping the disease progression. Earlier reports on the inhibition of both tau protein phosphorylation and Aβ peptide aggregation involved the use of nonselective natural compounds such as curcumin or plant extracts (reviewed in ref 20). However, such plant-derived compounds are known to inhibit a plethora of enzymes; hence, the mechanism(s) of action remain poorly defined, and target-oriented optimization is not possible. In contrast, single small molecules able to specifically interfere with only the disease-relevant pathways, amyloid formation and tau phosphorylation, were—to the best of our knowledge—not reported yet.

Herein, we present the first selective dual inhibitors that inhibit a major tau kinase, Dyrk1A, and exhibit an anti-Aβ aggregating activity, thus targeting two of the major pathogenic mechanisms involved in AD progression.

Screening of an in-house library of enzyme inhibitors devoid of typical kinase inhibitor motifs identified compound **1** as a hit (Figure 1, IC_{50} = 1.8 μM).[22] Interestingly, we found that

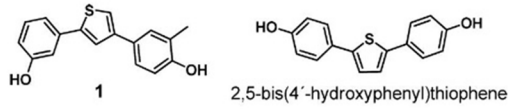

Figure 1. Hit and reference compound.[21]

structurally similar compounds were previously described to bind to Aβ peptide aggregates with high affinity, for example, 2,5-bis(4′-hydroxyphenyl)thiophene (K_i = 4.0 nM)[21] (Figure 1). Since it was possible that compounds with such a structural motif would also bind to the soluble monomeric or oligomeric Aβ peptides, thus potentially preventing aggregation, we tested the Dyrk1A inhibitor **1** and structurally related derivatives in Table 1 for this second biological activity. With a well consolidated experimental protocol in our hands,[18] we decided to use Aβ_{40} instead of the more toxic and aggregation prone Aβ_{42}, also because of its slower aggregation kinetics. We also explored the inverse approach, that is, testing of some 2,5-disubstituted thiophene isomers that were more similar to the described Aβ ligands,[21] and an analogous thiazole derivative against Dyrk1A; however, this group of analogues did not show any inhibitory activity (Table S1, Supporting Information). Hence, we focused on the 2,4-disubstituted thiophene isomers.

Initially, we observed only a weak inhibition of the in vitro Aβ_{40} peptide aggregation by compound **1** (46% at 100 μM). We then explored whether it was possible to optimize this activity, starting with a variation of the hydroxyl position. Moving of the hydroxyl on the A ring from the *meta*- to the *para*-position clearly enhanced the potency to prevent the self-assembly of the Aβ peptide in all cases, and eventually gave rise to the most potent compounds (**3**, **5**−**8**, Table 1). Importantly, these modifications did not strongly affect the inhibition of Dyrk1A. The addition of an aliphatic moiety was identified as a key step for the enhancement of the Aβ aggregation inhibition. Especially the *meta*-methyl substitution of the A ring resulted in the most potent compounds in this regard (**7** and **8**). However, longer aliphatic chains were unfavorable (e.g., *m*-ethyl in **6**) and were even detrimental to the Dyrk1A inhibition (compare **6** vs **5**). Concerning the B ring, the hydroxyl in *meta*-position was favorable for the inhibition of Dyrk1A, whereas the *para*-hydroxyl conferred a higher potency against the Aβ aggregation (cf. **5** vs **7**). The comparison of **1** with **2** revealed that the inhibition of Dyrk1A by compounds that are *p*-hydroxy−substituted at the B ring could be increased by the introduction of *m*-methyl (**1**), while ethyl at the same position was already too large (**4**). Thus, compound **8** was synthesized aiming at creating the best balance between the two desired biological activities. The most favorable substitution pattern on the A ring was kept (from **5** and **7**), while an additional methyl group was introduced in the *meta*-position of the B ring. Indeed, **8** displayed a slightly enhanced inhibition of Dyrk1A compared with **7**, while the potency to prevent the Aβ aggregation was also improved. The comparison of **8** to its methoxy precursor **8i** showed that at least one H-bond donor function of the hydroxyl groups was essential to both biological activities (**8i**, Table 1). Altogether, our structure−activity relationship indicated that with the 2,4-diphenyl thiophene scaffold, the

Table 1. Biological Activities of 2,4-Diphenyl Thiophene Derivatives

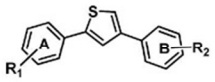

name	R1	R2	Dyrk1A IC_{50} (μM)[ab]	Aβ_{40} % inhibition @ 100 μM
1	3-OH	3-CH_3; 4-OH	1.8	46 ± 2
2	3-OH	4-OH	4.0	38 ± 2
3	4-OH	3-OH	4.5	55 ± 2
4	3-OH	3-CH_2CH_3; 4-OH	5.0	49 ± 3
5	3-CH_3; 4-OH	3-OH	2.0	73 ± 2
6	3-CH_2CH_3; 4-OH	3-OH	28%[c]	62 ± 2
7	3-CH_3; 4-OH	4-OH	6.7	78 ± 1
8	3-CH_3; 4-OH	3-CH_3; 4-OH	5.0	91 ± 1
8i	3-CH_3; 4-OCH_3	3-CH_3; 4-OCH_3	n.i.[d]	37 ± 3

[a]SD < 10%. [b][ATP] = 100 μM. [c]Percent inhibition at 5 μM. [d]n.i., no inhibition.

dx.doi.org/10.1021/cn5001815 | ACS Chem. Neurosci. 2014, 5, 1198−1202

potency toward $A\beta_{40}$ aggregation could be increased without loss of activity against Dyrk1A. In contrast, the previously described class of hydroxybenzothiophene analogues, derived from the bis(phenol)thiophenes following a ring condensation strategy,[23] proved to be markedly less potent in preventing the $A\beta$ aggregation (Table S2, Supporting Information). Therefore, it failed to provide an appropriate balance between the inhibition of Dyrk1A and the $A\beta$ aggregation, similarly to our previously published bis(pyrimidinyl)thiophene series[22] (Table S3, Supporting Information). Although it was suggested that phenolic compounds in general can interfere with $A\beta$ peptide aggregation,[24] the lack of activity with the hydroxybenzothiophene analogs underlines that the spatial arrangement of the thiophene to the phenolic structures is important, also indicating a specific binding interaction.

Based on their highest potencies to prevent $A\beta$ aggregation (cf. IC_{50} values in Table 2), compounds **5**, **7**, and **8** were selected for testing their cellular activity. To this end, we developed a cell-based assay that provided conditions for a strong tau phosphorylation specifically by Dyrk1A due to overexpression of both proteins (cf. Supporting Information, HEK293-tau-Dyrk1A cell assay). All three compounds were found to inhibit the intracellular, Dyrk1A-catalyzed tau phosphorylation with a remarkable efficacy, as there was only a slight decline of potency compared with that in the cell-free assay (Figure 2; cf. Table 1); the weakest Dyrk1A inhibitor **7** showed the lowest cellular potency. Altogether, compound **8** exhibited the best profile with a balanced inhibitory potency toward both targets (Table 2).

Table 2. IC_{50}'s of the Best Compounds for the Inhibition of $A\beta_{40}$ Aggregation and Intracellular Tau Phosphorylation

name	$A\beta_{40}$ inhibition (cell free assay, $IC_{50} \pm$ SEM, μM)	Inhibition of tau phosphorylation in cells (IC_{50}, μM)[a]
5	33 ± 4	8.5
7	16 ± 2	11.6
8	11 ± 3	8.3

[a]SD < 15%.

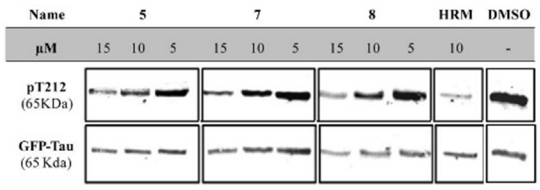

Figure 2. HEK293-tau-Dyrk1A cell assay. Compounds **5**, **7**, and **8** inhibit Dyrk1A-catalyzed tau phosphorylation in stably transfected HEK293 cells. The test compounds, DMSO, or the reference inhibitor harmine (HRM)[25,26] were added to the cell medium at the indicated concentrations. After immunoblotting, the level of phospho-tau-Thr212 was detected using a phosphospecific antibody. To normalize the signals, total recombinant tau protein was quantified using an anti-GFP antibody. One representative experiment out of two is shown.

A major obstacle for the application of kinase inhibitors is often their poor selectivity. Therefore, we tested the selectivity of **8** against a panel of carefully selected kinases, which not only included a member of each branch of the human kinome but also the complete list of frequently reported off-targets for Dyrk1A inhibitors.[27] This challenging screening revealed that **8** was rather selective for the Dyrk family of kinases, with the only exception of Clk4 (Table S4, Supporting Information). Coinhibition of the latter kinase might be advantageous with respect to its involvement in the alternative splicing of tau, which results in a pathogenic imbalance between 3R-tau and 4R-tau isoforms through skipping of exon 10.[28] As Dyrk1A shares this pathogenic role,[29] coinhibition of Dyrk and Clk kinases by our compounds might efficiently correct the tau splicing isoform imbalance. It should be noted that the clean selectivity profile versus the chosen kinase panel ruled out any nonselective inhibitory properties such as those found with plant−derived compounds like curcumin.[30]

In conclusion, using a focused multitarget approach, we identified a new bis(hydroxphenyl)thiophene-based family of dual Dyrk1A and β-amyloid inhibitors. Of note, the chemical class of bis(hydroxyphenyl)-substituted thiophenes was previously reported to display a good metabolic stability in rat liver microsomes and a high permeability in the CaCo-2 assay,[31] and was orally available in rats.[32] Although the substitution pattern of those derivatives was different, these studies demonstrated that bis(hydroxyphenyl)-substituted thiophenes can show favorable pharmacokinetic properties in spite of the phenolic substructure. Moreover, the penetration of the blood-brain barrier is another important requirement for AD therapeutics; interestingly, bisphenolic compounds with comparable physicochemical properties (bis(hydroxyphenyl) bis-styrylbenzenes) were shown to readily cross the blood-brain barrier.[33]

For proof-of-concept studies, it is preferable to optimize the potencies of our lead compounds; however, **8** might be considered to be just at the border of being potentially applicable to in vivo AD models—provided that no dose-limiting toxicities occur. For comparison, Hirohata and coworkers reported that ibuprofen inhibits α-synuclein fibril formation with an IC_{50} of 12.1 μM, similar to the potency range of our compounds, and pointed out that such levels can be reached in cerebrospinal fluid after an oral dose of 800 mg in humans.[34] While the kinase inhibitory activity can certainly be optimized, it is unclear to what extent the antifibrillogenic potency can be increased, since the underlying mode of action may involve stoichiometric binding rather than a catalytic mechanism. Thus, the in vivo efficacy might also depend on the concentration of the $A\beta$ peptides in the affected neurons, which may, at least partially, be lower than the 30 μM in our cell-free assay.

METHODS

HEK293-Tau-Dyrk1A Cell Assay. HEK293-tau-Dyrk1A cells, generated as described in the Supporting Information, were seeded in 12-well plates and grown in full medium without G418 until 70% confluence was reached. The medium was then exchanged by DMEM containing 0.1% of FCS and tetracycline (0.3 μg/mL) to induce the expression of Dyrk1A, resulting in a strong increase of Dyrk1A activity in the cells (see experimental validation of the assay, Figure S1 in the Supporting Information). The test compounds or DMSO (control) were then added from stock solutions in DMSO to the desired final concentration (DMSO concentration $\leq$ 0.2%). Initially, potential cytotoxicity of the compounds was checked; no signs of toxicity were observed after incubation for 2 days at the highest concentrations (20 μM) of the compounds. Under the assay conditions, the incubation with the compounds was carried out overnight in an incubator at 37 °C and 5% CO_2. The next day, the medium was removed from each well and the plate frozen at −80 °C for 10−15 min to facilitate the cell disruption. Then, 200 μL of SDS-PAGE sample buffer per well was added to the frozen cells and cell lysis was completed by passing several times through a micro syringe (Hamilton). Aliquots of 24 μL of the samples were then separated by SDS-PAGE (10% gels), and the

dx.doi.org/10.1021/cn5001815 | ACS Chem. Neurosci. 2014, 5, 1198−1202

proteins blotted on a PVDF membrane (Immobilon-FL, Millipore) using a semidry blotting apparatus (Biometra). Free binding sites on the membrane were then blocked for 1 h using blocking buffer (3% bovine serum albumin in Tris buffered saline (TBS), pH 7.2), followed by an incubation with the first primary antibody (pT212) diluted 1:1000 in blocking buffer overnight at 4 °C. On the following day, the membrane was washed with TBS containing 0.1% Tween-20 for three times and one time with TBS. Then it was incubated with the second primary antibody (anti-GFP, dilution 1:1000) in blocking buffer for 1 h at room temperature. After a second wash, the membrane was incubated with secondary antibodies (IR-Dye-labeled anti-mouse and anti-rabbit, both diluted 1:7500 in blocking buffer) for 1 h at room temperature. The signals of the washed membrane were finally detected by using an Odyssey infrared imager (LI-COR).

■ ASSOCIATED CONTENT

Supporting Information

Biological activities of 2,5-bis(hydroxyphenyl)thiophenes, hydroxybenzothiophenes, and bis(pyridinyl)thiophenes (Tables S1–S3); selectivity screening (Table S4); experimental details for all assays and syntheses; HEK293-tau-Dyrk1A assay validation (Figure S1). This material is available free of charge via the Internet at http://pubs.acs.org.

■ AUTHOR INFORMATION

Corresponding Author

*E-mail: ma.engel@mx.uni-saarland.de. Phone: +4968130270312.

Author Contributions

M.M. developed and performed the cellular tau phosphorylation assay and repeated kinase inhibition assays; C.S. and P.M. contributed to inhibitor design and performed synthetic chemistry; C.S. performed most kinase inhibition assays; M.C. conducted Aβ aggregation assays and interpreted data; R.W.H., A.C., and M.E. conceived the project, interpreted data, and oversaw the research. The manuscript was written by M.M., M.C., and M.E..

Funding

We are grateful for the financial support by the DFG to M.E. (EN 381/3-1).

Notes

The authors declare no competing financial interest.

■ ACKNOWLEDGMENTS

We thank Prof. Dr. Walter Becker, Institute of Pharmacology and Toxicology, RWTH Aachen, and Prof. Dr. Roland Brandt, University Osnabrück, for providing the pEGFP-DYRK1A HEK293 cell line and the pEGFP-htau352wt plasmid, respectively.

■ ABBREVIATIONS

AD, Alzheimer's disease; DS, Down syndrome; Dyrk, dual specificity tyrosine (Y) phosphorylation regulated kinase; Aβ, amyloid β; NFT, neurofibrillary tangles; DSCR, Down syndrome critical region; APP, amyloid precursor protein; GSK3β, glycogen synthase kinase 3β; PKA, protein kinase A; CDK5, cyclin dependent kinase 5; HRM, harmine

■ REFERENCES

(1) Murphy, S. L., Xu, J., and Kochanek, K. D. (2013) Deaths: Final Data for 2010. *National Vital Statistics Reports* , Vol. *61*, National Center for Health Statistics, Hyattsville, MD.

(2) Ittner, L. M., and Götz, J. (2011) Amyloid-B and Tau—A Toxic Pas de Deux in Alzheimer's Disease. *Nat. Rev. Neurosci. 12*, 65–72.

(3) Hawkes, C. A., Carare, R. O., and Weller, R. O. (2014) Amyloid and Tau in the Brain in Sporadic Alzheimer's Disease: Defining the Chicken and the Egg. *Acta Neuropathol. 127*, 617–618.

(4) Martin, L., Latypova, X., Wilson, C. M., Magnaudeix, A., Perrin, M.-L., Yardin, C., and Terro, F. (2013) Tau Protein Kinases: Involvement in Alzheimer's Disease. *Ageing Res. Rev. 12*, 289–309.

(5) Wisniewski, K. E., Wisniewski, H. M., and Wen, G. Y. (1985) Occurrence of Neuropathological Changes and Dementia of Alzheimer's Disease in Down's Syndrome. *Ann. Neurol. 17*, 278–282.

(6) Wegiel, J., Dowjat, K., Kaczmarski, W., Kuchna, I., Nowicki, K., Frackowiak, J., Mazur Kolecka, B., Wegiel, J., Silverman, W. P., Reisberg, B., Deleon, M., Wisniewski, T., Gong, C.-X., Liu, F., Adayev, T., Chen-Hwang, M.-C., and Hwang, Y.-W. (2008) The Role of Overexpressed DYRK1A Protein in the Early Onset of Neurofibrillary Degeneration in Down Syndrome. *Acta Neuropathol. 116*, 391–407.

(7) Liu, F., Liang, Z., Wegiel, J., Hwang, Y.-W., Iqbal, K., Grundke-Iqbal, I., Ramakrishna, N., and Gong, C.-X. (2008) Overexpression of Dyrk1A Contributes to Neurofibrillary Degeneration in Down Syndrome. *FASEB J. 22*, 3224–3233.

(8) Kimura, R., Kamino, K., Yamamoto, M., Nuripa, A., Kida, T., Kazui, H., Hashimoto, R., Tanaka, T., Kudo, T., Yamagata, H., Tabara, Y., Miki, T., Akatsu, H., Kosaka, K., Funakoshi, E., Nishitomi, K., Sakaguchi, G., Kato, A., Hattori, H., Uema, T., and Takeda, M. (2007) The DYRK1A Gene, Encoded in Chromosome 21 Down Syndrome Critical Region, Bridges between Beta-Amyloid Production and Tau Phosphorylation in Alzheimer Disease. *Hum. Mol. Genet. 16*, 15–23.

(9) Park, J., Yang, E. J., Yoon, J. H., and Chung, K. C. (2007) Dyrk1A Overexpression in Immortalized Hippocampal Cells Produces the Neuropathological Features of Down Syndrome. *Mol. Cell. Neurosci. 36*, 270–279.

(10) Tejedor, F. J., and Hämmerle, B. (2011) MNB/DYRK1A as a Multiple Regulator of Neuronal Development. *FEBS J. 278*, 223–235.

(11) Larson, M. E., Sherman, M. A., Greimel, S., Kuskowski, M., Schneider, J. A., Bennett, D. A., and Lesné, S. E. (2012) Soluble A-Synuclein Is a Novel Modulator of Alzheimer's Disease Pathophysiology. *J. Neurosci. 32*, 10253–10266.

(12) Ferrer, I., Barrachina, M., Puig, B., Martínez de Lagrán, M., Martí, E., Avila, J., and Dierssen, M. (2005) Constitutive Dyrk1A Is Abnormally Expressed in Alzheimer Disease, Down Syndrome, Pick Disease, and Related Transgenic Models. *Neurobiol. Dis. 20*, 392–400.

(13) Roher, A. E., Lowenson, J. D., Clarke, S., Woods, A. S., Cotter, R. J., Gowing, E., and Ball, M. J. (1993) Beta-Amyloid-(1–42) Is a Major Component of Cerebrovascular Amyloid Deposits: Implications for the Pathology of Alzheimer Disease. *Proc. Natl. Acad. Sci. U.S.A. 90*, 10836–10840.

(14) Lemere, C. A., Blusztajn, J. K., Yamaguchi, H., Wisniewski, T., Saido, T. C., and Selkoe, D. J. (1996) Sequence of Deposition of Heterogeneous Amyloid Beta-Peptides and APO E in Down Syndrome: Implications for Initial Events in Amyloid Plaque Formation. *Neurobiol. Dis. 3*, 16–32.

(15) Anighoro, A., Bajorath, J., and Rastelli, G. (2014) Polypharmacology: Challenges and Opportunities in Drug Discovery. *J. Med. Chem.*, DOI: 10.1021/jm5006463.

(16) Rizzo, S., Rivière, C., Piazzi, L., Bisi, A., Gobbi, S., Bartolini, M., Andrisano, V., Morroni, F., Tarozzi, A., Monti, J.-P., and Rampa, A. (2008) Benzofuran-Based Hybrid Compounds for the Inhibition of Cholinesterase Activity, Beta Amyloid Aggregation, and Abeta Neurotoxicity. *J. Med. Chem. 51*, 2883–2886.

(17) Brogi, S., Butini, S., Maramai, S., Colombo, R., Verga, L., Lanni, C., De Lorenzi, E., Lamponi, S., Andreassi, M., Bartolini, M., Andrisano, V., Novellino, E., Campiani, G., Brindisi, M., and Gemma, S. (2014) Disease-Modifying Anti-Alzheimer's Drugs: Inhibitors of Human Cholinesterases Interfering with β-Amyloid Aggregation. *CNS Neurosci. Ther. 20*, 624–632.

(18) Catto, M., Berezin, A. A., Lo Re, D., Loizou, G., Demetriades, M., De Stradis, A., Campagna, F., Koutentis, P. A., and Carotti, A. (2012) Design, Synthesis and Biological Evaluation of Benzo[*e*]-

[1,2,4]triazin-7(1*H*)-one and [1,2,4]-Triazino[5,6,1-Jk]carbazol-6-one Derivatives as Dual Inhibitors of Beta-Amyloid Aggregation and Acetyl/butyryl Cholinesterase. *Eur. J. Med. Chem. 58*, 84−97.
(19) Rook, Y., Schmidtke, K.-U., Gaube, F., Schepmann, D., Wünsch, B., Heilmann, J., Lehmann, J., and Winckler, T. (2010) Bivalent Beta-Carbolines as Potential Multitarget Anti-Alzheimer Agents. *J. Med. Chem. 53*, 3611−3617.
(20) Calcul, L., Zhang, B., Jinwal, U. K., Dickey, C. A., and Baker, B. J. (2012) Natural Products as a Rich Source of Tau-Targeting Drugs for Alzheimer's Disease. *Future Med. Chem. 4*, 1751−1761.
(21) Chandra, R., Kung, M.-P., and Kung, H. F. (2006) Design, Synthesis, and Structure-Activity Relationship of Novel Thiophene Derivatives for Beta-Amyloid Plaque Imaging. *Bioorg. Med. Chem. Lett. 16*, 1350−1352.
(22) Schmitt, C., Kail, D., Mariano, M., Empting, M., Weber, N., Paul, T., Hartmann, R. W., and Engel, M. (2014) Design and Synthesis of a Library of Lead-like 2,4-Bisheterocyclic Substituted Thiophenes as Selective Dyrk/Clk Inhibitors. *PLoS One 9*, e87851.
(23) Miralinaghi, P., Schmitt, C., Hartmann, R. W., Frotscher, M., and Engel, M. (2014) 6-Hydroxybenzothiophene Ketones: Potent Inhibitors of 17β-Hydroxysteroid Dehydrogenase Type 1 (17β-HSD1) Owing to Favorable Molecule Geometry and Conformational Preorganization. *ChemMedChem*, DOI: 10.1002/cmdc.201402050.
(24) Porat, Y., Abramowitz, A., and Gazit, E. (2006) Inhibition of Amyloid Fibril Formation by Polyphenols: Structural Similarity and Aromatic Interactions as a Common Inhibition Mechanism. *Chem. Biol. Drug Des. 67*, 27−37.
(25) Frost, D., Meechoovet, B., Wang, T., Gately, S., Giorgetti, M., Shcherbakova, I., and Dunckley, T. (2011) B-Carboline Compounds, Including Harmine, Inhibit DYRK1A and Tau Phosphorylation at Multiple Alzheimer's Disease-Related Sites. *PLoS One 6*, e19264.
(26) Bain, J., Plater, L., Elliott, M., Shpiro, N., Hastie, C. J., McLauchlan, H., Klevernic, I., Arthur, J. S. C., Alessi, D. R., and Cohen, P. (2007) The Selectivity of Protein Kinase Inhibitors: A Further Update. *Biochem. J. 408*, 297−315.
(27) Schmitt, C., Miralinaghi, P., Mariano, M., Hartmann, R. W., and Engel, M. (2014) Hydroxybenzothiophene Ketones Are Efficient Pre-mRNA Splicing Modulators Due to Dual Inhibition of Dyrk1A and Clk1/4. *ACS Med. Chem. Lett. 5*, 963−967.
(28) Hartmann, A. M., Rujescu, D., Giannakouros, T., Nikolakaki, E., Goedert, M., Mandelkow, E. M., Gao, Q. S., Andreadis, A., and Stamm, S. (2001) Regulation of Alternative Splicing of Human Tau Exon 10 by Phosphorylation of Splicing Factors. *Mol. Cell. Neurosci. 18*, 80−90.
(29) Yin, X., Jin, N., Gu, J., Shi, J., Zhou, J., Gong, C.-X., Iqbal, K., Grundke-Iqbal, I., and Liu, F. (2012) Dual-Specificity Tyrosine Phosphorylation-Regulated Kinase 1A (Dyrk1A) Modulates Serine/arginine-Rich Protein 55 (SRp55)-Promoted Tau Exon 10 Inclusion. *J. Biol. Chem. 287*, 30497−30506.
(30) Aggarwal, B. B., and Sung, B. (2009) Pharmacological Basis for the Role of Curcumin in Chronic Diseases: An Age-Old Spice with Modern Targets. *Trends Pharmacol. Sci. 30*, 85−94.
(31) Bey, E., Marchais-Oberwinkler, S., Werth, R., Negri, M., Al-Soud, Y. A., Kruchten, P., Oster, A., Frotscher, M., Birk, B., and Hartmann, R. W. (2008) Design, Synthesis, Biological Evaluation and Pharmacokinetics of Bis(hydroxyphenyl) Substituted Azoles, Thiophenes, Benzenes, and Aza-Benzenes as Potent and Selective Nonsteroidal Inhibitors of 17beta-Hydroxysteroid Dehydrogenase Type 1 (17beta-HSD1). *J. Med. Chem. 51*, 6725−6739.
(32) Bey, E., Marchais-Oberwinkler, S., Negri, M., Kruchten, P., Oster, A., Klein, T., Spadaro, A., Werth, R., Frotscher, M., Birk, B., and Hartmann, R. W. (2009) New Insights into the SAR and Binding Modes of Bis(hydroxyphenyl)thiophenes and -Benzenes: Influence of Additional Substituents on 17β-Hydroxysteroid Dehydrogenase Type 1 (17β-HSD1) Inhibitory Activity and Selectivity. *J. Med. Chem. 52*, 6724−6743.
(33) Flaherty, D. P., Kiyota, T., Dong, Y., Ikezu, T., and Vennerstrom, J. L. (2010) Phenolic Bis-Styrylbenzenes as β-Amyloid Binding Ligands and Free Radical Scavengers. *J. Med. Chem. 53*, 7992−7999.
(34) Hirohata, M., Ono, K., Morinaga, A., and Yamada, M. (2008) Non-Steroidal Anti-Inflammatory Drugs Have Potent Anti-Fibrillogenic and Fibril-Destabilizing Effects for Alpha-Synuclein Fibrils in Vitro. *Neuropharmacology 54*, 620−627.

First selective dual inhibitors of tau phosphorylation and beta-amyloid aggregation, two major pathogenic mechanisms in Alzheimer's disease

Marica Mariano[1], Christian Schmitt[1], Parisa Miralinaghi[1], Marco Catto[2], Rolf W. Hartmann[1], Angelo Carotti[2], Matthias Engel[1]

[1]Department of Pharmaceutical and Medicinal Chemistry, Saarland University, Saarbrücken, Germany; [2]Dipartimento di Farmacia-Scienze del Farmaco, Università degli Studi di Bari "Aldo Moro", via Orabona 4, 70125 Bari, Italy

Supporting Information:

Table S1

2,5-Bis(hydroxyphenyl)thiophenes and a thiazole analogue that are inactive against Dyrk1A

cmpd. name and structure	screening concentration	% inhibition of Dyrk1A[b)]
harmine	1 µM	90.2
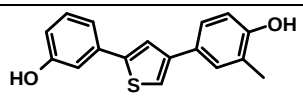 **1 (hit cmpd.)**	5 µM	78.0
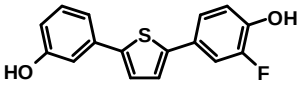 [a)]**21**	5 µM	8.3
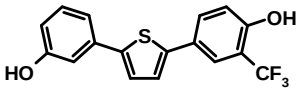 [a)]**24**	5 µM	7.5
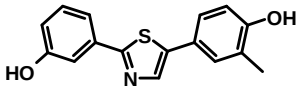 [a)]**37**	5 µM	11.5

[a)]compound numbers as published in Bey et al., *J. Med. Chem.* **2009**, *52*, 6724–6743; [b)] S.D. <10%.

Table S2

Biological activities of hydroxybenzothiophenes.

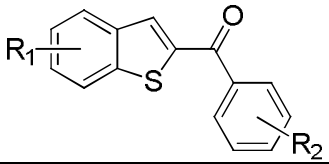

Compound	R1	R2	DYRK1A IC_{50} (μM) [a),b)]	Aβ % inhibition @ 100μM
9	6-OH	3-OH	1.6	24±6
10	3-CH_3;6-OH	3-OH	2.2	15±9
11	5-OH	3-OH	0.33	36±2
12	5-OH	4-OH	3.4	46±4
13	5-OH	2-F,3-OH	0.26	39±2
14	5-OH	3-OH,4-F	0.8	47±6
15	5-OH	3-CN	6.0	31±3

[a)]ATP concentration in the assay: 100 μM; [b)]S.D. <10%.

Table S3

Biological activities of bis(pyrimidinyl)thiophenes.

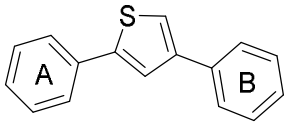

Compound	A	B	DYRK1A IC_{50} (μM) [a),b)]	Aβ % inhibition @ 100μM
16	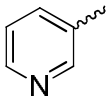	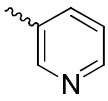	0.67	19±5
17	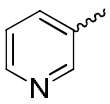	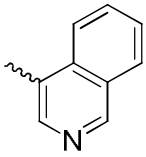	3.2	18±2
18	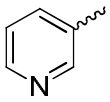	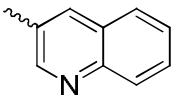	1.13	32±3
19	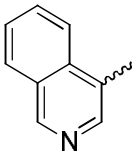	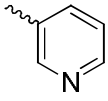	1.5	25±1

[a)]ATP concentration in the assay: 100 μM; [b)]S.D. <10%.

Table S4

Selectivity profile of compound **8** (10 µM) *vs.* a panel of selected kinases[a)]

Kinase Tested	%Inhibition[b)]
ABL1	-1
CAMK2A (CaMKII alpha)	-5
CDK5/p25	-5
CLK1	1
CLK2	2
CLK3	-1
CLK4	104
CSNK1D (CK1 delta)	-1
CSNK1E (CK1 epsilon)	-1
CSNK1G2 (CK1 gamma 2)	0
CSNK1G3 (CK1 gamma 3)	1
CSNK2A1 (CK2 alpha 1)	0
DYRK1B	55
DYRK2	86
DYRK3	0
DYRK4	-8
GSG2 (Haspin)	36
GSK3B (GSK3 beta)	2
HIPK1 (Myak)	-1
MAP3K9 (MLK1)	-3
MAPK14 (p38 alpha)	0
MAPK8 (JNK1)	-7
MLCK (MLCK2)	81
MST4	-7
MYLK (MLCK)	34
MYLK2 (skMLCK)	5
NTRK2 (TRKB)	-3
PIK3CG (p110 gamma)	0
PIM1	-19
PIM2	-3
PRKACA (PKA)	-10
PRKCA (PKC alpha)	-11
PRKD2 (PKD2)	-1
ROS1	2
STK17A (DRAK1)	69

[a)]The screening list was especially composed to include all kinases that were frequently reported as off-targets for diverse chemical classes of Dyrk inhibitors[69–73]. Hence, the low hit rate besides the main targets Dyrk and Clk4 suggests a very high degree of selectivity. Screenings were performed as a service at Life Technologies Labs; [b)]ATP concentration in the assay: 100 µM; S.D. <15%.

A1. Chemistry

A1.1. Synthesis Scheme

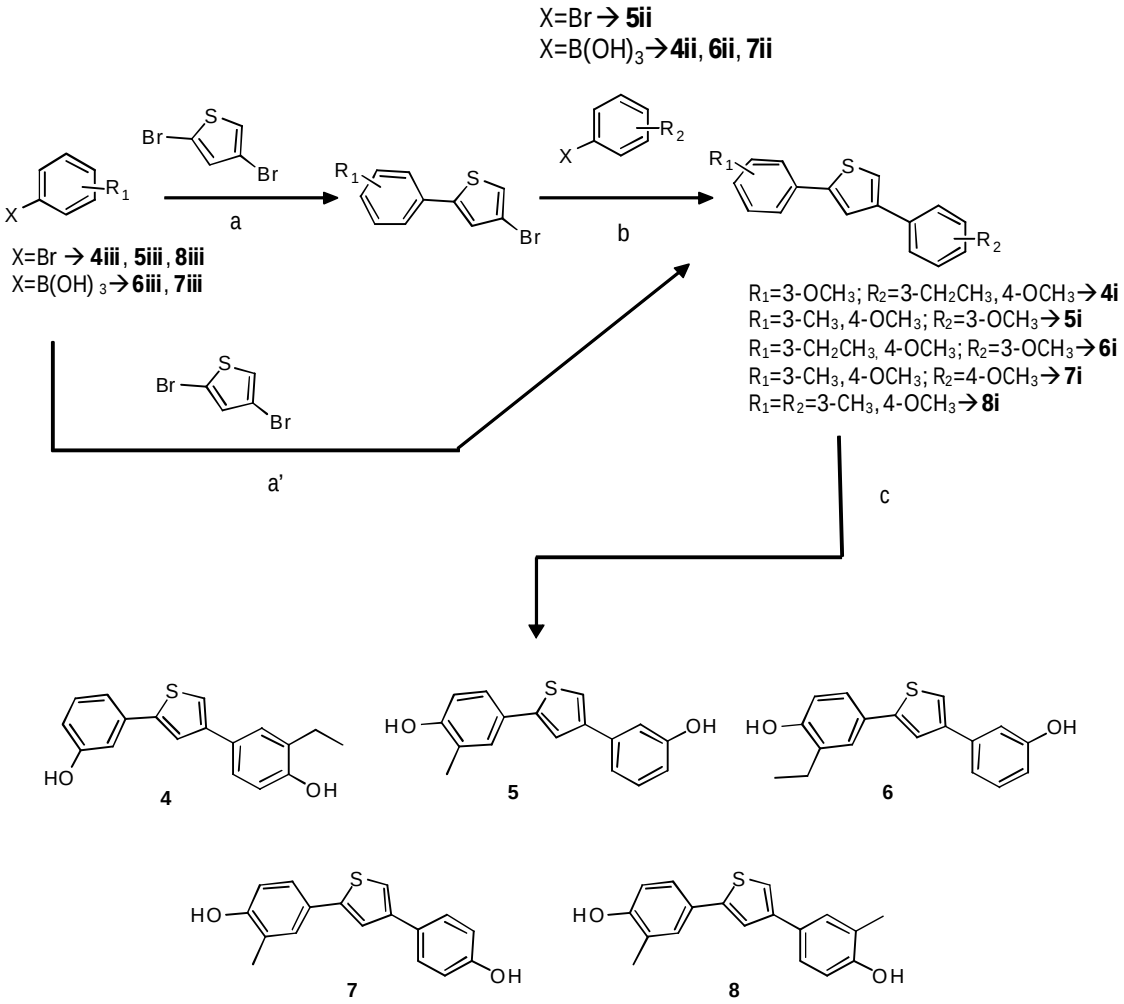

Scheme S1. Reagents and conditions: (a) For compound **4iii**: (1) Mg, dry THF, rt, 3 h, (2) $Pd(dppf)Cl_2$, -78°C to rt, 18 h; for compound **5iii**: Method A: (1) nBuLi, dry THF, -78°, 60 min, (2) $(BuO)_3B$, -78°C, 90 min, (3) $Pd(PPh_3)_4$, Na_2CO_3aq, reflux; for compounds **6iii** and **7iii**: Method B: $Pd(PPh_3)_4$, DMF/H_2O, 100°C, 14 h; (a') For compound **8iii**: Method A; (b) For compound **4ii**: $Pd(PPh_3)_4$, Na_2CO_3aq, reflux; for compound **5ii**: Method A, for compounds **6ii** and **7ii**: Method B; (c) For compounds **4-8**: Method C: BBr_3, CH_2Cl_2, -78°C to rt; for compound **8**: Pyridinium hydrochloride, µw 190°C, 2 h.

A1.2. General Chemical Methods

All chemical starting materials purchased from Sigma-Aldrich, Acros Organics, CombiBlocks, and Alfa Aesar were directly used without further purification. The purity of the synthesized compounds was determined by reversed phase chromatography (Nucleodur 100-3 c18ec from Macherey Nagel) using an Agilent 1100 series HPLC system from Agilent Technologies and a GC Trace Ultra from Thermo. The purity of the compounds used in the biological assays was ≥ 95%. Mass spectra (ESI) were measured on an AB Sciex Qtrap2000 from AB Sciex. Mass spectra (EI) were measured on a DSQ II from Thermo. ^{1}H and ^{13}C NMR spectra were recorded on either a Bruker DRX-500 (^{1}H, 500 MHz; ^{13}C, 126 MHz) instrument at 300 K or on a Bruker Fourier300 (^{1}H, 300 MHz; ^{13}C, 75 MHz) NMR spectrometer at 300 K in the deuterated solvents indicated. Flash column chromatography was performed using silica gel 60 (Merck, 35-70 µm). Reaction/flash monitoring was done by TLC on ALUGRAM SIL G/UV254 (Macherey-Nagel) employing UV detection.

A1.3. Synthesis and Compounds Characterization

4-(5-(3-hydroxyphenyl)thiophen-3-yl)-2-methylphenol (1): The detailed synthesis and compound characterization of the title compound is described in *Bey et al*[74]

3-(4-(4-hydroxyphenyl)thiophen-2-yl)phenol (2): The detailed synthesis and compound characterization of the title compound is described in *Bey et al*[75]

3-(5-(4-hydroxyphenyl)thiophen-3-yl)phenol (3): The detailed synthesis and compound characterization of the title compound is described in *Bey et al.*[75]

Method A. 1 equivalent of arylbromide dissolved in 10 ml of degassed THF was cooled to -78°C. 1.2 eq. of n-butyllithium was slowly added (T < -70°C) and the reaction was stirred for 60 min at -78°C. Then 1.1 eq. of tributyl borate added dropwise and the reaction was stirred for additional 90 min at -78°C. The mixture was allowed to warm to room temperature before 10 ml of degassed THF, 4 mol % $Pd(PPh_3)_4$, 1equivalent of 2-4-dibromothiophene and 2.5 eq. of Na_2CO_3 in 2.5 ml of water were added. The reaction was heated to reflux and the progress was monitored by TLC.

Method B. 1 equivalent of the bromothiophene derivative and 2.5 equivalents of Cs_2CO_3 were dissolved in a mixture of 8 ml of dimethylformamide and 1 ml of water. The mixture was purged with nitrogen for 30 min and 1 equivalent of the corresponding boronic acid and 0.05 equivalents of $Pd(PPh_3)_4$ were added. The reaction mixture was stirred at 100°C for 14 hours. The progress of the reaction was monitored by TLC. After completion the mixture was cooled to room temperature and 20 ml of brine was added. The aqueous layer was extracted with diethyl ether (4x). The combined organic layer was dried over magnesium sulfate and the solvent was removed under reduced pressure. The crude product was purified by flash column chromatography.

Method C. To a solution of methoxybenzene derivative (1 equivalent) in 10 ml of dry dichloromethane at -78°C, boron tribromide (1 M, 3 equivalents per methoxy function) was added dropwise and the mixture was allowed to warm to room temperature. The progress of the reaction was monitored by TLC. After completion, the reaction was stopped by addition of 10 ml of water.

4-bromo-2-(3-methoxyphenyl)thiophene: 1 g of 3-bromoanisole **(4iii)** was slowly added to a suspension of 0.156 g of magnesium in dry THF under nitrogen atmosphere. The mixture was carefully heated to start the reaction and stirring was continued for at room temperature for 3 hours. The solution was then cooled to -78°C and 1 eq. of 2,4-dibromothiophene and 4 mol % of $Pd(dppf)Cl_2$ were added. The mixture was stirred at room temperature for 18 hours. The reaction mixture was poured into water. The organic layer was washed several times with water, dried over magnesium sulfate and the solvent was removed under removed pressure. The crude product was purified using flash column chromatography eluting with hexane/ethyl acetate 30:1 to give 0.3 g (1.1 mmol, 20 %) of 4-bromo-2-(3-methoxyphenyl)thiophene as colorless solid.^{1}H NMR (500MHz ,DMSO-d_6) δ = 7.68 (d, *J* = 1.5 Hz, 1 H), 7.61 (d, *J* = 1.5 Hz, 1 H), 7.37 - 7.32 (m, 1 H), 7.24 - 7.21 (m, 2 H), 6.94 (ddd, *J* = 1.1, 2.3, 8.2 Hz, 1 H), 3.83 - 3.82 (s, 3 H); ^{13}C NMR (126MHz ,DMSO-d_6) δ = 159.8, 144.6, 133.8, 130.3, 126.1, 123.1, 117.7, 114.2, 110.6, 109.8, 55.2. Purity (FID): 98 %; t_R: 6.97 min; MS (EI), *m/z* $[M]^+$: 269.89, calc. 269.95.

4-(3-ethyl-4-methoxyphenyl)-2-(3-methoxyphenyl)thiophene (4i): 0.3 g (1.1 mmol) of 4-bromo-2-(3-methoxyphenyl)thiophene was dissolved in THF under nitrogen atmosphere. Then, 0.2 g (0.75 mmol) of (3-ethyl-4-methoxyphenyl)boronic acid **(4ii)**, 4 mol % of $Pd(PPh_3)_4$ and 2.5 eq. of Na_2CO_3 were added. The mixture was stirred under reflux and the reaction was monitored by TLC. After completion, the crude product was washed with water and brine. The aqueous layer was then extracted with ethyl acetate. The combined organic layer was dried over magnesium sulfate and the solvent was removed under reduced pressure. The product was purified by flash column chromatography eluting with hexane/ethyl acetate 20:1 to give 0.15 g (0.46 mmol, 61 %) of 4-(3-ethyl-4-methoxyphenyl)-2-(3-methoxyphenyl)thiophene as a slight yellow solid. ^{1}H NMR (500MHz ,CHLOROFORM-d) δ = 7.51 (d, *J* = 1.6 Hz, 1 H), 7.40 - 7.37 (m, 2 H), 7.27 (d, *J* = 7.9 Hz, 1 H), 7.24 (d, *J* = 1.6 Hz, 1 H), 7.23 - 7.21 (m, 1 H), 7.17 - 7.15 (m, 1 H), 6.85 - 6.80 (m, 2 H), 3.83 (s, 3 H), 3.83 (s, 3 H), 2.67 (q, *J* = 7.6 Hz, 2 H), 1.22 (t, *J* = 7.6 Hz, 3 H); ^{13}C NMR (126MHz ,CHLOROFORM-d) δ = 160.0, 156.9, 144.6, 143.1, 135.8, 133.0, 129.9, 128.4, 127.2, 124.7, 122.6, 118.5, 118.3, 113.1, 111.5, 110.4, 55.4, 55.3, 23.4, 14.2. Purity (FID): 98 %; t_R: 9.61 min; MS (EI), *m/z* $[M]^+$: 324.044, calc. 324.12.

2-ethyl-4-(5-(3-hydroxyphenyl)thiophen-3-yl)phenol (4): The title compound was prepared by reaction of of 4-(3-ethyl-4-methoxyphenyl)-2-(3-methoxyphenyl)thiophene **(4i)** (75 mg, 0.23 mmol) according to the method C. The crude product was purified by flash column chromatography eluting with hexane/ethyl acetate 10:1 to give 58 mg (0.195 mmol, 85 %) of 2-ethyl-4-(5-(3-hydroxyphenyl)thiophen-3-yl)phenol as a colorless solid. ^{1}H NMR (500MHz ,CHLOROFORM-d) δ = 7.49 (d, *J* = 1.3 Hz, 1 H), 7.37 (d, *J* = 2.2 Hz, 1 H), 7.31 (dd, *J* = 2.4, 8.4 Hz, 1 H), 7.25 - 7.23 (m, 2 H), 7.23 - 7.19 (m, 1 H), 7.10 (dd, *J* = 1.6, 2.5 Hz, 1 H), 6.78 (d, *J* = 8.2 Hz, 1 H), 6.75 (ddd, *J* = 1.6, 2.4, 7.6 Hz, 1 H), 2.67 (q, *J* = 7.6 Hz, 2 H), 1.27 (t, *J* = 7.9 Hz, 3 H); ^{13}C NMR (126MHz ,CHLOROFORM-d) δ = 155.9, 152.8, 144.2, 143.0, 136.0, 130.3, 130.2, 129.0, 127.5, 125.0, 122.6, 118.5, 118.5, 115.5, 114.6, 112.7, 23.1, 14.0. Purity (FID): 95 %; t_R: 9.85 min; MS (EI), *m/z* $[M]^+$: 295.92, calc. 296.09.

4-bromo-2-(4-methoxy-3-methylphenyl)thiophene: The title compound was prepared by reaction of 4-bromo-1-methoxy-2-methylbenzene **(5iii)** (1 g , 4.97 mmol) and 2-4-dibromothiophene (1.2 g, 4.97 mmol) according to the method A. The reaction was stopped by addition of 10 % citric acid. The organic layer was separated and the aqueous layer was extracted with ethyl acetate. The combined organic layer was dried and concentrated under reduced pressure. The crude product was purified by flash column chromatography eluting with hexane/ethyl acetate 30:1 to give 847 mg (3 mmol, 60 %) of 4-bromo-2-(4-methoxy-3-methylphenyl)thiophene as a colorless solid. ^{1}H NMR (500MHz, Methanol-d_4) δ = 7.28 (dd, *J* = 0.6, 8.5 Hz, 1 H), 7.27 - 7.25 (m, 1 H), 7.13 (d, *J* = 1.6 Hz, 1 H), 7.05 (d, *J* = 1.6 Hz, 1 H), 6.80 (d, *J* = 8.5 Hz, 1 H), 3.74 (s, 3 H), 2.11 (s, 3 H) ^{13}C NMR (126MHz, Methanol-d_4) δ = 159.5, 128.9, 128.3, 125.4, 125.4, 122.0, 111.4, 111.2, 55.9, 16.3. Purity (FID): 95 %; t_R: 7.340 min; MS (EI), *m/z* $[M]^+$: 283.886, calc. 283.97.

2-(4-methoxy-3-methylphenyl)-4-(3-methoxyphenyl)thiophene (5i): The title compound was prepared by reaction of 3-bromoanisole **(5ii)** (62 mg, 0.33 mmol) and 4-bromo-2-(4-methoxy-3-methylphenyl)thiophene (100 mg, 0.33 mmol) according to the method A. The crude product was washed with small portions of water. The organic layer was then dried over magnesium sulfate and the solvent was removed under reduced pressure. The crude product was purified by flash column chromatography eluting with hexane/ethyl acetate 20:1 to give 71 mg (0.23 mmol, 70 %) of 2-(4-methoxy-3-methylphenyl)-4-(3-methoxyphenyl)thiophene as a white solid which was directly used for the next step without further characterization other than GC-MS. Purity (FID): 90 %; t_R: 9.427 min; MS (EI), *m/z* $[M]^+$: 310.024, calc. 310.10.

4-(4-(3-hydroxyphenyl)thiophen-2-yl)-2-methylphenol (5): The title compound was prepared by reaction of 2-(4-methoxy-3-methylphenyl)-4-(3-methoxyphenyl)thiophene **(5i)** (70 mg, 0.23 mmol) according to the method C. The crude product was purified by column flash chromatography eluting with hexane/ethyl acetate 5:1 to give 35 mg (0.12 mmol, 50 %) of 4-(4-(3-hydroxyphenyl)thiophen-2-yl)-2-methylphenol as a white solid. ^{1}H NMR (500MHz ,DMSO-d_6) δ = 9.54 (s, 1 H), 9.45 (s, 1 H), 7.65 (d, *J* = 1.3 Hz, 1 H), 7.60 (d, *J* = 1.6 Hz, 1 H), 7.45 (d, *J* = 1.9 Hz, 1 H), 7.35 (dd, *J* = 2.2,

8.2 Hz, 1 H), 7.23 - 7.18 (m, 1 H), 7.18 - 7.15 (m, 1 H), 7.12 - 7.10 (m, 1 H), 6.82 (d, *J* = 8.2 Hz, 1 H), 6.72 (ddd, *J* = 1.1, 2.2, 7.8 Hz, 1 H), 2.17 (s, 3 H); ^{13}C NMR (126MHz ,DMSO-d_6) δ = 157.7, 155.5, 144.6, 142.3, 136.5, 129.7, 127.8, 124.7, 124.5, 124.0, 120.6, 118.5, 116.9, 115.0, 114.2, 112.8, 15.9. Purity (FID): 96 %; t_R: 10.27 min; MS (EI), *m/z* $[M]^+$: 281.91, calc. 282.07.

4-bromo-2-(3-ethyl-4-methoxyphenyl)thiophene: The title compound was prepared by reaction of 2,4-dibromothiophene (489 mg, 2 mmol) and (3-ethyl-4-methoxyphenyl)boronic acid **(6iii)** (400 mg, 2.2 mmol) according to the method B. The crude product was purified by flash column chromatography eluting with a mixture of hexane and dichloromethane (95:5) to give 505 mg (1.7 mmol, 84 %) of 4-bromo-2-(3-ethyl-4-methoxyphenyl)thiophene as colorless solid. ^{1}H NMR (500MHz, DMSO-d_6) δ = 7.48 (d, *J* = 1.6 Hz, 1 H), 7.40 - 7.35 (m, 2 H), 7.33 (d, *J* = 1.3 Hz, 1 H), 6.90 (d, *J* = 8.5 Hz, 1 H), 3.73 (s, 3 H), 2.51 (q, *J* = 7.5 Hz, 2 H), 1.07 (t, *J* = 7.4 Hz, 3 H); ^{13}C NMR (126MHz, DMSO-d_6) d = 157.2, 145.1, 132.4, 126.0, 124.9, 124.4, 124.2, 121.7, 111.1, 109.6, 55.5, 22.7, 14.1. Purity (FID): 98 %; t_R: 7.85 min; MS (EI), *m/z* $[M]^+$: 296.157, calc. 295.99.

2-(3-ethyl-4-methoxyphenyl)-4-(3-methoxyphenyl)thiophene (6i): The title compound was prepared by reaction of 4-bromo-2-(3-ethyl-4-methoxyphenyl)thiophene (150 mg, 0.5 mmol) and (3-methoxyphenyl)boronic acid **(6ii)** (70 mg, 0.5 mmol according to the method B. The crude product was purified by flash column chromatography eluting with a mixture of hexane and dichloromethane 5:1 to give 120 mg (0.37 mmol, 80 %) of 2-(3-ethyl-4-methoxyphenyl)-4-(3-methoxyphenyl)thiophene as a white solid. ^{1}H NMR (500MHz, DMSO-d_6) δ = 7.86 (d, *J* = 1.6 Hz, 1 H), 7.78 (d, *J* = 1.6 Hz, 1 H), 7.54 - 7.53 (m, 1 H), 7.53 - 7.51 (m, 1 H), 7.37 - 7.32 (m, 3 H), 7.00 (d, *J* = 9.1 Hz, 1 H), 6.88 (ddd, *J* = 1.7, 2.6, 7.3 Hz, 1 H), 3.83 (s, 3 H), 3.82 (s, 3 H), 2.62 (q, *J* = 7.6 Hz, 2 H), 1.18 (t, *J* = 7.6 Hz, 3 H); ^{13}C NMR (126MHz, DMSO-d_6) δ = 159.7, 156.8, 144.2, 142.1, 136.5, 132.2, 129.8, 126.1, 126.1, 124.2, 121.4, 119.4, 118.4, 112.7, 111.6, 111.0, 55.4, 55.1, 22.8, 14.3. Purity (FID): 98 %; t_R: 9.696 min; MS (EI), *m/z* $[M]^+$: 324.188, calc. 324.12.

2-ethyl-4-(4-(3-hydroxyphenyl)thiophen-2-yl)phenol (6): The title compound was prepared by reaction of 2-(3-ethyl-4-methoxyphenyl)-4-(3-methoxyphenyl)thiophene **(6i)** (110 mg) according to

the method C. The crude product was purified by flash column chromatography eluting with a mixture of hexane and dichloromethane 1:1 to give 88 mg (0.3 mmol, 88 %) of 2-ethyl-4-(4-(3-hydroxyphenyl)thiophen-2-yl)phenol as a white solid. ^{1}H NMR (500MHz, DMSO-d_6) δ = 9.45 (s, 1 H), 9.38 (br. s., 1 H), 7.59 (d, *J* = 1.3 Hz, 1 H), 7.53 (d, *J* = 1.6 Hz, 1 H), 7.36 (d, *J* = 2.5 Hz, 1 H), 7.27 (dd, *J* = 2.4, 8.4 Hz, 1 H), 7.15 - 7.11 (m, 1 H), 7.11 - 7.08 (m, 1 H), 7.05 - 7.03 (m, 1 H), 6.75 (d, *J* = 8.5 Hz, 1 H), 6.64 (ddd, *J* = 1.3, 2.4, 7.7 Hz, 1 H), 2.51 (q, *J* = 7.5 Hz, 2 H), 1.10 (t, *J* = 7.3 Hz, 3 H); ^{13}C NMR (126MHz, DMSO-d_6) δ = 157.7, 155.1, 144.7, 142.3, 136.5, 130.6, 129.7, 126.3, 124.9, 124.0, 120.6, 118.5, 116.9, 115.3, 114.2, 112.8, 22.8, 14.2. Purity (FID): 98 %; t_R: 10.129 min; MS (EI), *m/z* $[M]^+$: 296.128, calc. 296.09.

4-bromo-2-(4-methoxy-3-methylphenyl)thiophene: The title compound was prepared by reaction of 2,4-dibromothiophene (0.5 g, 2.2 mmol, 0.25 ml) and (4-methoxy-3-methylphenyl)boronic acid **(7iii)** (0.4 g, 2.4 mmol) according to method B. The resulting crude product was purified by flash column chromatography eluting with a mixture of hexane and dichloromethane (98:2) to give 0.5 g (1.8 mmol, 82 %) of 4-bromo-2-(4-methoxy-3-methylphenyl)thiophene as a colorless solid. ^{1}H NMR (500MHz, DMSO-d_6) δ = 7.56 (d, *J* = 1.3 Hz, 1 H), 7.48 - 7.45 (m, 2 H), 7.40 (d, *J* = 1.6 Hz, 1 H), 6.98 - 6.95 (m, 1 H), 3.81 (s, 3 H), 2.18 (s, 3 H); ^{13}C NMR (126MHz, DMSO-d_6) δ = 157.6, 145.0, 127.5, 126.4, 124.7, 124.4, 124.2, 121.7, 110.7, 109.6, 55.4, 15.9. Purity (FID): 99 %; t_R: 7.75 min; MS (EI), *m/z* $[M]^+$: 284.15, calc. 283.97.

2-(4-methoxy-3-methylphenyl)-4-(4-methoxyphenyl)thiophene (7i) : The title compound was prepared by reaction of 4-bromo-2-(4-methoxy-3-methylphenyl)thiophene **(7ii) (**150 mg, 0.48 mmol) and (4-methoxyphenyl)boronic acid (70 mg, 0.48 mmol) according to method B. The resulting crude product was purified by flash column chromatography eluting with a mixture of hexane and dichloromethane (5:1) to give 115 mg (0.37 mmol, 77 %) of 2-(4-methoxy-3-methylphenyl)-4-(4-methoxyphenyl)thiophene. ^{1}H NMR (500MHz, DMSO-d_6) δ = 7.78 (d, *J* = 1.6 Hz, 1 H), 7.72 - 7.70 (m, 1 H), 7.70 - 7.68 (m, 1 H), 7.60 (d, *J* = 1.6 Hz, 1 H), 7.54 - 7.52 (m, 1 H), 7.52 - 7.49 (m, 1 H), 7.00 - 6.96 (m, 3 H), 3.82 (s, 3 H), 3.79 (s, 3 H), 2.20 (s, 3 H); ^{13}C NMR

(126MHz, DMSO-d_6) δ = 158.5, 157.1, 144.0, 141.9, 127.9, 127.5, 127.1, 126.2, 126.0, 124.1, 121.1, 117.5, 114.2, 110.7, 55.4, 55.1, 16.0. Purity (FID): 95 %; t_R: 9.66 min; MS (EI), *m/z* $[M]^+$: 310.08, calc. 310.10.

4-(4-(4-hydroxyphenyl)thiophen-2-yl)-2-methylphenol (7): The title compound was prepared by reaction of 2-(4-methoxy-3-methylphenyl)-4-(4-methoxyphenyl)thiophene **(7i)** according to method C. The mixture was extracted with dichloromethane (4x) and the combined organic layer was dried over magnesium sulfate. The solvent was removed under reduced pressure and the crude product was purified by flash column chromatography eluting with a mixture of hexane and dichloromethane (1:1) to give 81 mg (0.29 mmol, 89 %) of 4-(4-(4-hydroxyphenyl)thiophen-2-yl)-2-methylphenol as a white solid. ^{1}H NMR (500MHz, DMSO-d_6) δ = 9.53 (s, 1 H), 9.49 (s, 1 H), 7.64 (d, *J* = 1.6 Hz, 1 H), 7.57 - 7.56 (m, 1 H), 7.56 - 7.55 (m, 1 H), 7.46 (d, *J* = 1.6 Hz, 1 H), 7.44 - 7.43 (m, 1 H), 7.34 (ddd, *J* = 0.6, 2.8, 8.2 Hz, 1 H), 6.83 - 6.81 (m, 1 H), 6.81 - 6.80 (m, 1 H), 6.80 - 6.79 (m, 1 H), 2.17 (s, 3 H); ^{13}C NMR (126MHz, DMSO-d_6) d = 156.7, 155.4, 144.4, 142.3, 127.8, 127.1, 126.5, 124.9, 124.5, 123.9, 120.4, 116.2, 115.5, 115.0, 15.9. Purity (FID): 97 %; t_R: 10.26 min; MS (EI), *m/z* $[M]^+$: 282.199, calc. 282.07.

2,4-bis(4-methoxy-3-methylphenyl)thiophene (8i): The title compound was prepared by reaction of 4-bromo-2-methylanisole **(8iii)** (2 g, 9.94 mmol) and 2,4-dibromothiophene (1.2 g, 4.97 mmol) according to method A. The reaction was stopped and the crude mixture was washed with saturated NaCl solution. The aqueous layer was extracted with ethyl acetate (4x) and the combined organic layer was dried over magnesium sulfate. The solvent was removed under reduced pressure and the resulting crude oil was purified by flash column chromatography eluting with hexane/ethyl acetate 30:1 to give a 0.8 g (2.47 mmol) of 2,4-bis(4-methoxy-3-methylphenyl)thiophene as a white solid. ^{1}H NMR (500MHz, DMSO-d_6) δ = 7.81 - 7.74 (m, 1 H), 7.65 - 7.48 (m, 5 H), 7.02 - 6.90 (m, 2 H), 3.81 (s, 6 H), 2.21 (s, 6 H); ^{13}C NMR (126MHz, DMSO-d_6) δ = 157.1, 156.7, 143.9, 142.1, 128.2, 127.5, 127.4, 126.2, 126.1, 125.8, 124.5, 124.1, 121.1, 117.2, 110.7, 110.4, 55.4, 55.3, 16.1, 16.0. Purity (FID): 98 %; t_R: 9.55 min; MS (EI), *m/z* $[M]^+$: 324.04, calc. 324.12.

4,4'-(thiophene-2,4-diyl)bis(2-methylphenol) (8): 100 mg (0.3 mmol) of (2,4-bis(4-methoxy-3-methylphenyl)thiophene **(8i)** and 50 eq. of pyridinium hydrochloride were added to a microwave glass vial and heated to 190°C for 2 hours. Then the melt was cooled to room temperature and dissolved in 20 ml of 3 N HCl. The aqueous layer was thoroughly extracted with diethyl ether (5x) and the combined organic layer was washed with saturated $NaHCO_3$. The organic layer was separated and dried over magnesium sulfate. The solvent was removed under reduced pressure and the crude product was purified by flash column chromatography eluting with hexane/ethyl acetate 5:1 to give 62 mg (0.21 mmol, 70 %) of 4,4'-(thiophene-2,4-diyl)bis(2-methylphenol) as colorless solid. ^{1}H NMR (500MHz, DMSO-d_6) δ = 7.63 (d, *J* = 1.6 Hz, 1 H), 7.48 - 7.46 (m, 1 H), 7.44 - 7.43 (m, 2 H), 7.37 (ddd, *J* = 0.6, 2.5, 8.2 Hz, 1 H), 7.33 (ddd, *J* = 0.6, 1.9, 8.2 Hz, 1 H), 6.81 (d, *J* = 6.3 Hz, 1 H), 6.80 (d, *J* = 6.6 Hz, 1 H), 2.17 (s, 6 H); ^{13}C NMR (126MHz, DMSO-d_6) δ = 155.4, 154.8, 144.3, 142.5, 128.4, 127.7, 126.3, 124.9, 124.5, 124.4, 124.1, 123.9, 120.5, 116.0, 115.0, 114.8, 16.0, 15.9. Purity (FID): 99 %; t_R: 9.94 min; MS (EI), *m/z* $[M]^+$: 296.0, calc. 296.09.

(6-hydroxybenzo[b]thiophen-2-yl)(3-hydroxyphenyl)methanone (9): The detailed synthesis and compound characterization is described in Miralinaghi *et al.*[76]

(6-hydroxy-3-methylbenzo[b]thiophen-2-yl)(3-hydroxyphenyl)methanone (10): The detailed synthesis and compound characterization is described in Miralinaghi *et al.* [76]

(5-hydroxybenzo[b]thiophen-2-yl)(3-hydroxyphenyl)methanone (11): The detailed synthesis and compound characterization is described in Miralinaghi *et al.* [76]

(5-hydroxybenzo[b]thiophen-2-yl)(4-hydroxyphenyl)methanone (12): The detailed synthesis and compound characterization is described in Miralinaghi *et al.* [76]

(2-fluoro-5-hydroxyphenyl)(5-hydroxybenzo[b]thiophen-2-yl)methanone (13): The detailed synthesis and compound characterization is described in Miralinaghi *et al.*[76]

(4-fluoro-3-hydroxyphenyl)(5-hydroxybenzo[b]thiophen-2-yl)methanone (14): The detailed synthesis and compound characterization is described in Miralinaghi *et al.*[76]

3-(5-hydroxybenzo[b]thiophene-2-carbonyl)benzonitrile (15): The detailed synthesis and compound characterization is described in Miralinaghi *et al.*[76]

3,3'-(thiophene-2,4-diyl)dipyridine (16): The detailed synthesis and compound characterization of the title compound is described in Schmitt et al.[77]

4-(5-(pyridin-3-yl)thiophen-3-yl)isoquinoline (17): The detailed synthesis and compound characterization of the title compound is described in Schmitt et al.[77]

3-(5-(pyridin-3-yl)thiophen-3-yl)quinoline (18): The detailed synthesis and compound characterization of the title compound is described in Schmitt et al.[77]

4-(4-(pyridin-3-yl)thiophen-2-yl)isoquinoline (19): The detailed synthesis and compound characterization of the title compound is described in Schmitt et al.[77]

A2. Biology

A2.1. Kinase assay

Dyrk1A reaction was performed in a reaction buffer containing 50 mM Tris/HCl, pH 7.4, 0.1 mM EGTA, 0.5 mM DTT, 10 mM $MgCl_2$, 10 µM or 100 µM ATP (as indicated) and 0.33 µM [γ-^{32}ATP] as well as 100 µM Woodtide (KKISGRLSPIMTEQ-NH_2). The kinase reactions were performed at 30 °C for 15 min and terminated by spotting 5 µL of the reaction mixture onto a P81 phosphocellulose membrane (Whatman). The membrane was washed four times with 0.3 % phosphoric acid and one time with acetone and dried. The dry membrane was exposed in a cassette to a Phosphor Screen Imaging Plate (FujiFilm) and the signals detected by scanning of the imaging plate in a Fuji FLA-3000 PhosphoImager. The spots were quantified using AIDA software (Raytest, Version 3.52) to determine the activities of the kinases in the assay reactions. For IC_{50} determinations, eight concentrations of each compound were used in triplicates, and the percentage of inhibition at 10 µM was also calculated from the average of triplicate values. IC_{50} values were

calculated by fitting the data with Origin Pro 8.6 (OriginLabs). The IC_{50} values given in the Tables are representative of at least two independent determinations.

A2.2. Aβ40 peptide aggregation assay

The in vitro inhibition of $A\beta_{40}$ aggregation was determined following a previously reported thioflavin T (ThT) fluorescence–based method involving the use of hexafluoroisopropanol (HFIP) as aggregation enhancer[78]. To obtain batches of $A\beta_{1-40}$ free from preaggregates, commercial peptides (purity >95%; EzBiolab, Carmel, USA) were dissolved in HFIP, lyophilized and stored at -20 °C. The solution of ThT (25 µM) used for fluorimetric measurements was prepared in 0.025 M phosphate buffer, pH 6.0, filtered through 0.45 µm nylon filters and stored at 4 °C. Compounds were first tested at 100 µM; test samples were co-incubated with 30 µM Aβ peptide in phosphate buffered saline (PBS; 0.01 M phosphate buffer, 0,1 M NaCl, pH 7.4) also containing 2% HFIP and 10% (v/v) DMSO as co-solvents. Blank samples were prepared for each concentration, devoid of peptide, and their fluorescence value subtracted from the corresponding fluorescence values of the co-incubated samples. As the control, a sample of peptide was incubated in the same PBS/2% HFIP/10% DMSO buffer, without inhibitor. Incubations were run in triplicate at 25 °C for 2 h. Fluorimetric measurements were performed in a 700 µL cuvette with a Perkin–Elmer LS55 spectrofluorimeter, using FLWinlab software. 470 µL of the ThT solution were mixed with 30 µL of sample, and the resulting fluorescence measured with parameters set as follows: excitation at 440 nm (slit 5 nm); emission at 485 nm (slit 10 nm); integration time 2 s. Biological activity was determined as percent of inhibitory activity V_i for each concentration, according to the formula:

$$V_i = 100 - [(F_i - F_b)/F_0] \times 100$$

where F_i is the fluorescence value of the sample, F_b its blank value, and F_0 the fluorescence value of Aβ control (already subtracted of its blank). For the most active inhibitors (≥ 80% Aβ aggregation inhibition), IC_{50} values were determined by testing in duplicate 5–7 concentrations, ranging from 200 to 0.01 µM. Statistics from three independent experiments were calculated within GraphPad Prism® v. 5 software; data are reported in Tables 1, 2, S2 and S3.

A2.3. Development of a cell–based Dyrk1A-tau phosphorylation assay

Plasmid. The pEGFP-htau352wt plasmid encoding for full length human tau protein fused to N-terminal enhanced green fluorescent protein (EGFP) was kindly provided by Prof. Dr. Roland Brandt, University Osnabrück, and originally constructed by J. Eidenmüller in his group. Before it was used for cell transfections, the plasmid was analysed by digestion using the restriction enzyme NheI and sequenced by GATC Biotech service, Germany.

Antibodies. For the western blot, the primary antibodies rabbit anti-phospho-Threonine 212-tau (pT212, Life Technologies GmbH, cat no. 444-740G) and mouse anti-GFP antibody (LifeTechnologies GmbH, Cat n. 33-2600) were used. The same pT212 antibody had been previously used by Dan Li et al.[79] who showed that it was specifically detecting the Dyrk1A–catalyzed phosphorylation (see Figure 5C therein). As secondary antibodies we used goat anti-mouse IgG IR-Dye 800 CW (LI-COR Biosciences, cat n. 926-32210) and goat anti-rabbit IgG IR-Dye 680 RD (LI-COR Biosciences Cat n. 926-68071).

Generation of a stable double-transfected HEK293-tau-Dyrk1A cell line. In the brains of Alzheimer´s disease patients with Down Syndrome, Dyrk1A is overexpressed and physically associated with tau fibrils[80], which is thought to favor strong phosphorylation of the tau protein specifically by Dyrk1A. To mimic this setting in a cellular assay for our compounds, we aimed at overexpressing both proteins. To this end, a plasmid coding for EGFP-tau was transfected into a human embryonic kidney cell line (HEK293-Dyrk1A) that had been modified with a stably integrated pEGFP-DYRK1A expression vector under control of a tetracycline–responsive promoter (kind gift from Prof. Dr. Walter Becker, Institute of Pharmacology and Toxicology, RWTH Aachen). The cell line was grown in DMEM with 10% fetal calf serum (FCS) and 1% penicillin-streptomycin mix (PenStrep). For the transfection, the cells were seeded in 12-well plates at a density of $0.7 \cdot 10^6$ cells per ml. To minimize cell detachment during the transfection and later during the assays, the plates were coated before with poly-L-lysine (100µg/ml in water). The transfection was performed using polyethyleneimine (PEI) as a DNA-complexing agent (Cat. No. 23966-2, Polysciences Inc., USA). We optimized the ratio of DNA:PEI (1:3) and also the amount of DNA

(1.2 µg). The best transfection condition was identified by measuring in each well the intensity of EGFP fluorescence corresponding to the EGFP-tau fusion protein in the absence of tetracycline in an Omega Polastar plate reader (BMG Labtech, Germany), using the setting for fluorescein detection (excitation 485 nm, emission 520 nm). The DNA/PEI complex was prepared in DMEM + 0.1% FCS, vortexted and added to the cells. After 4–5 hours in an incubator (37 °C, 5 % CO_2), the transfection medium was supplemented by FCS (final concentration of 10%), and 1% PenStrep, and the incubation continued overnight. The next day, the medium was exchanged by fresh full medium containing geneticin (G418, 800µg/ml) as selection agent. The generation of a stable double-transfected EFGP-Dyrk1A/EGFP-hTau HEK293 cell line proceeded over two weeks by exchanging the old medium by fresh selection medium each time when the old medium started to turn yellow. After two weeks, more than 95% of the cells showed green fluorescence in the absence of tetracycline, indicative of resistant clones expressing EFGP-tau.

A2.4. Figure S1

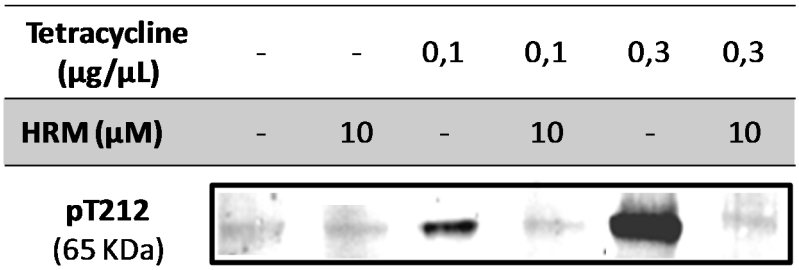

The tau protein phosphorylation at threonine 212 in the HEK293-tau-Dyrk1A cells is dependent on Dyrk1A and can be fully suppressed by harmine. The expression of Dyrk1A is induced upon addition of the transcription enhancer tetracycline in a concentration–dependent manner, as seen by the increase in tau phosphorylation (pT212) (detected using the anti-phospho-tau-Thr212 antibody described under "Antibodies**"**). In the absence of the inducer tetracycline, only a weak background signal is observed. The phospho-tau-Thr212 signal can be completely abolished by addition of the selective Dyrk1A inhibitor harmine (HRM) to the cell medium. These results confirm that under the experimental conditions, Thr212 on the overexpressed tau protein is specifically phosphorylated by Dyrk1A, as previously described by Kimura et al.[81]

3.2. Publication B: Systematic diversification of benzylidene heterocycles yields novel inhibitor scaffolds selective for Dyrk1A, Clk1 and CK2

Marica Mariano, Rolf W. Hartmann, Matthias Engel

European Journal of Medicinal Chemistry 2016 vol: 112 pp: 209-216;
http://dx.doi.org/10.1016/j.ejmech.2016.02.017

European Journal of Medicinal Chemistry 112 (2016) 209–216

Contents lists available at ScienceDirect

European Journal of Medicinal Chemistry

journal homepage: http://www.elsevier.com/locate/ejmech

Research paper

Systematic diversification of benzylidene heterocycles yields novel inhibitor scaffolds selective for Dyrk1A, Clk1 and CK2

Marica Mariano [a], Rolf W. Hartmann [a, b], Matthias Engel [a, *]

[a] Department of Pharmaceutical and Medicinal Chemistry, Saarland University, Saarbrücken, Germany
[b] Helmholtz Institute for Pharmaceutical Research Saarland (HIPS), Campus C2-3, D 66123 Saarbrücken, Germany

ARTICLE INFO

Article history:
Received 14 December 2015
Received in revised form
4 February 2016
Accepted 5 February 2016
Available online 9 February 2016

Keywords:
Dyrk1A
PI3 kinase
Alzheimer
Glioma
Multi-targeted inhibitor

ABSTRACT

The dual-specificity tyrosine-regulated kinase 1A (Dyrk1A) has gathered much interest as a pharmacological target in Alzheimer's disease (AD), but it plays a role in malignant brain tumors as well. As both diseases are multi-factorial, further protein kinases, such as Clk1 and CK2, were proposed to contribute to the pathogenesis. We designed a new class of α-benzylidene−γ-butyrolactone inhibitors that showed low micromolar potencies against Dyrk1A and/or Clk1 and a good selectivity profile among the most frequently reported off-target kinases. A systematic replacement of the heterocyclic moiety gave access to further inhibitor classes with interesting selectivity profiles, demonstrating that the benzylidene heterocycles provide a versatile tool box for developing inhibitors of the CMGC kinase family members Dyr1A/1B, Clk1/4 and CK2. Efficacy for the inhibition of Dyrk1A−mediated tau phosphorylation was demonstrated in a cell-based assay. Multi-targeted but not non-specific kinase inhibitors were also obtained, that co-inhibited the lipid kinases PI3Kα/γ. These compounds were shown to inhibit the proliferation of U87MG cells in the low micromolar range. Based on the molecular properties, the inhibitors described here hold promise for CNS activity.

1. Introduction

The dual-specificity tyrosine-regulated kinases (Dyrk) and CDC2-like kinases (Clk) both belong to the CMGC branch of the kinome and share the ability to phosphorylate tyrosine as well as serine/threonine residues; however, only the activating autophosphorylation occurs actually at tyrosine.

The Dyrk1A isoform is expressed ubiquitously while the most closely related homolog, Dyrk1B, is mainly found in testes and muscle tissue [1]. In the last decade, Dyrk1A, but not Dyrk1B, received much attention due to its implication in the development of Down Syndrome−related and sporadic Alzheimer's disease (AD) [2,3], where it promotes neurodegeneration by hyperphosphorylating the microtubule-associated protein tau [4]. Furthermore, Dyrk1A was also shown to phosphorylate amyloid precursor protein (APP) and presenilin-1, a key component of the γ-secretase complex, thereby accelerating the formation of neurotoxic Aβ peptides [5].

Recently, Dyrk1A was also proposed as a new target in glioblastoma [6]. Glioma are among the most malignant types of solid tumors and survival rates for patients are still very poor: less than 5% of patients survive for 5 years after having been diagnosed with glioblastoma multiforme, the most aggressive subtype [7]. Hence, more effective therapeutic agents are urgently needed. Of note, Dyrk1A was reported to act as an enhancer of receptor tyrosine kinase signaling; known examples include FGFR [8] and EGFR [6,9]. Pozo and coworkers found Dyrk1A to be strongly overexpressed in glioblastoma, paralleling EGFR expression [6]. Dyrk1A prevents endocytosis−mediated degradation of EGFR by a mechanism that requires phosphorylation of the EGFR signaling modulator Sprouty2 [9]. Moreover, Dyrk1A−catalyzed phosphorylation of FOXO (also called FKHR) was shown to promote nuclear exclusion, thus maintaining cell cycle progression and suppressing the activation of pro-apoptotic genes [10,11]. Compared with healthy tissue, the mRNA of Dyrk1A, but not of the homologous kinases Dyrk1B or Dyrk2, was strongly overexpressed in glioblastoma, medulloblastoma, astrocytoma and oligodendroglioma (analyzed using the Oncomine portal, www.oncomine.org) [12,13]. This suggests that Dyrk1A could be an interesting anti-cancer target in EGFR−overexpressing tumors.

The Clk1 and -4 isoforms do not only share a strong structural

* Corresponding author.
E-mail address: ma.engel@mx.uni-saarland.de (M. Engel).

http://dx.doi.org/10.1016/j.ejmech.2016.02.017
0223-5234/

homology with the Dyrk family but also some physiological functions: Both are involved in the regulation of alternative mRNA splicing through the phosphorylation of serine/arginine-rich (SR) proteins, including AF2/ASF, SC35 and SRp55 [14–18].

SR proteins mostly promote the inclusion of exons *via* binding to exonic splicing enhancers, and their activity is mainly regulated by multiple phosphorylations [19,20]. Upon dysregulation of the kinase activities in the case of Alzheimer's disease, the alternative splicing of tau is influenced, which results in a pathogenic imbalance between 3R-tau and 4R-tau isoforms through skipping of exon 10 [17]. Thus, co-inhibition of Dyrk and Clk kinases might efficiently correct the tau splicing isoform imbalance. Indeed, we could show that dual inhibitors of Dyr1A and Clk1 are more efficient pre-mRNA splicing modulators than selective Dyrk1A or Clk1 inhibitors [21]. Furthermore, Leucettine L41, a dual Dyrk1A/Clk1 inhibitor [22] was recently reported to prevent memory impairments and neurotoxicity induced by oligomeric $A\beta_{25-35}$ peptide administration in mice [23].

However, whether the benefit of such multi-targeted approaches outweighs the potential accumulation of side effects related to target inhibitions, will only be seen in long term *in vivo*-studies. Therefore, a selective inhibitor of Dyrk1A is a primary goal of drug development efforts, in particular with respect to Down Syndrome–related neurodegeneration, for which the overexpression of Dyrk1A is a main cause [24].

Rather selective Dyrk1A inhibitors have been described previously, such as harmine, INDY, KH-CB19, Leucettines and pyridinylthiophenes [25–29], however, they still inhibited Clk1/4 with equal potency. Recently, Falke et al. [30] reported some 10-iodo-11*H*-indolo[3,2-c]quinoline-6-carboxylic acid derivatives as highly selective inhibitors of Dyrk1A, but the carboxylic acid function may impair CNS penetration [31].

From a medicinal chemistry point of view, it is advantageous that Dyrk1A can potently be inhibited by very small molecules with molecular weights below 300 g/mol [25,26], suggesting that the binding site can adapt to small ligands. This property contributes to the attractiveness of Dyrk1A as a target for CNS diseases, because as a rule of thumb, the smaller the inhibitor, the higher are the chances to pass the blood brain barrier [31].

In the following, we describe the development of small benzylidene derivatives, which cover a broad range of selectivity and potency profiles, depending on the combined heterocycles.

2. Results and discussion

2.1. Design strategy and synthesis

Two of the most important factors that determine the CNS permeability of small molecules are the molecular mass, which showed a median of 305 Da in a thorough analysis of CNS drugs, and the number of H-bond donors, which should be ≤ 1 [31]. Therefore, our design of new Dyrk1A inhibitors was based on previously published inhibitors that fulfilled the following criteria: i) low mass, ii) no requirement for an H-bond donor contacting the hinge region, and iii) good potency in cellular systems. One of the most compact but yet potent and orally available inhibitor of Dyrk1A is the β-carboline alkaloid harmine (Fig. 1). *In vitro* studies showed good activity against Dyrk1A, particularly in cells, and a slight selectivity toward other members of the Dyrk family. However, it also exerts several adverse CNS effects due to its potent monoaminoxidase-A inhibition [32]. The benzothiazole TG003 is a synthetic inhibitor of Dyrk1A which was identified in a high-throughput screening [26]. This compound is able to block the negative regulatory activity of Dyrk1A in the NFAT pathway. Unfortunately, its potency is not sufficient for *in vivo* applications (cell-free IC_{50} for Dyrk1A: 0.8 μM) [21]. Another rather small compound with inhibitory activity against Dyrks and Clk1 is leucettamine B, which was isolated from a marine sponge [22].

A superimposition of harmine, INDY (the 5-hydroxy derivative of TG003, Fig. 1) and Leucettine L41 (a synthetic derivative of Leucettamine B [22]) as bound to Dyrk1A in published cocrystal structures revealed some common pharmacophoric features, which were used as starting points for the design of new Dyrk1A inhibitors (Fig. 2). Obviously, two H-bond acceptor (HBA) functions at the molecule ends and an aromatic system connected to one HBA were sufficient for strong binding affinity to the ATP binding cleft of Dyrk1A. The smallest possible linker to connect two suitable moieties, which preserved the planar overall geometry, was a methine bridge. This was already present in the Leucettamine derivatives (Fig. 1), in which the 2-aminoimidazolone carbonyl oxygen was functioning as HBA for Lys188. Employing Claisen–Schmidt chemistry, a large variety of different HBA ring combinations was accessible, which were expected to have a strong impact on the potency and selectivity profile due to differences in lipophilicity, acidity and molecular electrostatic potentials. Since a systematic study of the most straightforward combinations had not been done before, we decided to synthesize and explore a set of new scaffolds exhibiting the minimum pharmacophor features according to Fig. 2. In order to maintain a good probability of CNS penetration, the molecular weight was kept below 280 g/mol.

2.2. Structure-activity relationships (SAR)

First, several γ-butyrolactone moieties were combined with different benzylidene units, and the influence on potency and selectivity was tested. The kinases chosen for the primary screening panel were (i) frequently reported off-targets for diverse classes of Dyrk1A inhibitors (first five kinases in Tables 1 and 2, all from the CMGC family) [21], and (ii) kinases from more distant families (last two in Tables 1 and 2). In this way, conclusive selectivity data were immediately obtained.

The first synthesized compound **1** was moderately active as Dyrk1A inhibitor (Table 1) and quite selective against our panel of kinases. It did not appreciably inhibit Dyrk2 and showed weaker activity even against Dyrk1B. In order to increase its activity and selectivity, we decided to rigidify the *p*-methoxy-benzene into a chromane (compound **2**). This non-planar, partially saturated system was favorable for the inhibition of Dyrk1A but less well tolerated by Dyrk1B, resulting in increased selectivity towards the latter isoform. This modification may take advantage – at least indirectly – of the only difference between the ATP binding pockets of Dyrk1A and Dyrk1B, which is the exchange of the linear side chain of hinge region residue Met240 in Dyrk1A by a branched leucine in Dyrk1B. Although pointing away from the ATP pocket, the Leu side chain might restrict the flexibility of some β-sheet residues that form the lid of the pocket to adapt to sterically more demanding cyclic moieties. An extension of the lactone ring to a six-membered cycle (**3**) or by a methyl substituent (**4**) confirmed the trend that the ATP-binding pocket of Dyrk1A accepts more bulky structures than that of Dyrk1B, as indicated by the 9 times higher potency of **4** for Dyrk1A. Consistent with this finding, the less bulky coumaran moiety in **5** caused a drop of the selectivity towards Dyrk1B (compared with **2**) – and particularly towards Dyrk2 –, while the inhibition of Dyrk1A was conserved. Reintroducing a methyl substituent in **6** not only recovered the selectivity toward Dyrk1B but markedly increased the potency toward Dyrk1A (IC_{50}: 0.17 μM). Thus, the potency was similar to that of harmine but the selectivity towards Dyrk1B was considerably improved, reaching a remarkable selectivity factor of 15.5 (cf. Table 1). The 5-methyl substituent in **6** increased the selectivity in general, which

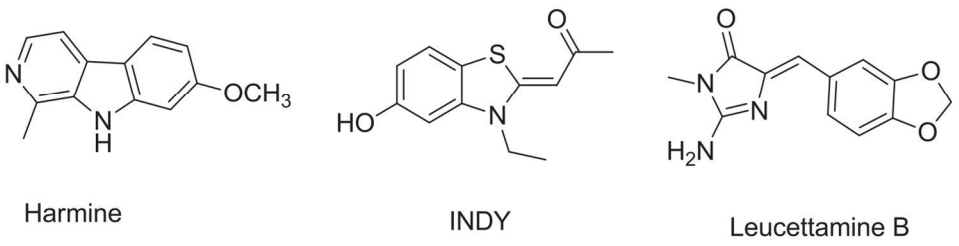

Fig. 1. 2D structures of harmine, INDY and Leucettamine B.

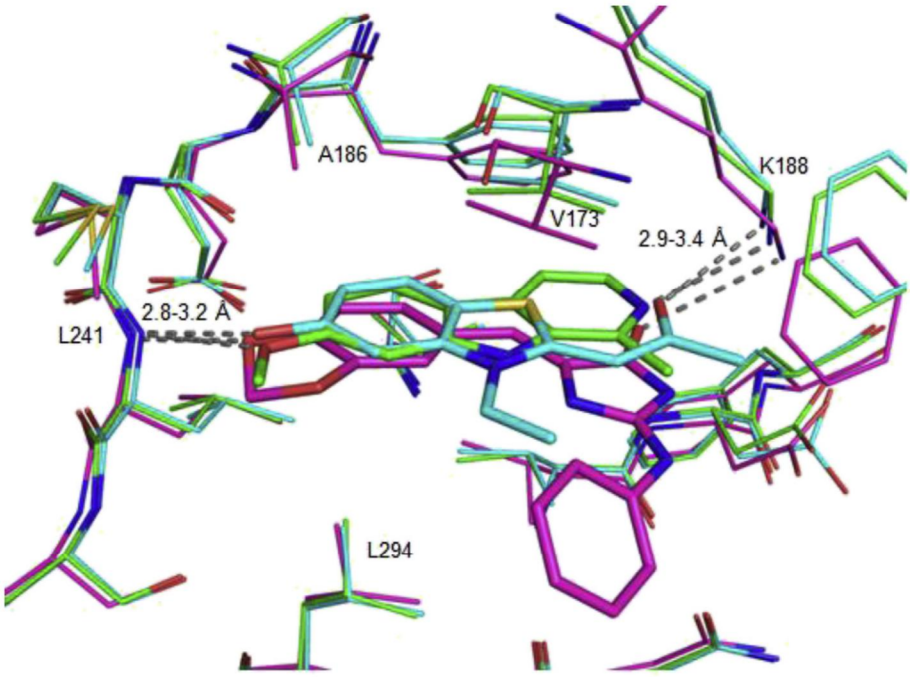

Fig. 2. Superimposition of harmine (green), INDY (cyan) and Leucettine L41 (magenta) cocrystallized with Dyrk1A (PDB codes 3ANR, 3ANQ and 4AZE, respectively). All ligands are bound in the ATP-binding cleft *via* two H-bonds, formed with Leu241-NH at the hinge region and Lys188 (indicated by the grey dashed lines). The measured ranges of the N–O distances are given in Å. Additional contacts comprise van der Waals-interactions with the side chains of Ala186, Val173 and Leu294, which mainly involve the left aromatic rings. (For interpretation of the references to colour in this figure legend, the reader is referred to the web version of this article.)

became particularly evident from the negligible inhibition of the atypical kinase haspin by **6** (43% at 5 μM) compared to **7** (75% at 5 μM) (Table 3). Haspin was reported as a notorious off-target even for some of the most selective Dyrk1A inhibitors, including TG003 and harmine [27,33]. An extended selectivity profiling for compound **6** revealed that besides Dyrk1A and Clk1, only Clk4 was affected in our panel (Table S1, Supplementary Material). The IC_{50} for Clk4 as determined by the LanthaScreen® Kinase Binding Assay was 32 nM. However, this assay is based on the competition of the test compound with an Alexa Fluor®–conjugated tracer compound for binding to the ATP site, thus the IC_{50} is difficult to compare with IC_{50}s obtained by peptide phosphorylation assays. The next most strongly inhibited kinase was PI3Kα, with an IC_{50} of 0.65 μM (determined by a substrate phosphorylation assay in the presence of 100 μM ATP). The PI3 lipid kinases had been included in the screening panel for reasons stated below.

Because **6** still significantly inhibited Clk1 (and probably Clk4), we tried to further optimize the selectivity by modifying the benzylidene part of the molecule. Our strategy of including a second oxygen atom was unsuccessful as both potency and selectivity decreased (cf. compounds **8** and **9**). Subsequently, we decided to replace the coumaran of compound **5** by a benzothiazole moiety, leading to a potent inhibitor (**7**) with dual selectivity for Dyrk1A and Clk1. Surprisingly, our attempt to further increase the potency and selectivity for Dyrk1A by introducing a methyl on the γ-butyrolactone ring failed (compound **10**). Probably the methyl group forced the compound into a slightly different binding orientation, which negatively affected the H-bond interaction between the benzothiazole nitrogen and the hinge region. The distinct behavior of compound **6** might be explained by the different spatial orientation of the oxygen lone pairs. However, the affinity to Clk1 was less affected, thus rendering compound **10** moderately selective for Clk1.

Our second set of compounds (Table 2) was designed by modifying the lactone part of the molecule in order to establish stronger interactions in the binding site and thus boost the potency. For the first compounds, we decided to use again 4-methoxybenzaldehyde as coupling partner, since the plain methoxy substituent on the benzene had conferred the highest selectivity towards Clk1 so far (cf. compounds **1** and **3** in Table 1). The first designed compound **11** was not active, suggesting that the combination of two carbonyls in the pyrrolidinedione was too polar for the binding site (Table 2). Similarly, the hydantoin derivative **12** exhibited only a weak inhibitory activity toward Dyrk1A.

Table 1
Inhibitory activity of α-benzylidene-γ-butyrolactone derivatives against Dyrk1A and selectivity profiling against a panel of selected kinases.

#	Structure	D1A	D1B	D2	CK2	Clk1	EGFR	PKCβ
		(IC_{50}, μM)[a]						
1	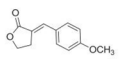	1.81	3.80	>10	n.i.	>10	n.i.	n.i.
2	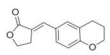	0.93	6.70	>10	>10	3.90	>10	n.i.
3	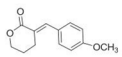	1.10	5.80	>10	>10	7.52	n.i.	n.i.
4	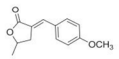	1.20	10.5	n.i.	>10	4.37	n.d.	n.i.
5	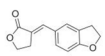	0.96	2.17	0.82	>10	>10	>10	n.i.
6	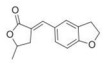	0.17	2.64	0.43	>10	>10	>10	n.i.
7	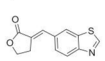	0.13	1.05	0.06	>10	>10	>10	n.i.
8	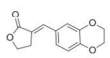	0.88	4.29	2.04	>10	>10	>10	n.i.
9	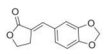	0.60	2.63	0.99	>10	>10	>10	n.i.
10	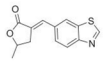	1.08	1.68	>10	>10	0.17	>10	n.i.
Hrm	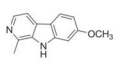	0.13	0.18	3.00	n.d.	0.22	n.d.	n.d.

[a] S.D. ≤ 18%, [ATP] = 100 μM; D1A = Dyrk1A, D1B = Dyrk1B, D2 = Dyrk2; Hrm = Harmine; n.i., no inhibition; n.d., not determined.

Table 2
Inhibitory activity of benzylidene thioxothiazolidinone–based derivatives against Dyrk1A and selectivity profiling against a panel of selected kinases.

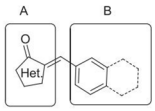

#	A	B	D1A	D1B	D2	CK2	Clk1	EGFR	PKCβ
			(IC_{50}, μM)[a]						
11			>10	n.d.	n.d.	n.d.	n.d.	n.d.	n.d.
12			6.4	>10	n.i.	n.i.	10	n.d.	n.i.
13			1.3	5.2	9.2	0.17	3.6	n.i.	n.i.
14			0.25	1.5	>10	0.22	5.7	n.i.	n.i.
15			0.1	0.3	1.0	0.1	0.5	>10	>10
16			0.04	0.07	0.20	0.06	0.1	>10	9.2
17			0.02	0.06	0.06	0.04	0.2	>10	>10
18			0.7	0.9	1.5	2.4	0.02	>10	>10
AS			0.03	0.08	0.1	0.02	0.07	>10	n.i.

[a] S.D. ≤ 18%, [ATP] = 100 μM; D1A = Dyrk1A, D1B = Dyrk1B, D2 = Dyrk2, AS = AS605240; n.d., not determined; n.i., no inhibition.

Nonetheless, when the NH heteroatom unit was replaced by sulfur leading to the thiazolidinedione ring, appreciable inhibition was observed (compound **13**). Interestingly, **13** was mainly selective for CK2, exhibiting an IC_{50} of 0.17 μM. Since CK2 is known to preferably bind acidic compounds in the ATP-binding site [34,35], the relatively low pKa value of the thiazolidinedione group (reported to be 6.14 for the unsubstituted analog [36]) may account for this selectivity. Indeed, the NH acidity of the CK2-inactive analog **12** is considerably weaker (pka value: 8.9 [37]). We further explored the effects of sulfur atoms by incorporating the rhodanine system (2-thioxothiazolidin-4-one). This resulted in 5-fold increase in the Dyrk1A inhibitory potency (compare compound **14** with **13**), while the CK2 inhibition remained unchanged. This was again in accordance with the acidic pka of **14**, which was previously reported to be 5.8 [38]. Thus, **14** was a dual inhibitor of Dyrk1A and CK2; of note, the overall selectivity did not drop, even though the rhodanine system was frequently present in hits identified for many different enzymes [39]. In particular, the high selectivity (23-fold) of **14** over Clk1 was remarkable. CK2 is also believed to be involved in the pathology of Alzheimer's disease [40–42]. Thus, **14** might allow to evaluate whether simultaneous inhibition of Dyrk1A and CK2 has any benefit in Alzheimer's disease models without significantly affecting Clk1.

In the course of our study, we found that the selectivity of the rhodanine moiety was strongly modulated by the extent of the aromatic system. The selectivity toward Dyrk1B and Dyrk2 was reduced stepwise when the coumaran (**15**) and particularly the benzothiazole (**16**) and quinoline (**17**) rings were introduced. The resulting nanomolar inhibitors **16** and **17** were multi-targeted within the CMGC kinase family, but not promiscuous, since PKCβ and EGFR kinase were not affected.

Table 3
Extended selectivity profiling of **6**, **7**, **16** and **17**.

Kinase	**6**	**7**	**16**	**17**
	% inhibition/(IC_{50} [nM][c])			
STK17A (DRAK1)	28%[a]	n.d.	n.d.	97%[b] (12.8)
PIM1	19%[a]	n.d.	n.d.	89%[b] (103)
Haspin	43%[a]	75%[a]	93%[b] (255)	93%[b] (259)
PI3K-C2β	8%[a]	13%[a]	56%[b]	62%[b]
PI3K-p110-α	84%[a] (650)	90%[a]	98%[b] (2.2)	100%[b] (2.6)
PI3K-p110-δ	73%[a]	77%[a]	90%[b] (12.4)	97%[b] (16.1)
PI3K-p110-γ	75%[a]	79%[a]	97%[b] (2.3)	97%[b] (2.3)

[a] % inhibition at 5 μM; [b] % inhibition at 1 μM; [a,b] shown are mean values of two different measurements performed in duplicates (S.D. ≤ 2.5%); [c] data were calculated based on mean values of duplicates that differed by less than 7%.

Because the benzothiazole moiety in **16** generated a moderate selectivity over Dyrk2, it was also combined with thiohydantoin (cpd. **18**) to test whether this favorable inhibitory profile and the potency of the rhodanine analog **16** might be retained. While the activities against Dyrk1A and CK2 dropped, compound **18** displayed an impressive selectivity for Clk1 (35 fold over Dyrk1A). Thus, our scaffold diversification identified thiohydantoin as a novel moiety mediating strong and selective affinity for Clk1.

Because of the obvious structural similarity of our compounds **16** and **17** with the thiazolidinedione AS605240 (Table 2), which was previously described as a rather selective PI3Kγ inhibitor (IC_{50}: 8 nM) [43], it was straightforward to enlarge our panel of screened

kinases by some of the PI3K isoforms; in turn, we tested AS605240 against our kinase targets. Indeed, AS605240 turned out to be a nanomolar inhibitor of Dyrk1A and CK2 as well (Table 2), and not surprisingly, both **16** and **17** were highly active against PI3Kγ and–α (Table 3). Compound **17** was slightly more selective than **16**, exhibiting lower activity toward PI3Kδ and Clk1 (Tables 2 and 3; see also extended screening in Table S1, Supplementary Material). Of note, both for **16** and **17**, a reduced activity against the atypical kinase haspin was noted (Table 3), corroborating that the rhodanine moiety does not *a priori* confer non-specific behavior. Collectively, we identified CK2α, Clk1, STK17A and PI3Kα/γ as additional targets for **16** and **17** (Tables 2 and 3 and S1), of which, however, PI3Kα/γ turned out to be most potently inhibited. Literature data on the pathogenic roles of these kinases in glioma suggest that they can all be considered as potential targets in this brain malignancy (Table S2, Supplementary Material). In light of this, the compounds presented here might display a favorable profile as multi-target agents for the treatment of glioma. Indeed, we found that **16**, **17** and AS605240 inhibited the growth of U87MG glioma cells with submicromolar IC_{50}s, being more potent than the rather Dyrk1A/1B–selective reference compound harmine (Table S3, Supplementary Material).

To the best of our knowledge, this is the first report showing that AS605240 is a strong inhibitor of Dyrk1A, CK2 and Clk1, and that dual inhibitors of PI3 lipid kinases and protein kinases can be developed. However, inhibition of multiple kinases might be associated with severe side effects. In this regard, it is noteworthy that AS605240, which exhibits an *in vitro* inhibitory profile similar to **16** and **17**, found a widespread use in many murine models of inflammatory diseases, including rheumatoid arthritis, systemic lupus erythematosus, atherosclerosis, colitis, liver fibrosis and pulmonary fibrosis [44–46]. No signs of toxicity were observed in any of these studies, even though some used high oral dosage, e. g., 50 mg/kg twice per day over 14 days [44]. Moreover, in a xenograft model using PI3Kγ–expressing neuroblastoma cells in SCID mice, AS605240 effectively suppressed tumor growth at 20 mg/kg [47]. In the light of our findings – although the inhibition of PI3Kγ may account for a large part of the observed therapeutic effects – it is fair to ask retrospectively what contribution was made by the inhibition of the kinase targets that were identified for AS605240 in our screening, Dyrk1A, CK2α and Clk1. At any rate, the absence of toxic effects of AS605240 proves that in rodents, multi-targeted inhibitions involving even a pleiotropic kinase such as CK2, are not harmful to the organism, at least in short-term treatments.

Having discovered new Dyrk1A inhibitory scaffolds with diverse selectivity profiles, we were interested to evaluate their potency to inhibit the Dyrk1A–catalyzed tau phosphorylation in intact cells. To this end, we used a HEK293 cell line which overexpressed both Dyrk1A and human tau protein. Under the chosen conditions, phosphorylation of tau at Thr212 is solely dependent on the Dyrk1A activity [48]. Testing of the most potent Dyrk1A inhibitors from Tables 1 and 2, **6**, **7**, **16** and **17**, along with AS605240, revealed that the tau phosphorylation was suppressed at low micromolar and sub-micromolar concentrations (Fig. 3). There was no obvious correlation with the inhibitory activities of the compounds against purified Dyrk1A, since the most potent compounds in the cell free assay, **16**, **17** and AS506240 were inferior to harmine and compound **7**. Probably the distinct physicochemical properties of the scaffolds accounted for variable degrees in cell permeability and further pharmacokinetic properties. The high cellular potency of **7** was encouraging, suggesting that benzothiazolylmethylene-γ-butyrolactone might be a suitable core structure for the development of novel therapeutic agents against Alzheimer's disease and also against diseases involving abnormal pre-mRNA splicing, since Clk1 was strongly co-inhibited by **7** in the cell free assay (Table 1). Given the low molecular weight (231.3 g/mol), the small polar surface area (tPSA = 38.66 $Å^2$) and the absence of H-bond donors, the compound fulfills the major criteria for CNS availability [31].

However, most of our new scaffolds exhibited two metabolically weak spots, which might impede *in vivo* applications. One was the lactone ring structure, which might be hydrolyzed by esterases present in the serum and/or cells, and the other one was the potential Michael acceptor motif, which may also have toxicological implications. The Michael-type acceptor reactivity of some of the scaffolds disclosed as kinase inhibitors in this study, including 5-benzylidene thiazolidinediones, hydantoins, thiohydantoins and rhodanines, had been analyzed previously by Arsovska et al. [49]. The authors found that the 5-benzylidene five-membered oxo-heterocycles revealed almost insignificant reactivity toward cysteamine as an exemplary biological nucleophile.

Hydrolytic instability was mainly a concern for the lactone derivatives in Table 1. Therefore we decided to test the stability of some selected compounds in rat plasma. As reference compounds, diltiazem and *N*-acetyl-L-phenylalanine ethyl ester were chosen, possessing a plasma-stable [50] and a labile ester function [51], respectively. As can be seen from Table 4, all analyzed compounds exhibited a long half-life in rat plasma, similar to or better than that of diltiazem ($t_{1/2} = 125$ min), indicating a high metabolic stability in plasma. In contrast, *N*-acetyl-L-phenylalanine ethyl ester was completely metabolized within a few minutes, as it was expected. Thus, it can be concluded that the lactone and lactam rings of our compounds are not hydrolyzed by plasma enzymes.

3. Conclusions

Systematic variation of benzylidene–coupled heterocycles, differing in acceptor strength, lipophilicity and electrostatic potential, was highly effective to generate new scaffolds with different kinase selectivities and potencies, while keeping the molecular weight below 280 g/mol. Although we could not provide experimental evidence for a blood–brain–barrier penetration of our inhibitors within the scope of this study, the close structural similarity to some benzylidene derivatives previously reported to be brain–permeable suggests that at least some of our lead compounds might share this property, including the benzylidene hydantoins (similar to compound 28 in Ref. [52]) and the thiazolidinediones that are structurally similar to AS605240 [53].

With respect to novel agents against neurodegenerative diseases, compound **7** displayed the most promising activity in our cell–based tau phosphorylation assay. In a cytotoxicity assay, **7** was not toxic toward HEK293 cells at concentrations up to 20 μM (data not shown). The compound might be useful as a tool to further explore the effects of co-inhibition of Dyrk1A and Clk1/4 on the pathogenic mechanisms of Alzheimer's disease. Other compounds, such as **3** and **4,** were not very potent but showed an appreciable selectivity towards Dyrk1B and Clk1. These compounds might be considered as elaborated, selective fragments with still good ligand efficiencies (0.55 and 0.54, respectively). In order to optimize the potency, they might be extended analogously to the leucettines, through functionalization e. g., at position 5 of the γ-butyrolactone in **4**.

Within our panel of frequent off-target kinases for Dyrk1A inhibitors, the thiazolidinedione **13** and thiohydantion **18** were selective for CK2, probably because of their elevated acidity. The presence of thione sulfur in the five-membered ring generally increased the potency, however, mostly at the expense of selectivity. The loss of selectivity remained limited when the aromatic portion of the benzylidene moiety was restricted to a single ring (cf. compounds **14** and **16**). Upon introducing a bicyclic aromatic system, however, the selectivity toward Dyrk1B, Dyrk2 and CK2 was

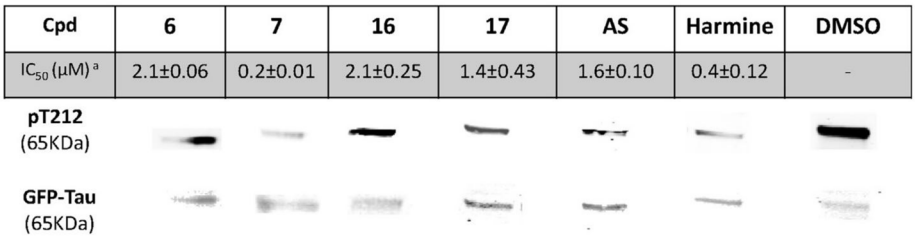

Fig. 3. Inhibition of Dyrk1A–catalyzed tau-Thr212 phosphorylation in stably transfected HEK293 cells. The test compounds, DMSO or the reference inhibitor harmine [54] were added to the cell medium and the Dyrk1A expression induced as described. After immunoblotting of the total cell proteins, the level of phospho-tau-Thr212 was detected using a phosphospecific antibody. To normalize the signals, total recombinant GFP-tau protein was quantified on the same blot using an anti-GFP antibody (fluorescence image converted to grey scales). Initial screenings were performed at 1 μM compound concentrations (lower panel; one representative experiment out of two is shown). [a]IC_{50} values were determined after cell treatment with different concentrations in triplicates, referring to the signal derived from DMSO–treated cells as 100%. Values represent averages from at least two independent determinations (±S.D.); AS, AS605240.

Table 4
Metabolic stability in rat plasma.

Compound	$t_{1/2}$ in rat plasma [min][a]
6	≫120[b]
5	≫120[b]
7	186
16	101
Diltiazem	125
N-acetyl-*L*-phenylalanine ethyl ester	<5

[a] Mean values from two experiments, S.D. < 17%.
[b] No degradation detected after 120 min.

abolished, yielding potent, multi-targeted inhibitors with enhanced anti-proliferative effect on the U87MG glioma cell line (Table S3, Supplementary Material). Interestingly, this class of compounds included the widely studied AS605240, formerly reported as rather selective PI3Kγ inhibitor. Altogether, our results showed that inhibitors which simultaneously target PI3 kinases and oncogenic protein kinases can be developed, with potential benefit in anti-cancer applications.

4. Methods

4.1. Chemistry. Synthesis of the key compounds **6**, **16** and **17**

4.1.1. Synthesis of (E)-3-((2,3-dihydrobenzofuran-5-yl)methylene)-5-methyldihydrofuran-2(3H)-one (**6**)

To a solution of NaH in dry toluene (0.162 g, 4.05 mmol), a solution of the δ-valerolactone (0.324 g, 3.24 mmol, 0.309 mL) was added, and the mixture stirred overnight at room temperature. On the next day, the mixture was cooled in an ice bath and 2,3-dihydrobenzo-furan-5-carboxaldehyde (0.300 g, 2.025 mmol) dissolved in dry toluene was added dropwise. The temperature was slowly increased to reflux until the starting materials were consumed. After cooling down, a solution of 10% H_2SO_4 was added and the solution stirred at room temperature for few minutes. Then 10 mL of water were added and the mixture extracted 3 times with ethyl acetate (10 mL). The organic phase was washed with brine and dried over Na_2SO_4. After evaporating the solvent *in vacuo*, crude product was purified the column chromatography. Yield: 31%. Mp: 131 °C. ^{1}H NMR (500 MHz, DMSO-d_6) δ ppm 1.36 (d, J = 6.31 Hz, 3H) 2.72–2.84 (m, 1H) 3.23 (t, J = 8.67 Hz, 2H) 3.33–3.40 (m, 1H) 4.60 (t, J = 8.67 Hz, 2H) 4.69–4.79 (m, 1H) 6.87 (d, J = 8.20 Hz, 1H) 7.35 (s, 1H) 7.37–7.41 (m, 1H) 7.51 (s, 1H). ^{13}C NMR (126 MHz, DMSO-d_6) δ ppm 22.03 (s, 1C) 28.66 (s, 1C) 34.63 (s, 1C) 71.66 (s, 1C) 73.64 (s, 1C) 109.37 (s, 1C) 122.20 (s, 1C) 126.72 (s, 1C) 127.18 (s, 1C) 128.47 (s, 1C) 131.34 (s, 1C) 135.15 (s, 1C) 161.17 (s, 1C) 171.65 (s, 1C). LC-MS (ESI): m/z MH^+ = 231.

General procedure A: rhodanine or hydantoine (1 eq), the corresponding aldehyde (1 eq) and sodium acetate (3 eq) were dissolved in 5 mL of acetic acid and the solution heated at 110 °C, if necessary under microwave conditions (130 W for ~10 min). After cooling, the precipitate was filtered off, washed to remove all the acetic acid and dried *in vacuo*. The reaction has been described in Mendgen et al. [39] to be stereospecific producing the Z-isomer as confirmed by the single peak in the HPLC.

4.1.2. Synthesis of (Z)-5-(benzo[d]thiazol-6-ylmethylene)-2-thioxothiazolidin-4-one (**16**)

Rhodanine (0.254 g, 1.84 mmol), 1,3-benzothiazole-6-carbaldehyde (0.300 g, 1.84 mmol) and sodium acetate (0.452 g, 5.51 mmol) were used following the general procedure A described above. Yield: 2%. Mp: > 300 °C. ^{1}H NMR (500 MHz, DMSO-d_6) δ ppm 7.76 (d, J = 8.51 Hz, 1H) 7.78 (s, 1H) 8.21 (d, J = 8.51 Hz, 1H) 8.47 (s, 1H) 9.50–9.58 (m, 1H) 13.88 (br. s., 1H). ^{13}C NMR (126 MHz, DMSO-d_6) δ ppm 123.74 (s, 1C) 125.09 (s, 1C) 125.97 (s, 1C) 128.30 (s, 1C) 130.26 (s, 1C) 131.13 (s, 1C) 134.94 (s, 1C) 153.93 (s, 1C) 159.56 (s, 1C) 169.43 (s, 1C) 195.71 (s, 1C). LC-MS (ESI): m/z MH^+ = 279.

4.1.3. Synthesis of (Z)-5-(quinolin-6-ylmethylene)-2-thioxothiazolidin-4-one (**17**)

Rhodanine (0.254 g, 1.909 mmol), 6-quinoline-carbaldehyde (0.300 g, 1.909 mmol) and sodium acetate (0.470 g, 5.73 mmol) were used following the general procedure A described above. Yield: 90%. Mp: >300 °C. ^{1}H NMR (500 MHz, DMSO-d_6) δ ppm 7.62 (dd, J = 8.35, 4.26 Hz, 1H) 7.82 (s, 1H) 7.95 (dd, J = 8.83, 2.21 Hz, 1H) 8.13 (d, J = 8.83 Hz, 1H) 8.24 (d, J = 2.21 Hz, 1H) 8.52–8.56 (m, 1H) 8.98 (dd, J = 4.26, 1.73 Hz, 1H) 13.69–14.22 (m, 1H). ^{13}C NMR (126 MHz, DMSO-d_6) δ ppm 122.53 (s, 1C) 126.93 (s, 1C) 127.13–128.39 (m, 1C) 130.06 (s, 1C) 130.25–130.44 (m, 1C) 130.55–130.76 (m, 1C) 131.03 (s, 1C) 131.15 (s, 1C) 136.95 (s, 1C) 147.74 (s, 1C) 152.34 (s, 1C) 169.45 (s, 1C) 195.72 (s, 1C) LC-MS (ESI): m/z MH^+ = 273.

4.2. Biology

4.2.1. Kinase assay

Inhibition assays for Dyrk1A, Dyrk1B, Dyrk2, CK2alpha, Clk1, EGFR and PKCβ were performed using purified recombinant kinase protein in the presence of 100 μM ATP as described previously [29].

4.2.2. HEK293-tau-Dyrk1A cell assay

The cell line was developed, and the assays for the inhibition of cellular Dyrk1A activity were performed as described previously [48]. In brief, HEK293-tau-Dyrk1A cells which stably overexpress EGFP-fused human full length tau protein and

tetracycline–inducible EGFP–fused Dyrk1A were grown in 12-well plates to 70% confluency; then tetracycline (0.3 μg/mL) and test compounds were added from stock solutions. The next day, the cells were lysed and the lysates analyzed by immunoblotting using an anti-phospho-tau-Thr212 antibody (pT212, Life Technologies GmbH, Cat No. 444–740 g, dil. 1:1000) and a mouse anti-GFP antibody (Life Technologies GmbH, Cat. No. 33–2600, dil. 1:1000) for normalization of the signals. After incubation with dye-labeled secondary antibodies, the signals for pT212 and EGFP were simultaneously detected using an Odyssey infrared imager (LI-COR). Fig. 3 shows the image converted to grey scales.

4.2.3. Metabolic stability tests in rat plasma

The test or reference compounds (1 μM) were incubated with rat plasma (pooled, heparinized) at 37 °C for 0, 5, 15, 30, 60, and 120 min. The incubation was stopped by precipitation of plasma proteins with 5 volumes of cold acetonitrile containing an internal standard, and the remaining compound concentration was analyzed by LC-MS/MS. N-Acetyl-L-phenylalanine ethyl ester (Cat. No. A4251) and diltiazem hydrochloride (Cat. No. D2521) were from Sigma.

4.2.4. Calculation of ligand efficiency

The calculations were done by dividing the Gibbs free energy of binding by the number of non-hydrogen atoms. K_i values were calculated from the IC_{50}s using the Cheng-Prussoff equation. The K_M value of our Dyrk1A preparation for ATP was previously determined to be 64 μM [29].

Acknowledgments

The authors thank Mrs. Nadja Weber and Dr. Christian Schmitt for performing some kinase inhibition assays. The financial support by the Deutsche Forschungsgemeinschaft (DFG) to M.E. (grant EN 381/2-3) is also greatly acknowledged.

Appendix A. Supplementary data

Supplementary data related to this article can be found at http://dx.doi.org/10.1016/j.ejmech.2016.02.017.

References

[1] S. Aranda, A. Laguna, S. de la Luna, DYRK family of protein kinases: evolutionary relationships, biochemical properties, and functional roles, FASEB J. 25 (2011) 449–462, http://dx.doi.org/10.1096/fj.10-165837.

[2] W.J. Song, L.R. Sternberg, C. Kasten-Sportès, M.L. Keuren, S.H. Chung, A.C. Slack, D.E. Miller, T.W. Glover, P.W. Chiang, L. Lou, D.M. Kurnit, Isolation of human and murine homologues of the Drosophila minibrain gene: human homologue maps to 21q22.2 in the Down syndrome "critical region", Genomics 38 (1996) 331–339, http://dx.doi.org/10.1006/geno.1996.0636.

[3] R. Kimura, K. Kamino, M. Yamamoto, A. Nuripa, T. Kida, H. Kazui, R. Hashimoto, T. Tanaka, T. Kudo, H. Yamagata, Y. Tabara, T. Miki, H. Akatsu, K. Kosaka, E. Funakoshi, K. Nishitomi, G. Sakaguchi, A. Kato, H. Hattori, T. Uema, M. Takeda, The DYRK1A gene, encoded in chromosome 21 Down syndrome critical region, bridges between beta-amyloid production and tau phosphorylation in Alzheimer disease, Hum. Mol. Genet. 16 (2007) 15–23, http://dx.doi.org/10.1093/hmg/ddl437.

[4] Y.L. Woods, P. Cohen, W. Becker, R. Jakes, M. Goedert, X. Wang, G.C. Proud, The kinase DYRK phosphorylates protein-synthesis initiation factor eIF2Bepsilon at Ser539 and the microtubule-associated protein tau at Thr212: potential role for DYRK as a glycogen synthase kinase 3-priming kinase, Biochem. J. 355 (2001) 609–615.

[5] F.J. Tejedor, B. Hämmerle, MNB/DYRK1A as a multiple regulator of neuronal development, FEBS J. 278 (2011) 223–235, http://dx.doi.org/10.1111/j.1742-4658.2010.07954.x.

[6] N. Pozo, C. Zahonero, P. Fernández, J.M. Liñares, A. Ayuso, M. Hagiwara, A. Pérez, J.R. Ricoy, A. Hernández-Laín, J.M. Sepúlveda, P. Sánchez-Gómez, Inhibition of DYRK1A destabilizes EGFR and reduces EGFR-dependent glioblastoma growth, J. Clin. Invest 123 (2013) 2475–2487, http://dx.doi.org/10.1172/JCI63623.

[7] S. Agarwal, R.K. Mittapalli, D.M. Zellmer, J.L. Gallardo, R. Donelson, C. Seiler, S.A. Decker, K.S. Santacruz, J.L. Pokorny, J.N. Sarkaria, W.F. Elmquist, J.R. Ohlfest, Active efflux of Dasatinib from the brain limits efficacy against murine glioblastoma: broad implications for the clinical use of molecularly targeted agents, Mol. Cancer Ther. 11 (2012) 2183–2192, http://dx.doi.org/10.1158/1535-7163.MCT-12-0552.

[8] S. Aranda, M. Alvarez, S. Turró, A. Laguna, S. de la Luna, Sprouty2-mediated inhibition of fibroblast growth factor signaling is modulated by the protein kinase DYRK1A, Mol. Cell. Biol. 28 (2008) 5899–5911, http://dx.doi.org/10.1128/MCB.00394-08.

[9] S.R. Ferron, N. Pozo, A. Laguna, S. Aranda, E. Porlan, M. Moreno, C. Fillat, S. de la Luna, P. Sánchez, M.L. Arbonés, I. Fariñas, Regulated segregation of kinase Dyrk1A during asymmetric neural stem cell division is critical for EGFR-mediated biased signaling, Cell Stem Cell. 7 (2010) 367–379, http://dx.doi.org/10.1016/j.stem.2010.06.021.

[10] Y.L. Woods, G. Rena, N. Morrice, A. Barthel, W. Becker, S. Guo, T.G. Unterman, P. Cohen, The kinase DYRK1A phosphorylates the transcription factor FKHR at Ser329 in vitro, a novel in vivo phosphorylation site, Biochem. J. 355 (2001) 597–607.

[11] H.S. Chang, C.H. Lin, C.H. Yang, M.S. Yen, C.R. Lai, Y.R. Chen, Y.L. Liang, W.C. Yu, Increased expression of Dyrk1a in HPV16 immortalized keratinocytes enable evasion of apoptosis, Int. J. Cancer 120 (2007) 2377–2385, http://dx.doi.org/10.1002/ijc.22573.

[12] S.L. Pomeroy, P. Tamayo, M. Gaasenbeek, L.M. Sturla, M. Angelo, M.E. McLaughlin, J.Y.H. Kim, L.C. Goumnerova, P.M. Black, C. Lau, J.C. Allen, D. Zagzag, J.M. Olson, T. Curran, C. Wetmore, J.A. Biegel, T. Poggio, S. Mukherjee, R. Rifkin, A. Califano, G. Stolovitzky, D.N. Louis, J.P. Mesirov, E.S. Lander, T.R. Golub, Prediction of central nervous system embryonal tumour outcome based on gene expression, Nature 415 (2002) 436–442, http://dx.doi.org/10.1038/415436a.

[13] R. Shai, T. Shi, T.J. Kremen, S. Horvath, L.M. Liau, T.F. Cloughesy, P.S. Mischel, S.F. Nelson, Gene expression profiling identifies molecular subtypes of gliomas, Oncogene 22 (2003) 4918–4923, http://dx.doi.org/10.1038/sj.onc.1206753.

[14] J. Shi, T. Zhang, C. Zhou, M.O. Chohan, X. Gu, J. Wegiel, J. Zhou, Y.W. Hwang, K. Iqbal, I. Grundke-Iqbal, C.X. Gong, F. Liu, Increased dosage of Dyrk1A alters alternative splicing factor (ASF)-regulated alternative splicing of tau in down syndrome, J. Biol. Chem. 283 (2008) 28660–28669, http://dx.doi.org/10.1074/jbc.M802645200.

[15] W. Qian, H. Liang, J. Shi, N. Jin, I. Grundke-Iqbal, K. Iqbal, C.X. Gong, F. Liu, Regulation of the alternative splicing of tau exon 10 by SC35 and Dyrk1A, Nucleic Acids Res. 39 (2011) 6161–6171, http://dx.doi.org/10.1093/nar/gkr195.

[16] X. Yin, N. Jin, J. Gu, J. Shi, J. Zhou, C.-X. Gong, K. Iqbal, I. Grundke-Iqbal, F. Liu, Dual-specificity tyrosine phosphorylation-regulated kinase 1A (Dyrk1A) modulates serine/arginine-rich protein 55 (SRp55)-promoted Tau exon 10 inclusion, J. Biol. Chem. 287 (2012) 30497–30506, http://dx.doi.org/10.1074/jbc.M112.355412.

[17] A.M. Hartmann, D. Rujescu, T. Giannakouros, E. Nikolakaki, M. Goedert, E.M. Mandelkow, Q.S. Gao, A. Andreadis, S. Stamm, Regulation of alternative splicing of human tau exon 10 by phosphorylation of splicing factors, Mol. Cell. Neurosci. 18 (2001) 80–90, http://dx.doi.org/10.1006/mcne.2001.1000.

[18] P. Jain, C. Karthikeyan, N.S. Hari Narayana Moorthy, D. Kumar Waiker, A. Kumar Jain, P. Trivedi, Human CDC2-Like Kinase 1 (CLK1): a novel target for Alzheimer's disease, Curr. Drug Targets 15 (2014) 539–550.

[19] S. Stamm, S. Ben-Ari, I. Rafalska, Y. Tang, Z. Zhang, D. Toiber, T.A. Thanaraj, H. Soreq, Function of alternative splicing, Gene 344 (2005) 1–20, http://dx.doi.org/10.1016/j.gene.2004.10.022.

[20] T. Misteli, J.F. Cáceres, J.Q. Clement, A.R. Krainer, M.F. Wilkinson, D.L. Spector, Serine phosphorylation of SR proteins is required for their recruitment to sites of transcription in vivo, J. Cell Biol. 143 (1998) 297–307.

[21] C. Schmitt, P. Miralinaghi, M. Mariano, R.W. Hartmann, M. Engel, Hydroxybenzothiophene ketones are efficient Pre-mRNA splicing modulators due to dual inhibition of Dyrk1A and Clk1/4, ACS Med. Chem. Lett. 5 (9) (2014) 963–967, http://dx.doi.org/10.1021/ml500059y.

[22] M. Debdab, F. Carreaux, S. Renault, M. Soundararajan, O. Fedorov, P. Filippakopoulos, O. Lozach, L. Babault, T. Tahtouh, B. Baratte, Y. Ogawa, M. Hagiwara, A. Eisenreich, U. Rauch, S. Knapp, L. Meijer, J.P. Bazureau, Leucettines, a class of potent inhibitors of cdc2-like kinases and dual specificity, tyrosine phosphorylation regulated kinases derived from the marine sponge leucettamine B: modulation of alternative pre-RNA splicing, J. Med. Chem. 54 (2011) 4172–4186, http://dx.doi.org/10.1021/jm200274d.

[23] G. Naert, V. Ferré, J. Meunier, E. Keller, S. Malmström, L. Givalois, F. Carreaux, J.P. Bazureau, T. Maurice, Leucettine L41, a DYRK1A-preferential DYRKs/CLKs inhibitor, prevents memory impairments and neurotoxicity induced by oligomeric Aβ25-35 peptide administration in mice, Eur. Neuropsychopharmacol. 25 (2015) 2170–2182, http://dx.doi.org/10.1016/j.euroneuro.2015.03.018.

[24] W. Becker, U. Soppa, F.J. Tejedor, DYRK1A: a potential drug target for multiple Down syndrome neuropathologies, CNS Neurol. Disord. Drug Targets 13 (2014) 26–33.

[25] C. Kuhn, D. Frank, R. Will, C. Jaschinski, R. Frauen, H.A. Katus, N. Frey, DYRK1A is a novel negative regulator of cardiomyocyte hypertrophy, J. Biol. Chem. 284 (2009) 17320–17327, http://dx.doi.org/10.1074/jbc.M109.006759.

[26] Y. Ogawa, Y. Nonaka, T. Goto, E. Ohnishi, T. Hiramatsu, I. Kii, M. Yoshida, T. Ikura, H. Onogi, H. Shibuya, T. Hosoya, N. Ito, M. Hagiwara, Development of

a novel selective inhibitor of the down syndrome-related kinase Dyrk1A, Nat. Commun. 1 (2010) 86, http://dx.doi.org/10.1038/ncomms1090.
[27] O. Fedorov, K. Huber, A. Eisenreich, P. Filippakopoulos, O. King, A.N. Bullock, D. Szklarczyk, L.J. Jensen, D. Fabbro, J. Trappe, U. Rauch, F. Bracher, S. Knapp, Specific CLK inhibitors from a novel chemotype for regulation of alternative splicing, Chem. Biol. 18 (2011) 67–76, http://dx.doi.org/10.1016/j.chembiol.2010.11.009.
[28] T. Tahtouh, J.M. Elkins, P. Filippakopoulos, M. Soundararajan, G. Burgy, E. Durieu, C. Cochet, R.S. Schmid, D.C. Lo, F. Delhommel, A.E. Oberholzer, L.H. Pearl, F. Carreaux, J.P. Bazureau, S. Knapp, L. Meijer, Selectivity, cocrystal structures, and neuroprotective properties of leucettines, a family of protein kinase inhibitors derived from the marine sponge alkaloid leucettamine B, J. Med. Chem. 55 (2012) 9312–9330, http://dx.doi.org/10.1021/jm301034u.
[29] C. Schmitt, D. Kail, M. Mariano, M. Empting, N. Weber, T. Paul, R.W. Hartmann, M. Engel, Design and synthesis of a library of lead-like 2,4-bisheterocyclic substituted thiophenes as selective Dyrk/Clk inhibitors, PLoS One 9 (2014) e87851, http://dx.doi.org/10.1371/journal.pone.0087851.
[30] H. Falke, A. Chaikuad, A. Becker, N. Loaëc, O. Lozach, S. Abu Jhaisha, W. Becker, P.G. Jones, L. Preu, K. Baumann, S. Knapp, L. Meijer, C. Kunick, 10-iodo-11H-indolo[3,2-c]quinoline-6-carboxylic acids are selective inhibitors of DYRK1A, J. Med. Chem. 58 (2015) 3131–3143, http://dx.doi.org/10.1021/jm501994d.
[31] T.T. Wager, R.Y. Chandrasekaran, X. Hou, M.D. Troutman, P.R. Verhoest, A. Villalobos, Y. Will, Defining desirable central nervous system drug space through the alignment of molecular properties, in vitro ADME, and safety attributes, ACS Chem. Neurosci. 1 (2010) 420–434, http://dx.doi.org/10.1021/cn100007x.
[32] S. Udenfriend, B. Witkop, B.G. Redfield, H. Weissbach, Studies with reversible inhibitors of monoamine oxidase: harmaline and related compounds, Biochem. Pharmacol. 1 (1958) 160–165, http://dx.doi.org/10.1016/0006-2952(58)90025-X.
[33] G.D. Cuny, N.P. Ulyanova, D. Patnaik, J.-F. Liu, X. Lin, K. Auerbach, S.S. Ray, J. Xian, M.A. Glicksman, R.L. Stein, J.M. Higgins, Structure-activity relationship study of beta-carboline derivatives as haspin kinase inhibitors, Bioorg. Med. Chem. Lett. 22 (2012) 2015–2019, http://dx.doi.org/10.1016/j.bmcl.2012.01.028.
[34] R. Prudent, V. Moucadel, M. López-Ramos, S. Aci, B. Laudet, L. Mouawad, C. Barette, J. Einhorn, C. Einhorn, J.N. Denis, G. Bisson, F. Schmidt, S. Roy, L. Lafanechere, J.C. Florent, C. Cochet, Expanding the chemical diversity of CK2 inhibitors, Mol. Cell. Biochem. 316 (2008) 71–85, http://dx.doi.org/10.1007/s11010-008-9828-z.
[35] A.G. Golub, V.G. Bdzhola, N.V. Briukhovetska, A.O. Balanda, O.P. Kukharenko, I.M. Kotey, O.V. Ostrynska, S.M. Yarmoluk, Synthesis and biological evaluation of substituted (thieno[2,3-d]pyrimidin-4-ylthio)carboxylic acids as inhibitors of human protein kinase CK2, Eur. J. Med. Chem. 46 (2011) 870–876, http://dx.doi.org/10.1016/j.ejmech.2010.12.025.
[36] L.A. Dakin, M.H. Block, H. Chen, E. Code, J.E. Dowling, X. Feng, A.D. Ferguson, I. Green, A.W. Hird, T. Howard, E.K. Keeton, M.L. Lamb, P.D. Lyne, H. Pollard, J. Read, A.J. Wu, T. Zhang, X. Zheng, Discovery of novel benzylidene-1,3-thiazolidine-2,4-diones as potent and selective inhibitors of the PIM-1, PIM-2, and PIM-3 protein kinases, Bioorg. Med. Chem. Lett. 22 (2012) 4599–4604, http://dx.doi.org/10.1016/j.bmcl.2012.05.098.
[37] H. de Koning, W.N. Speckamp, Succinimide, in: Encycl. Reagents Org. Synth., John Wiley & Sons, Ltd, 2001, http://dx.doi.org/10.1002/047084289X.rs126.
[38] G.G. Alfonso, J.L.G. Ariza, Derivatives of rhodanine as spectrophotometric analytical reagents, Microchem. J. 26 (1981) 574–585, http://dx.doi.org/10.1016/0026-265X(81)90144-2.
[39] T. Mendgen, C. Steuer, C.D. Klein, Privileged scaffolds or promiscuous binders: a comparative study on rhodanines and related heterocycles in medicinal chemistry, J. Med. Chem. 55 (2012) 743–753, http://dx.doi.org/10.1021/jm201243p.
[40] M.A. Pagano, L. Cesaro, F. Meggio, L.A. Pinna, Protein kinase CK2: a newcomer in the "druggable kinome", Biochem. Soc. Trans. 34 (2006) 1303–1306, http://dx.doi.org/10.1042/BST0341303.
[41] D.I. Perez, C. Gil, A. Martinez, Protein kinases CK1 and CK2 as new targets for neurodegenerative diseases, Med. Res. Rev. 31 (2011) 924–954, http://dx.doi.org/10.1002/med.20207.
[42] S. Côté, P.-H. Carmichael, R. Verreault, J. Lindsay, J. Lefebvre, D. Laurin, Nonsteroidal anti-inflammatory drug use and the risk of cognitive impairment and Alzheimer's disease, Alzheimers. Dement. 8 (2012) 219–226, http://dx.doi.org/10.1016/j.jalz.2011.03.012.
[43] M. Camps, T. Rückle, H. Ji, V. Ardissone, F. Rintelen, J. Shaw, C. Ferrandi, C. Chabert, C. Gillieron, B. Françon, T. Martin, D. Gretener, D. Perrin, D. Leroy, P.A. Vitte, E. Hirsch, M.P. Wymann, R. Cirillo, M.K. Schwarz, C. Rommel, Blockade of PI3Kgamma suppresses joint inflammation and damage in mouse models of rheumatoid arthritis, Nat. Med. 11 (2005) 936–943, http://dx.doi.org/10.1038/nm1284.
[44] X. Peng, X. Wu, L. Chen, Z. Wang, X. Hu, L. Song, C.M. He, Y.F. Luo, Z.Z. Chen, K. Jin, H.G. Lin, X.L. Li, Y.S. Wang, Y.Q. Wei, Inhibition of phosphoinositide 3-kinase ameliorates dextran sodium sulfate-induced colitis in mice, J. Pharmacol. Exp. Ther. 332 (2010) 46–56, http://dx.doi.org/10.1124/jpet.109.153494.
[45] Z. Wang, X. Wu, L. Song, Y. Wang, X. Hu, Y.F. Luo, Z.Z. Chen, J. Ke, X.D. Peng, C.M. He, W. Zhang, L.J. Chen, Y.Q. Wei, Phosphoinositide 3-kinase gamma inhibitor ameliorates concanavalin A-induced hepatic injury in mice, Biochem. Biophys. Res. Commun. 386 (2009) 569–574, http://dx.doi.org/10.1016/j.bbrc.2009.06.060.
[46] X. Wei, J. Han, Z. Chen, B. Qi, G. Wang, Y.H. Ma, H. Zheng, Y.F. Luo, Y.Q. Wei, L.J. Chen, A phosphoinositide 3-kinase-gamma inhibitor, AS605240 prevents bleomycin-induced pulmonary fibrosis in rats, Biochem. Biophys. Res. Commun. 397 (2010) 311–317, http://dx.doi.org/10.1016/j.bbrc.2010.05.109.
[47] V. Spitzenberg, C. König, S. Ulm, R. Marone, L. Röpke, J.P. Müller, M. Grün, R. Bauer, I. Rubio, M.P. Wymann, A. Voigt, R. Wetzker, Targeting PI3K in neuroblastoma, J. Cancer Res. Clin. Oncol. 136 (2010) 1881–1890, http://dx.doi.org/10.1007/s00432-010-0847-2.
[48] M. Mariano, C. Schmitt, P. Miralinaghi, M. Catto, R.W. Hartmann, A. Carotti, M. Engel, First Selective dual inhibitors of tau phosphorylation and beta-amyloid aggregation, two major pathogenic mechanisms in Alzheimer's disease, ACS Chem. Neurosci. 5 (2014) 1198–1202, http://dx.doi.org/10.1021/cn5001815.
[49] E. Arsovska, J. Trontelj, N. Zidar, T. Tomašić, L.P. Mašič, D. Kikelj, J. Plavec, A. Zega, Evaluation of Michael-type acceptor reactivity of 5-benzylidenebarbiturates, 5-benzylidenerhodanines, and related heterocycles using NMR, Acta Chim. Slov. 61 (2014) 637–644.
[50] G. Caillé, L.M. Dubé, Y. Théorêt, F. Varin, N. Mousseau, I.J. McGilveray, Stability study of diltiazem and two of its metabolites using a high performance liquid chromatographic method, Biopharm. Drug Dispos. 10 (1989) 107–114.
[51] O.D. Ratnoff, I.H. Lepow, Some properties of an esterase derived from preparations of the first component of complement, J. Exp. Med. 106 (1957) 327–343.
[52] M.A. Khanfar, R.A. Hill, A. Kaddoumi, K.A. El Sayed, Discovery of novel GSK-3β inhibitors with potent in vitro and in vivo activities and excellent brain permeability using combined ligand- and structure-based virtual screening, J. Med. Chem. 53 (2010) 8534–8545, http://dx.doi.org/10.1021/jm100941j.
[53] G.F. Passos, C.P. Figueiredo, R.D.S. Prediger, K.A.B.S. Silva, J.M. Siqueira, F.S. Duarte, P.C. Leal, R. Medeiros, J.B. Calixto, Involvement of phosphoinositide 3-kinase gamma in the neuro-inflammatory response and cognitive impairments induced by beta-amyloid 1-40 peptide in mice, Brain. Behav. Immun. 24 (2010) 493–501, http://dx.doi.org/10.1016/j.bbi.2009.12.003.
[54] D. Frost, B. Meechoovet, T. Wang, S. Gately, M. Giorgetti, I. Shcherbakova, T. Dunckley, β-carboline compounds, including harmine, inhibit DYRK1A and tau phosphorylation at multiple Alzheimer's disease-related sites, PLoS One 6 (2011) e19264, http://dx.doi.org/10.1371/journal.pone.0019264.

Supplementary Material

Systematic diversification of benzylidene heterocycles yields novel inhibitor scaffolds selective for Dyrk1A, Clk1 and CK2

Marica Mariano[a] , Rolf W. Hartmann[a,b] and Matthias Engel[a, *]

[a] *Department of Pharmaceutical and Medicinal Chemistry, Saarland University, Saarbrücken, Germany.*
b Helmholtz Institute for Pharmaceutical Research Saarland (HIPS), Campus C2-3, D 66123 Saarbrücken, Germany

Index:

[*] Corresponding author. E-mail: ma.engel@mx.uni-saarland.de; phone: +4968130270312.

B1. Chemistry

B1.1. General Chemical Methods

All chemical starting materials purchased from Sigma-Aldrich, Acros Organics, CombiBlocks, and Alfa Aesar were directly used without further purification.

Column chromatography was performed on silica gel (70–200 μm) and reaction progress was monitored by TLC on ALUGRAM SIL G/UV254 (Macherey-Nagel) employing UV detection.

Mass spectrometry was performed on a TSQ® Quantum (ThermoFisher, Dreieich, Germany). The triple quadrupole mass spectrometer was equipped with an electrospray interface (ESI). The purity of the compounds was assessed by LC/MS. The Surveyor®-LC-system consisted of a pump, an auto sampler, and a PDA detector. The system was operated by the standard software Xcalibur®. An RP C18 NUCLEODUR® 100-5 (3 mm) column (Macherey–Nagel GmbH, Dühren, Germany) was used as stationary phase. All solvents were HPLC grade. In a gradient run the percentage of acetonitrile was increased from an initial concentration of 0% at 0 min to 100% at 15 min and kept at 100% for 5 min. The injection volume was 15 μL and the flow rate was set to 800 μL/min. MS analysis was carried out at the needle voltage of 3000 V and the capillary temperature of 350 °C. Mass spectra were acquired in positive mode from 100 to 1000 *m*/*z* and UV spectra were recorded at the wave length of 254 nm and in some cases at 360 nm.

^{1}H and ^{13}C NMR spectra were recorded on either a Bruker DRX-500 (^{1}H, 500 MHz; ^{13}C, 126 MHz) instrument at 500 K or on a Bruker Fourier300 (^{1}H, 300 MHz; ^{13}C, 75 MHz) NMR spectrometer at 300 K in the deuterated solvents indicated. Signals are described as br (broad), s (singlet), d (doublet), t (triplet), dd (doublet of doublets), ddd (doublet of doublet of doublets), dt (doublet of triplets) and m (multiplet). All coupling constants (*J*) are given in Hertz (Hz)

Melting points (mp) were measured in open capillaries on a Stuart Scientific SMP3 apparatus and are uncorrected.

All tested compounds exhibited ≥95% chemical purity as measured by HPLC/MS.

Although the stereoselectivity was not controlled, all compounds showed only one peak in the HPLC/MS analysis, suggesting that only one *E*/*Z* isomer was formed. It was previously shown that the synthesis of compounds **3** and **4**, according to the employed method, generated exclusively the *Z* isomer.[82]

B1.2. Synthesis and Compound Characterization

(E)-3-(4-methoxybenzylidene)dihydrofuran-2(*3H*)-one (1)

A total of 0.854 mmol of 4-iodoanisole, 1.28 mmol of α-methylene-γ-butyrolactone, 2.56 mmol of AcOK and 0.047 mmol of Pd_2Cl_2dppf were dissolved in 2mL of DMF, and the mixture was stirred under nitrogen at 80°C for ~3h. After it was cooled, the reaction mixture was washed with a mixture of ethyl acetate and saturated acqueous $NaHCO_3$. The phases were separated, and the combined organic phases were dried over Na_2SO_4. After removal of the solvent, the crude product was purified by column chromatography. The crude product corresponding to the main spot on TLC was treated with ethyl ether and filtered (3 times).

Yield: 23%. Mp: 124°C. ^{1}H NMR ($CDCl_3$): δ 3.21 (td, J = 3, J= 7 Hz, 2H), 3.84 (s, 3H), 4.44 (t, J = 7.5 Hz, 2H), 6.95 (dd, J = 2, J = 7 Hz, 2H), 7.45 (dd, J = 2, J = 6.5 Hz, 2H), 7.52 ppm (t, 1H). ^{13}C NMR ($CDCl_3$): δ 27.39, 55.40, 65.30, 114.44, 118.93, 120.63, 127.48, 131.80 ppm. LC-MS (ESI): m/z MH^+= 205.

Synthesis of *(E)*-3-(chroman-6-ylmethylene)-5-methyldihydrofuran-2(*3H*)-one (2)

The solution of chroman-6-carbaldehyde (0.250 g, 1.54 mmol) and γ-butyrolactone (0.133 g, 0.119 ml, 1.54 mmol) in ethanol was added drop by drop to a solution of NaOEt (0.252 g, 3.70 mmol) in ethanol in a ice-cooled bath. The mixture was stirred increasing slowly the temperature to 50°C, if necessary under microwave conditions (130W for ~10 minutes). Cool down and filter the precipitate, washing 3 times with ethanol. Purify by chromatography, if necessary.

Yield: 4%. Mp: 160°C. ^{1}H NMR (500 MHz, CHLOROFORM-*d*) δ ppm 2.01 - 2.08 (m, 2 H) 2.83 (t, *J*=6.31 Hz, 2 H) 3.22 (td, *J*=7.33, 3.00 Hz, 2 H) 4.22 - 4.27 (m, 2 H) 4.43 - 4.49 (m, 2 H) 6.85 (d, *J*=8.51 Hz, 1 H) 7.19 - 7.22 (m, 1 H) 7.29 (d, *J*=2.21 Hz, 1 H) 7.49 (t, *J*=2.84 Hz, 1 H). ^{13}C NMR (126 MHz, CHLOROFORM-*d*) δ ppm 22.03 (s, 1 C) 24.90 (s, 1 C) 27.43 (s, 1 C) 65.28 (s, 1 C) 66.84 (s, 1 C) 117.40 (s, 1 C) 120.15 (s, 1 C) 122.70 (s, 1 C) 126.93 (s, 1 C) 129.24 (s, 1 C) 132.44 (s, 1 C) 136.69 (s, 1 C) 156.58 (s, 1 C) 172.96 (s, 1 C). LC-MS (ESI): m/z MH^+= 231.

Synthesis of *(E)*-3-(4-methoxybenzylidene)tetrahydro-*2H*-pyran-2-one (3)

To a solution of NaH in toluene dry (0.00116 g, 2.94 mmol) add a solution of the δ-valerolactone (0.472 g, 0.420 mL, 4.70 mmol) and stir it at room temperature overnight. On the further day, add the 4-methoxybenzaldehyde (0.400 g, 0.356 mL, 2.94 mmol) dissolved in toluene dry drop by drop in an ice cooled bath. Slowly increase the temperature to reflux until the starting materials are consumed. Cool down, add a solution of H_2SO_4 10% and stir at room temperature for few minutes. Add 10 mL of water and extract 3

times with ethyl acetate (10 mL). Wash the last time with brine and dry the organic phases on Na_2SO_4. After evaporating the solvent *in vacuo*, purify the crude product by chromatography.

Yield: 48%. Mp: 105°C. ^{1}H NMR (500 MHz, CHLOROFORM-*d*) δ ppm 1.92 - 2.02 (m, 2 H) 2.86 (td, *J*=6.54, 2.36 Hz, 2 H) 3.83 (s, 3 H) 4.33 - 4.40 (m, 2 H) 6.90 - 6.96 (m, 2 H) 7.41 (d, *J*=8.51 Hz, 2 H) 7.86 (s, 1 H). ^{13}C NMR (126 MHz, CHLOROFORM-*d*) δ ppm 23.01 (s, 1 C) 26.03 (s, 1 C) 55.35 (s, 1 C) 68.46 (s, 1 C) 85.15 (s, 1 C) 114.06 (s, 2 C) 122.09 - 125.20 (m, 1 C) 127.74 (s, 1 C) 131.27 - 133.48 (m, 3 C) 141.41 (s, 1 C). LC-MS (ESI): m/z MH^+ = 219.

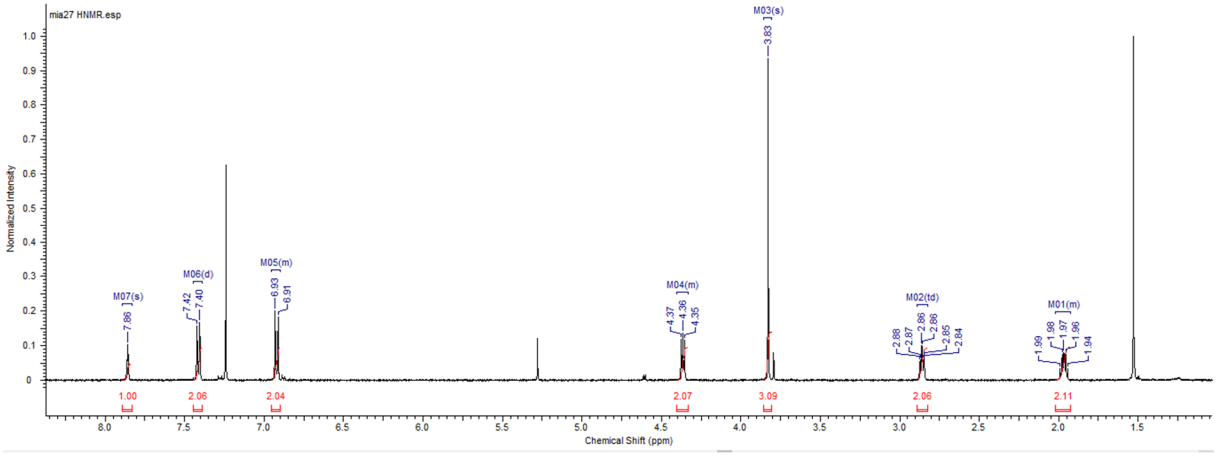

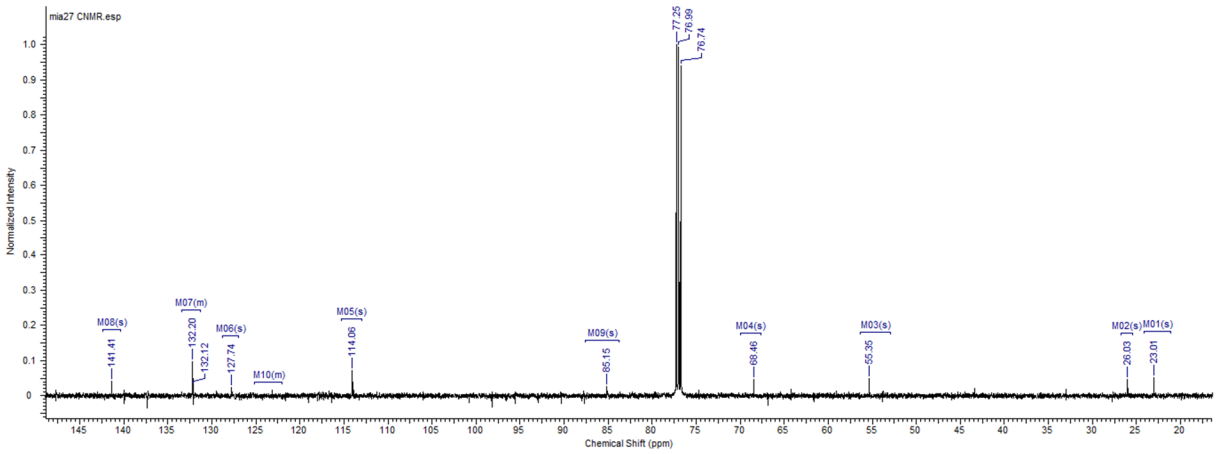

Synthesis of *(E)*-2-(4-methoxybenzylidene)cyclopentanone (4)

To a solution of NaH in toluene dry (0.0705 g, 2.94 mmol) add a solution of the γ-valerolactone (0.471 g, 0.448 mL, 4.70 mmol) and stir it at room temperature overnight. On the further day, add the 4-methoxybenzaldehyde (0.400 g, 0.356 mL, 2.94 mmol) dissolved in toluene dry drop by drop in an ice cooled bath. Slowly increase the temperature to reflux until the starting materials are consumed. Cool down, add a solution of H_2SO_4 10% and stir at room temperature for few minutes. Add 10 mL of water and extract 3 times with ethyl acetate (10 mL). Wash the last time with brine and dry the organic phases on Na_2SO_4. After evaporating the solvent *in vacuo*, purify the crude product by chromatography.

Yield: 52%. Mp: 87°C. ^{1}H NMR (500 MHz, CHLOROFORM-*d*) δ ppm 1.45 (d, *J*=6.31 Hz, 3 H) 2.70 - 2.79 (m, 1 H) 3.33 (ddd, *J*=17.18, 7.88, 2.68 Hz, 1 H) 3.84 (s, 3 H) 4.68 - 4.78 (m, 1 H) 6.90 - 6.97 (m, 2 H) 7.40 - 7.45 (m, 2 H) 7.49 (t, *J*=2.84 Hz, 1 H). ^{13}C NMR (126 MHz, CHLOROFORM-*d*) δ ppm 22.42 (s, 1 C) 35.25 (s, 1 C) 55.38 (s, 1 C) 73.87 (s, 1 C) 114.38 (s, 2 C) 122.03 (s, 1 C) 127.50 (s, 1 C) 131.72 (s, 2 C) 136.26 (s, 1 C) 160.81 (s, 1 C) 172.40 (s, 1 C). LC-MS (ESI): m/z MH^{+} = 219.

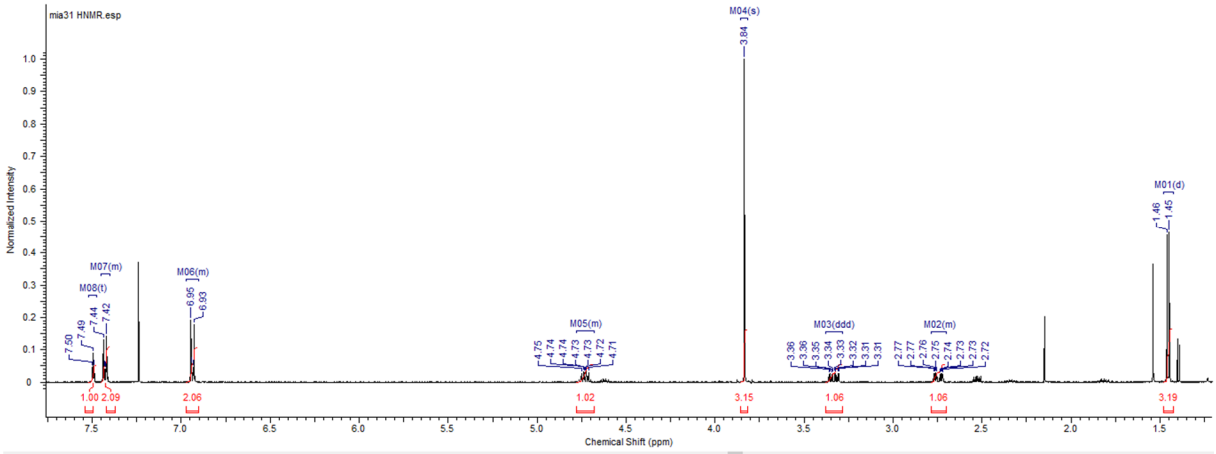

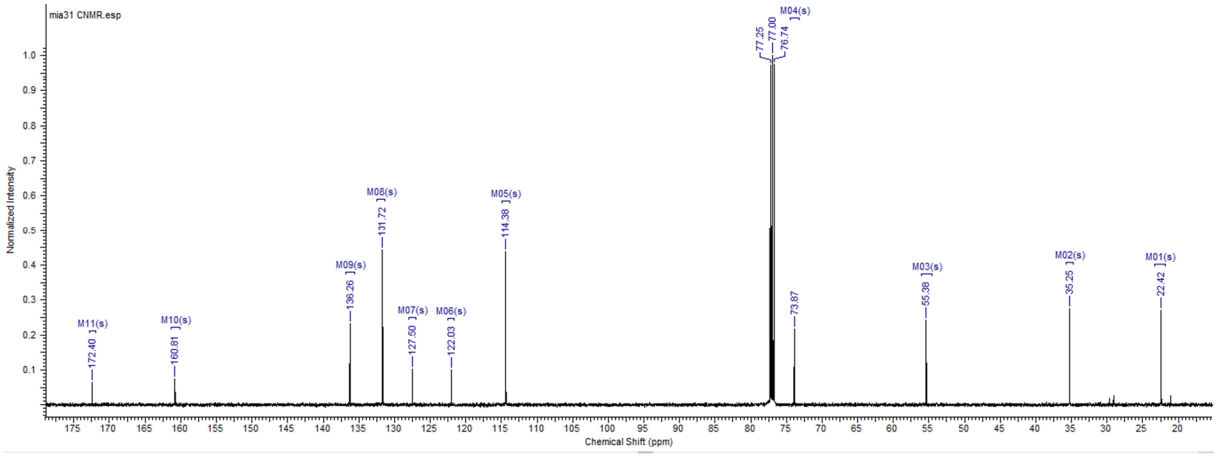

Synthesis of *(E)*-3-((2,3-dihydrobenzofuran-5-yl)methylene)dihydrofuran-2(*3H*)-one (5)

The solution of 2,3-dihydro-benzofuran-5-carboxaldehyde (0.300 g, 0.255 ml, 2.02 mmol) and γ-butyrolactone (0.174 g, 0.156 ml, 2.02 mmol) in ethanol was added drop by drop to a solution of NaOEt (0.275 g, 4.04 mmol) in ethanol in a ice-cooled bath. The mixture was stirred increasing slowly the temperature to 50°C, if necessary under microwave conditions (130W for ~10 minutes). Cool down and filter the precipitate, washing 3 times with ethanol. Purify by chromatography, if necessary.

Yield: 4%. Mp: n.d. ^{1}H NMR (500 MHz, CHLOROFORM-*d*) δ ppm 3.15 (td, *J*=7.39, 2.89 Hz, 2 H) 3.19 (t, *J*=8.68 Hz, 2 H) 4.39 (t, *J*=7.31 Hz, 2 H) 4.58 (t, *J*=8.83 Hz, 2 H) 6.78 (d, *J*=8.22 Hz, 1 H) 7.24 (d, *J*=8.22 Hz, 1 H) 7.29 (s, 1 H) 7.45 (t, *J*=2.89 Hz, 1 H). ^{13}C NMR (126 MHz, CHLOROFORM-*d*) δ ppm 27.52 (s, 1 C) 29.34 (s, 1 C) 65.26 (s,

1 C) 71.88 (s, 1 C) 109.88 (s, 1 C) 119.83 (s, 1 C) 126.90 (s, 1 C) 127.58 (s, 1 C) 128.11 (s, 1 C) 131.24 (s, 1 C) 136.90 (s, 1 C) 161.59 - 161.91 (m, 1 C) 172.98 (s, 1 C). LC-MS (ESI): m/z MH^+= 217.

Synthesis of *(E)*-3-((2,3-dihydrobenzofuran-5-yl)methylene)-5-methyldihydrofuran-2(*3H*)-one (6)

To a solution of NaH in toluene dry (0.162 g, 4.05 mmol) add a solution of the γ-valerolactone (0.324 g, 3.24 mmol, 0.309 mL) and stir it at room temperature overnight. On the further day, add the 2,3-dihydrobenzo-furan-5-carboxaldehyde (0.300 g, 2.025 mmol) dissolved in toluene dry drop by drop in an ice cooled bath. Slowly increase the temperature to reflux until the starting materials are consumed. Cool down, add a solution of H_2SO_4 10% and stir at room temperature for few minutes. Add 10 mL of water and extract 3 times with ethyl acetate (10 mL). Wash the last time with brine and dry the organic phases on Na_2SO_4. After evaporating the solvent *in vacuo*, purify the crude product by chromatography.

Yield: 31%. Mp: 131°C. ^{1}H NMR (500 MHz, DMSO-d_6) δ ppm 1.36 (d, *J*=6.31 Hz, 3 H) 2.72 - 2.84 (m, 1 H) 3.23 (t, *J*=8.67 Hz, 2 H) 3.33 - 3.40 (m, 1 H) 4.60 (t, *J*=8.67 Hz, 2 H) 4.69 - 4.79 (m, 1 H) 6.87 (d, *J*=8.20 Hz, 1 H) 7.35 (s, 1 H) 7.37 - 7.41 (m, 1 H) 7.51 (s, 1 H). ^{13}C NMR (126 MHz, DMSO-d_6) δ ppm 22.03 (s, 1 C) 28.66 (s, 1 C) 34.63 (s, 1 C) 71.66 (s, 1 C) 73.64 (s, 1 C) 109.37 (s, 1 C) 122.20 (s, 1 C) 126.72 (s, 1 C) 127.18 (s, 1 C) 128.47 (s, 1 C) 131.34 (s, 1 C) 135.15 (s, 1 C) 161.17 (s, 1 C) 171.65 (s, 1 C). LC-MS (ESI): m/z MH^+= 231.

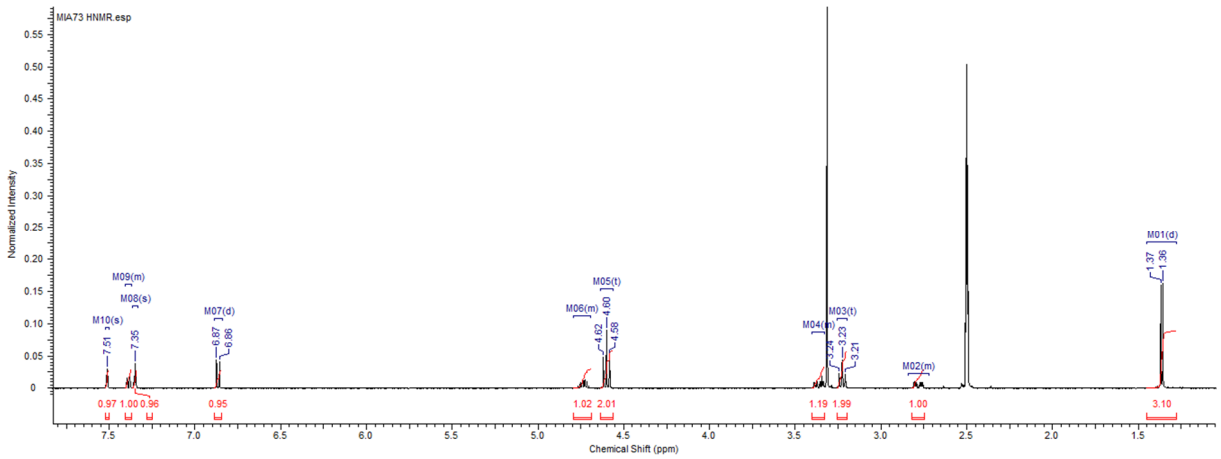

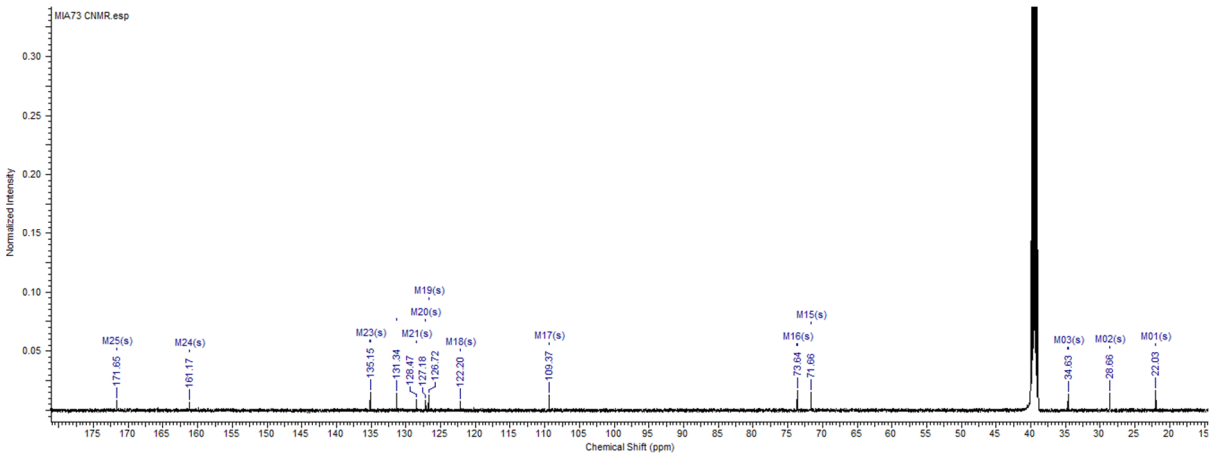

Synthesis of *(E)*-3-(benzo[d]thiazol-6-ylmethylene)dihydrofuran-2(*3H*)-one (7)

To a solution of NaH in toluene dry (0.146 g, 6.1 mmol) add a solution of the γ-butyrolactone (0.253 g, 2.94 mmol, 0.226 mL) and stir it at room temperature overnight. On the further day, add the 1,3-benzothiazole-6-carbaldehyde (0.300 g, 1.83 mmol) dissolved in toluene dry drop by drop in an ice cooled bath. Slowly increase the temperature to reflux until the starting materials are consumed. Cool down, add a solution of H_2SO_4 10% and stir at room temperature for few minutes. Add 10 mL of water and extract 3 times with ethyl acetate (10 mL). Wash the last time with brine and dry the organic phases on Na_2SO_4. After evaporating the solvent *in vacuo*, purify the crude product by chromatography.

Yield: 33%. Mp: 176°C. ^{1}H NMR (300 MHz, CHLOROFORM-*d*) δ ppm 3.35 (td, *J*=7.22, 2.89 Hz, 2 H) 4.53 (t, *J*=7.26 Hz, 2 H) 7.68 (dd, *J*=8.75, 1.68 Hz, 1 H) 7.72 (t, *J*=2.89 Hz, 1 H) 8.12 (d, *J*=1.49 Hz, 1 H) 8.20 (d, *J*=8.75 Hz, 1 H) 9.09 (s, 1 H). ^{13}C NMR (75 MHz, CHLOROFORM-*d*) δ ppm 27.53 (s, 1 C) 65.40 (s, 1 C) 123.71 (s, 1 C) 123.97 (s, 1 C) 124.27 (s, 1 C) 127.77 (s, 1 C) 132.33 (s, 1 C) 134.66 (s, 1 C) 135.91 (s, 1 C) 153.81 (s, 1 C) 155.96 (s, 1 C) 172.22 (s, 1 C). LC-MS (ESI): m/z MH^+= 232.

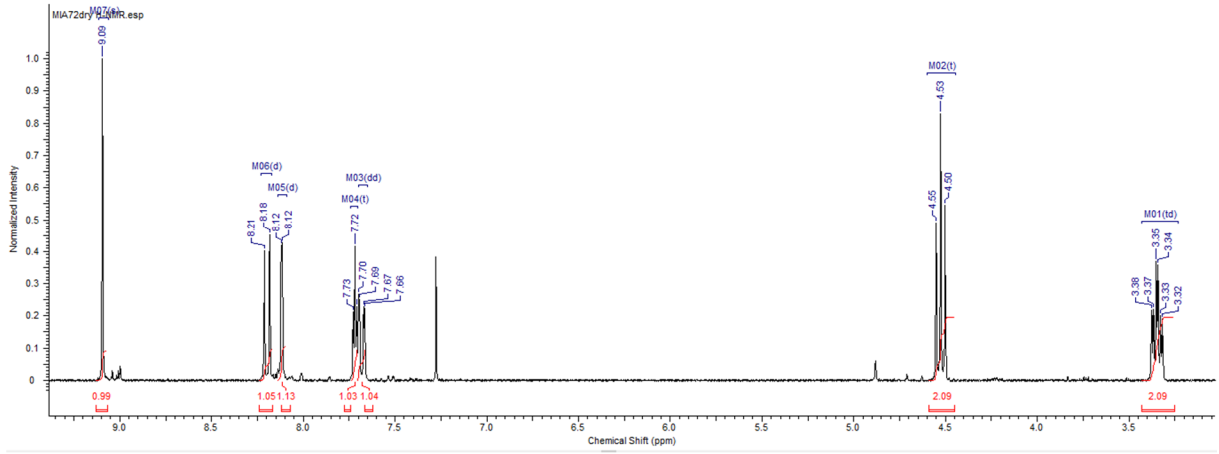

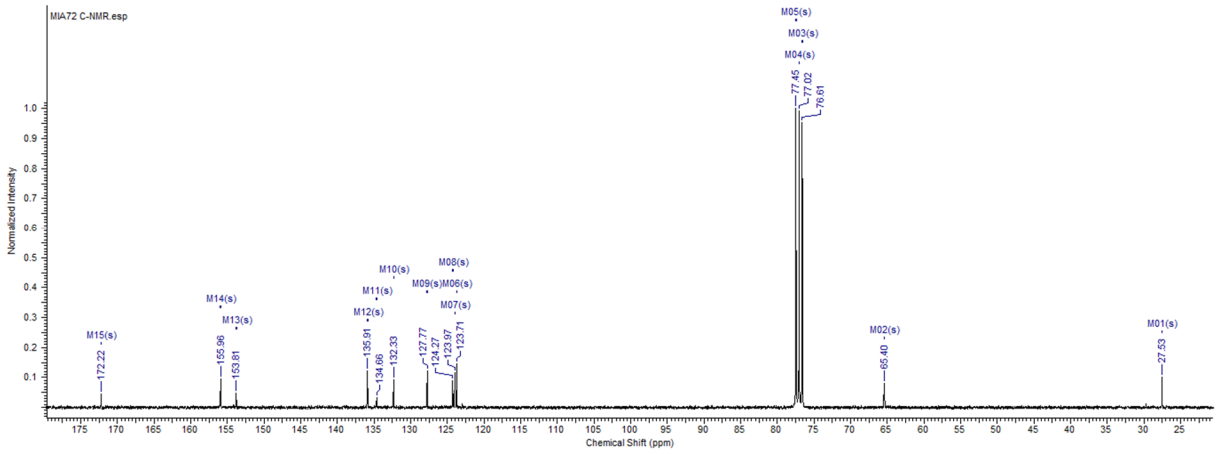

Synthesis of *(E)*-3-((2,3-dihydrobenzo[b][1,4]dioxin-6-yl)methylene)dihydrofuran-2(*3H*)-one (8).

To a solution of NaH in toluene dry (0.146 g, 6.1 mmol) add a solution of the γ-butyrolactone (0.252 g, 0.225 mL, 2.9 mmol) and stir it at room temperature overnight. On the further day, add the 1,4-benzodioxan-6-carbaldehyde (0.300 g, 1.8 mmol) dissolved in toluene dry drop by drop in an ice cooled bath. Slowly increase the temperature to reflux until the starting materials are consumed. Cool down, add a solution of H_2SO_4 10% and stir at room temperature for few minutes. Add 10 mL of water and extract 3 times with ethyl acetate (10 mL). Wash the last time with brine and dry the organic phases on Na_2SO_4. After evaporating the solvent *in vacuo*, purify the crude product by chromatography.

Yield: 19%. Mp: 188°C. ^{1}H NMR (300 MHz, CHLOROFORM-d) δ ppm 3.22 (td, J=7.33, 2.84 Hz, 2 H) 4.28 - 4.38 (m, 4 H) 4.47 (t, J=7.31 Hz, 2 H) 6.89 - 6.98 (m, 1 H) 6.99 - 7.09 (m, 2 H) 7.48 (t, J=2.89 Hz, 1 H). ^{13}C NMR (126 MHz, CHLOROFORM-d) δ ppm 23.07 (s, 1 C) 59.93 (s, 1 C) 60.30 (s, 1 C) 61.05 (s, 1 C) 113.50 (s, 1 C) 114.35 (s, 1 C) 117.00 (s, 1 C) 119.98 (s, 1 C) 124.05 (s, 1 C) 132.03 (s, 1 C) 139.35 (s, 1 C) 140.98 (s, 1 C) 168.47 (s, 1 C). LC-MS (ESI): m/z MH^+ = 233.

Synthesis of *(E)*-3-(benzo[d][1,3]dioxol-5-ylmethylene)dihydrofuran-2(*3H*)-one (9).

Step 1. A solution of piperonyl alcohol (1 g, 6.6 mmol) in dry dichloromethane (10 ml) was added to a solution of Dess-Martin reagent (3.35 g, 7.9 mmol) in dichloromethane (10 ml) at 0°C . The reaction was stirred at room temperature for about 72 hours. After a filtration on celite, the organic solution was extracted 3 times with water. The organic layers were dried on Na_2SO_4 and the solvent was evaporated *in vacuo*, obtaining a brown solid (benzo[d][1,3]dioxole-5-carbaldehyde).

Yield: 96%. Mp: 44°C. ^{1}H NMR (500 MHz, CHLOROFORM-d) δ ppm 6.06 (s, 2 H) 6.91 (d, J=7.88 Hz, 1 H) 7.32 (d, J=1.58 Hz, 1 H) 7.39 (dd, J=7.88, 1.58 Hz, 1 H) 9.79 (s, 1 H). ^{13}C NMR (126 MHz, CHLOROFORM-d) δ ppm 102.09 (s, 1 C) 106.92 (s, 1 C) 108.34 (s, 1 C) 128.66 (s, 1 C) 131.87 (s, 1 C) 148.70 (s, 1 C) 153.09 (s, 1 C) 190.28 (s, 1 C). LC-MS (ESI): m/z MH^+ = 151.

Step 2. To a solution of NaH in toluene dry (0.144 g, 6.0 mmol) add a solution of the γ-butyrolactone (0.275 g, 0.246 mL, 3.2 mmol) and stir it at room temperature overnight. On the further day, add the benzo[d][1,3]dioxole-5-carbaldehyde (0.300 g, 2 mmol) obtained from Step 1, dissolved in toluene dry drop by drop in an ice cooled bath. Slowly increase the temperature to reflux until the starting materials are consumed. Cool down, add a solution of H_2SO_4 10% and stir at room temperature for few minutes. Add 10 mL of water and extract 3 times with ethyl acetate (10 mL). Wash the last time with brine and dry the organic phases on Na_2SO_4. After evaporating the solvent *in vacuo*, purify the crude product by chromatography.

Yield: 26%. Mp: 162°C. ^{1}H NMR (500 MHz, CHLOROFORM-d) δ ppm 3.14 (td, J=7.31, 2.74 Hz, 2 H) 4.39 (t, J=7.31 Hz, 2 H) 5.96 (s, 2 H) 6.79 - 6.84 (m, 1 H) 6.92 (d, J=1.83 Hz, 1 H) 6.97 (dd, J=8.22, 1.52 Hz, 1 H) 7.42 (t, J=2.89 Hz, 1 H). ^{13}C NMR (126 MHz, CHLOROFORM-d) δ ppm 27.39 (s, 1 C) 65.27 (s, 1 C) 101.64 (s, 1 C) 108.81 (s, 1 C) 108.99 (s, 1 C) 121.18 (s, 1 C) 125.99 (s, 1 C) 129.04 (s, 1 C) 136.49 (s, 1 C) 148.27 (s, 1 C) 149.07 (s, 1 C) 172.63 (s, 1 C). LC-MS (ESI): m/z MH^+ = 219.

Synthesis of *(E)*-3-(benzo[d]thiazol-6-ylmethylene)-5-methyldihydrofuran-2(*3H*)-one (10)

To a solution of NaH in toluene dry (0.147 g, 3.68 mmol) add a solution of the γ-valerolactone (0.294 g, 2.94 mmol, 0.280 mL) and stir it at room temperature overnight. On the further day, add the 1,3-benzothiazole-6-carbaldehyde (0.300 g, 1.84 mmol) dissolved in toluene dry drop by drop in an ice cooled bath. Slowly increase the temperature to reflux until the starting materials are consumed. Cool down, add a solution of H_2SO_4 10% and stir at room temperature for few minutes. Add 10 mL of water and extract 3 times with ethyl acetate (10 mL). Wash the last time with brine and dry the organic phases on Na_2SO_4. After evaporating the solvent *in vacuo*, purify the crude product by chromatography.

Yield: 13%. Mp: oil. ^{1}H NMR (300 MHz, CHLOROFORM-*d*) δ ppm 1.53 (d, J=6.33 Hz, 3 H) 2.90 (m, J=7.82, 6.15, 5.22, 2.79 Hz, 1 H) 3.42 - 3.54 (m, 1 H) 4.77 - 4.88 (m, 1 H) 7.67 (m, J=8.57, 1.68 Hz, 1 H) 7.71 (t, J=2.89 Hz, 1 H) 8.11 (d, J=1.30 Hz, 1 H) 8.20 (d, J=8.57 Hz, 1 H) 9.09 (s, 1 H). ^{13}C NMR (75 MHz, CHLOROFORM-*d*) δ ppm 20.03 - 24.27 (m, 1 C) 33.00 - 37.74 (m, 1 C) 73.50 - 74.66 (m, 1 C) 123.30 - 123.80 (m, 1 C) 123.95 (s, 1 C) 125.19 - 126.64 (m, 1 C) 127.03 - 128.64 (m, 1 C) 131.70 - 133.10 (m, 1 C) 135.04 - 136.49 (m, 1 C) 153.13 - 154.15 (m, 1 C) 155.50 - 156.34 (m, 1 C) 171.78 (s, 1 C) 206.30 - 207.89 (m, 1 C). LC-MS (ESI): m/z MH^+= 256.

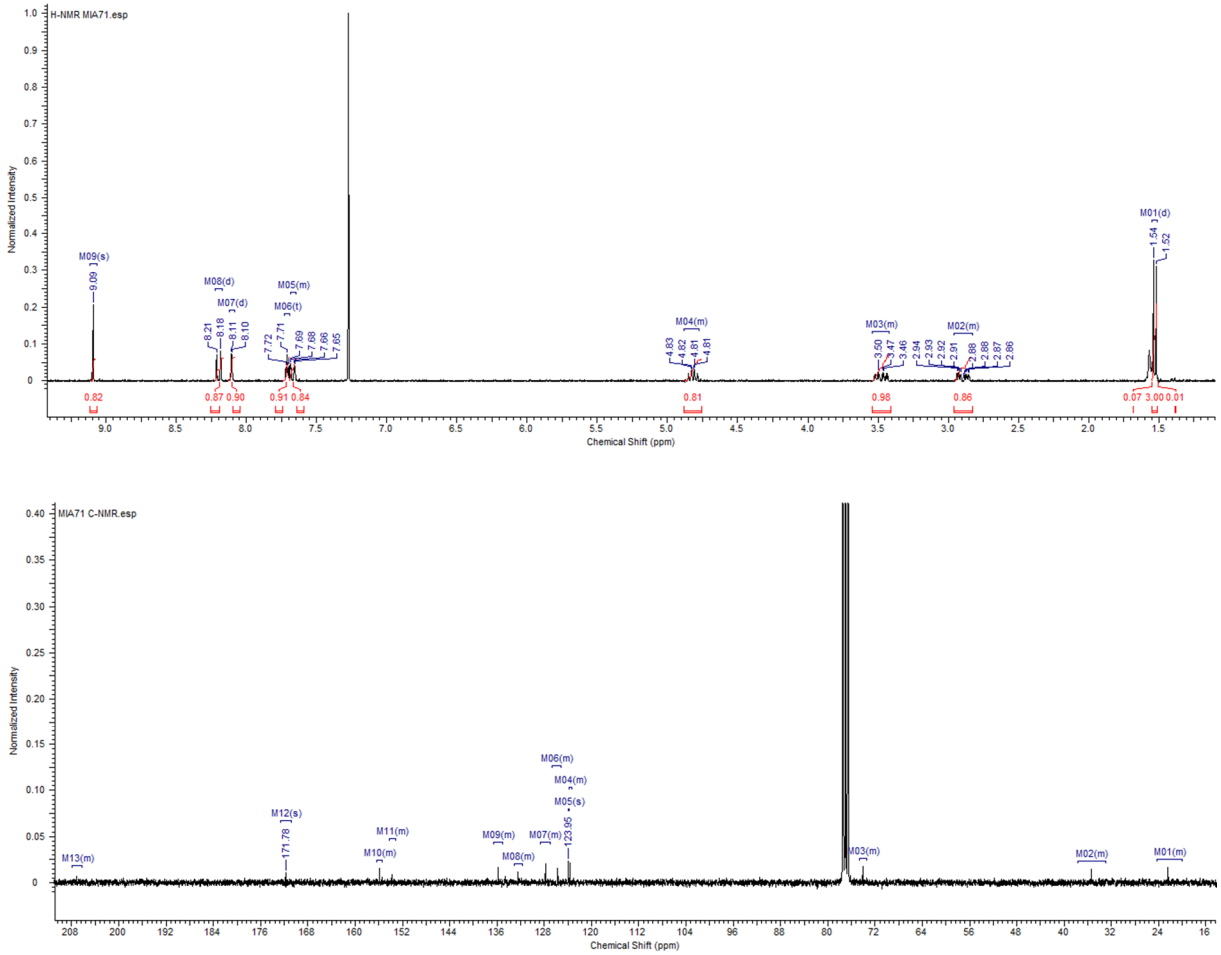

Synthesis of *(E)*-3-(4-methoxybenzylidene)pyrrolidine-2,5-dione (11)

Stir the maleimide (1,000 g, 10.3 mmol) with Ph_3P (2.702 g, 103 mmol) in acetone (10mL) for 1,5h at reflux. Cool down and filter the precipitate obtained**.**

Stir the precipitate (1.055g, 2.94 mmol) with 4-methoxybenzaldehyde (0.400 g, 0.357 mL, 2.94 mmol) in dry methanol (10 mL) at reflux for 48h. Cool down the reaction mixture and filtrate the precipitate through a Buchner funnel. The filter cake was washed with MeOH. Purify the solid by column chromatography.

Yield: 36 %. Mp: 248°C. ^{1}H NMR (500 MHz, DMSO-d_6) δ ppm 3.60 (d, *J*=2.21 Hz, 2 H) 3.81 (s, 3 H) 7.03 (d, *J*=8.83 Hz, 2 H) 7.34 (s, 1 H) 7.58 (d, *J*=8.83 Hz, 2 H) 11.28 - 11.38 (m, 1 H). ^{13}C NMR (126 MHz, DMSO-d_6) δ ppm 34.72 (s, 1 C) 55.32 (s, 1 C) 114.45 (s, 2 C) 124.04 (s, 1 C) 126.77 (s, 1 C) 131.37 (s, 1 C) 132.01 (s, 2 C) 160.41 (s, 1 C) 172.11 (s, 1 C) 175.81 (s, 1 C). LC-MS (ESI): m/z MH^+ =218.

Synthesis of *(Z)*-5-(4-methoxybenzylidene)imidazolidine-2,4-dione (12)

Hydantoine (0.400 g, 4 mmol) was dissolved in 4 mL of water stirring. After complete dissolution, the pH of the mixture was buffered to 7.0 with saturated $NaHCO_3$ solution. Ethanolammine (0.36 mL) was added at the reaction mixture, and the temperature was increased to 90°C gradually. The 4-methoxybenzaldehyde solution (0.544 g, 0.486 mL, 4 mmol) in 4 mL of ethanol was added dropwise with continuous stirring. The

temperature was raised to 120°C and kept under reflux for 48h. On cooling, a precipitate was formed and it was filtered and washed with H_20/EtOH 5:1.

Yield: 26%. Mp: 255°C. ^{1}H NMR (500 MHz, DMSO-d_6) δ ppm 3.79 (s, 3 H) 6.39 (s, 1 H) 6.96 (d, *J*=8.83 Hz, 2 H) 7.59 (d, *J*=8.83 Hz, 2 H) 10.18 - 10.61 (m, 1 H) 10.95 - 11.28 (m, 1 H) ^{13}C NMR (126 MHz, DMSO-d_6) δ ppm 55.25 (s, 1 C) 108.61 (s, 1 C) 114.27 (s, 2 C) 125.42 (s, 1 C) 126.06 (s, 1 C) 131.07 (s, 2 C) 155.63 (s, 1 C) 159.41 (s, 1 C) 165.59 (s, 1 C). LC-MS (ESI): m/z MH^+ = 219.

Synthesis of *(Z)*-4-(4-methoxybenzylidene)thiazolidine-2,5-dione (13)

2,4-thiazolidinedione (0.400 g, 3.415 mmol) was dissolved in water (4 mL) stirring. After complete dissolution, the pH of the mixture was buffered to 7 with sat. $NaHCO_3$ solution. Ethanolammine (0,36 mL) was added at the reaction mixture, and the temperature was increased to 90 °C gradually. The aldehyde (0.465 g, 3.415 mmol, 0.415 mL) solution in EtOH (4 mL) was added dropwise with continuous stirring. The temperature was raised to 120 °C and kept under reflux. After 48 h, cool down the reaction, add 10 ml of water and extract 3 times with ethyl acetate (10 mL). Wash with brine and dry on Na_2SO_4. Dry the solvent *in vacuo*. Add 20 mL of petroleum ether and few mL of water. Filter the precipitate.

Yield: 15%. Mp: 275°C. ^{1}H NMR (300 MHz, METHANOL-d_4) δ ppm 3.86 (s, 3 H) 4.57 (s, 1 H) 7.04 (d, *J*=8.94 Hz, 2 H) 7.52 (d, *J*=8.75 Hz, 2 H) 7.61 (s, 1 H). ^{13}C NMR (126 MHz, DMSO-d_6) δ ppm 39.60 (s, 1 C) 39.76 (s, 1 C) 39.93 (s, 1 C) 40.09 (s, 1 C) 55.32 (s, 1 C) 114.56 (s, 2 C) 127.04 (s, 1 C) 131.22 (s, 2 C) 159.86 (s, 1 C). LC-MS (ESI): m/z MH^+ =236.

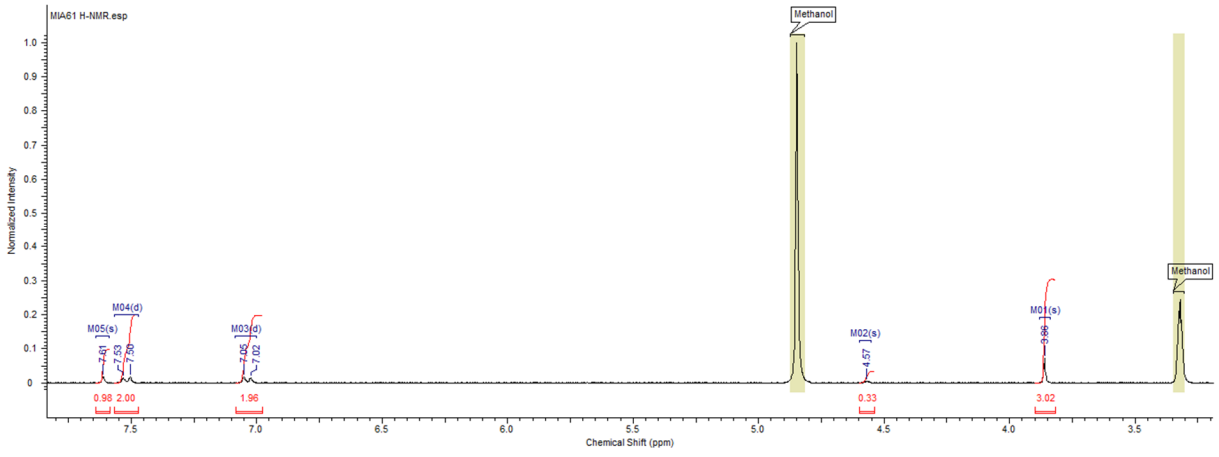

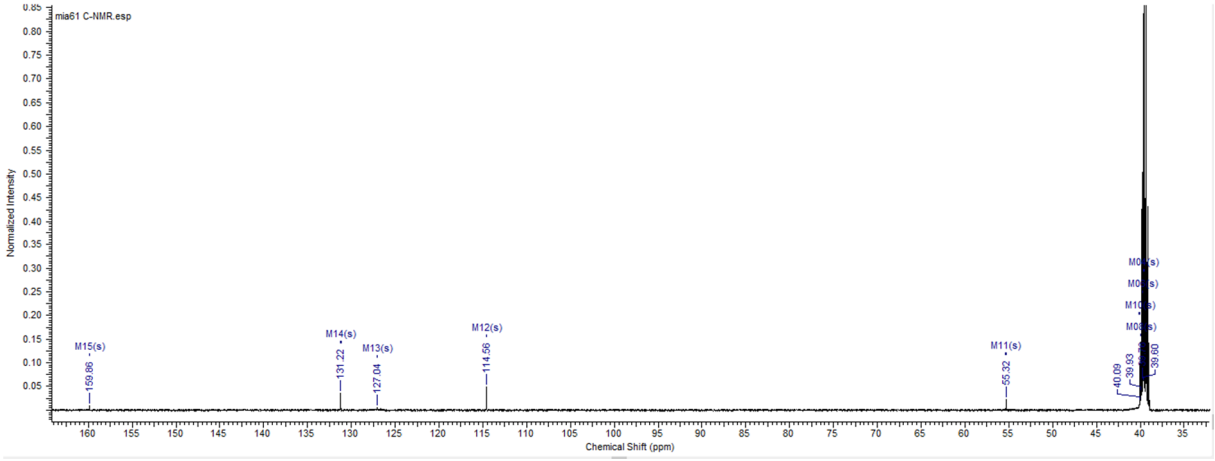

Synthesis of *(E)*-5-(4-methoxybenzylidene)-2-thioxothiazolidin-4-one (14)

To a solution of NaH in toluene dry (0.176 g, 4.4 mmol) add a solution of the rhodanine (0.469 g, 3.5 mmol) and stir it at room temperature overnight. On the further day, add the 4-methoxybenzaldehyde (0.300 g, 2.2 mmol, 0.268 mL) dissolved in toluene dry drop by drop in an ice cooled bath. Slowly increase the temperature to reflux until the starting materials are consumed. Cool down, add a solution of H_2SO_4 10% and stir at room temperature for few minutes. Add 10 mL of water and extract 3 times with ethyl acetate (10 mL). Wash the last time with brine and dry the organic phases on Na_2SO_4. After evaporating the solvent *in vacuo*, purify the crude product by chromatography.

Yield: 8 %. Mp: 255°C. ^{1}H NMR (300 MHz, DMSO-d_6) δ ppm 3.73 - 3.96 (m, 3 H) 7.03 - 7.23 (m, 2 H) 7.55 - 7.60 (m, 2 H) 7.62 (s, 1 H) 13.66 - 13.85 (m, 1 H). ^{13}C NMR (126 MHz, DMSO-d_6) δ ppm 55.55 (s, 1 C) 113.90 (s, 1 C) 115.09 (s, 2 C) 125.49 (s, 1 C) 131.82 (s, 1 C) 132.67 (s, 2 C) 134.09 (s, 1 C) 161.32 (s, 1 C) 194.25 - 196.09 (m, 1 C). LC-MS (ESI): m/z MH^+ =252.

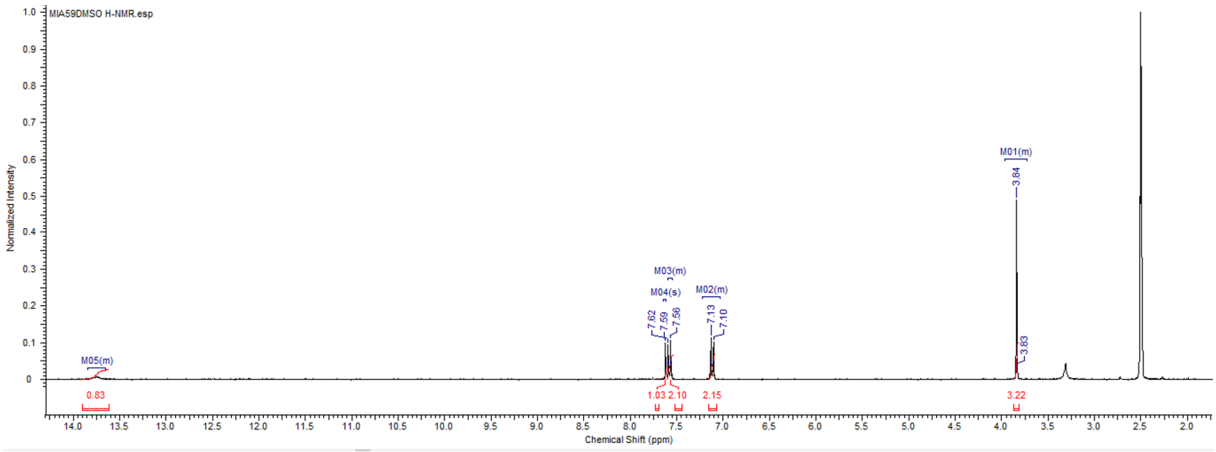

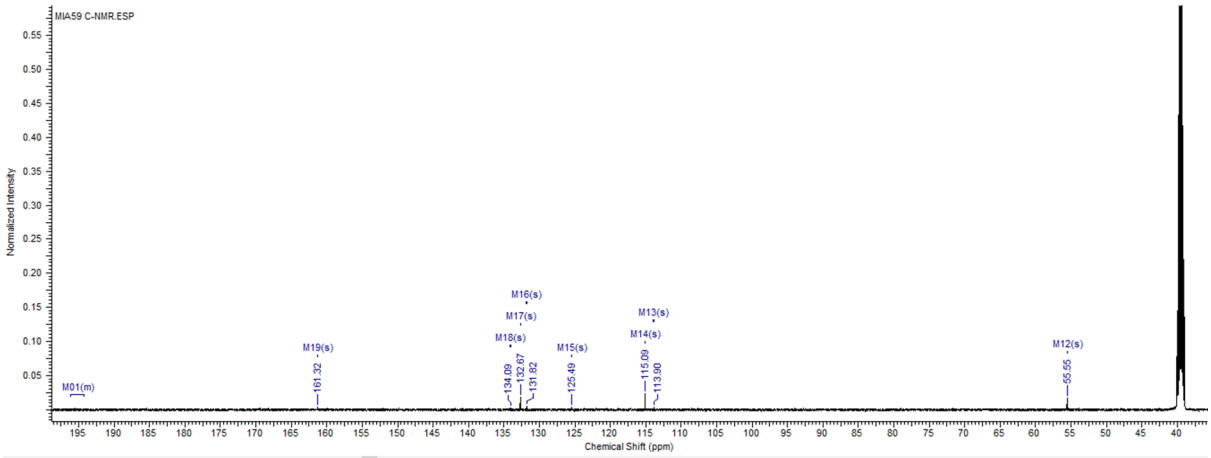

Synthesis of *(Z)*-5-((2,3-dihydrobenzofuran-5-yl)methylene)-2-thioxothiazolidin-4-one (15)

Dissolve the rhodanine (0.09 g, 0.675 mmol), 3-dihydrobenzo-furan-5-carboxaldehyde (0.100 g, 0.675 mmol) and sodium acetate (0.166 g, 2.025 mmol) in 5 mL of acetic acid and cook the solution at 110°C, if necessary under microwave conditions (130W for ~10 minutes). Cool down and collect the precipitate via filtration. Wash with an appropriate solvent to remove all the acetic acid. Dry *in vacuo*.

Yield: 20%. mp: >300°C. ^{1}H NMR (300 MHz, chloroform-d) δ ppm 3.30 (s, 2 H) 3.30 (t, j=8.75 Hz, 2 H) 4.70 (t, j=8.75 Hz, 2 H) 6.90 (d, j=8.29 Hz, 1 H) 7.30 - 7.34 (m, 1 H) 7.35 (s, 1 H) 7.63 (s, 1 H) 8.90 - 9.40 (br, 1 H). ^{13}C NMR (126 MHz, DMSO-d6) δ ppm 28.49 (s, 1 C) 72.13 (s, 1 C) 109.02 (s, 1 C) 110.06 (s, 1 C) 121.35 (s, 1 C) 125.57 (s, 1 C) 127.32 (s, 1 C) 129.47 (s, 1 C) 132.42 (s, 1 C) 132.63 (s, 1 C) 162.31 (s, 1 C) 195.48 (s, 1 C). LC-MS (ESI): m/z MH^{+}= 264.

Synthesis of *(Z)*-5-(benzo[*d*]thiazol-6-ylmethylene)-2-thioxothiazolidin-4-one (16)

Described in the Methods section of the main text.

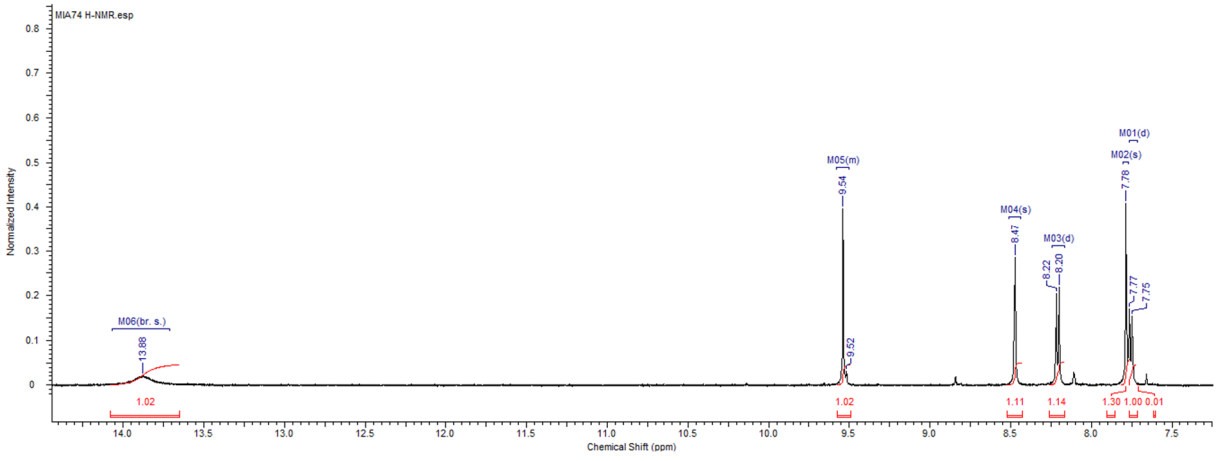

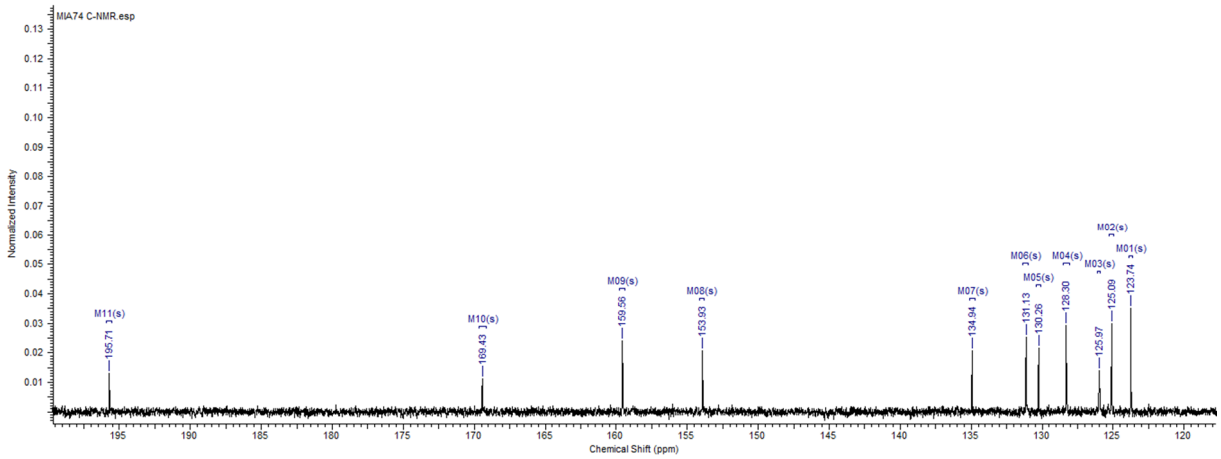

Synthesis of *(Z)*-5-(quinolin-6-ylmethylene)-2-thioxothiazolidin-4-one (17)

Described in the Methods section of the main text.

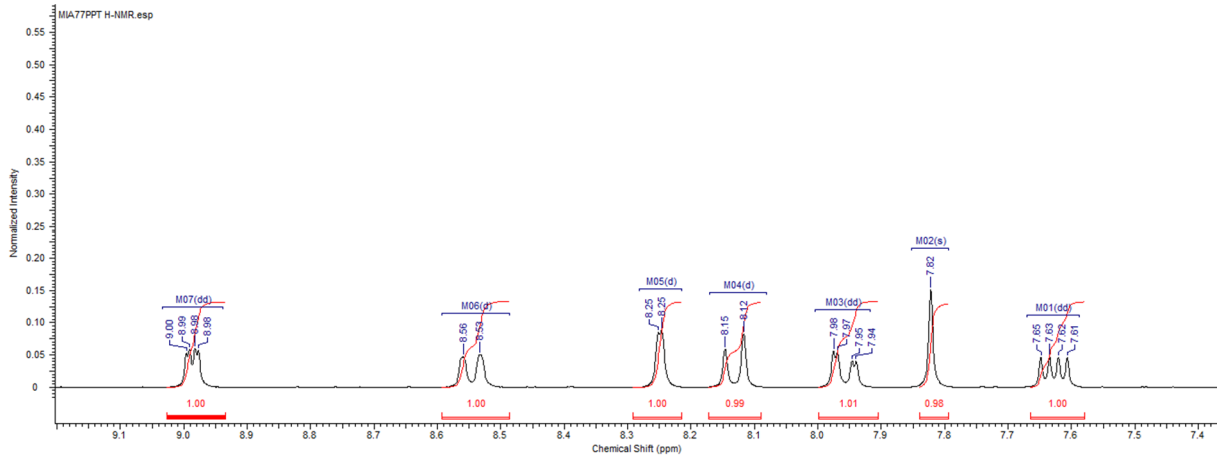

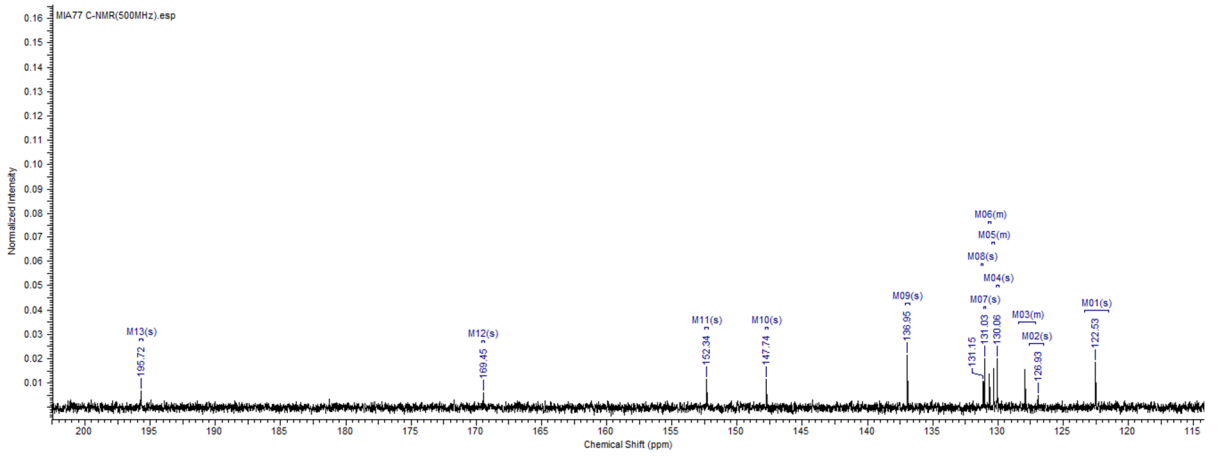

Synthesis of *(Z)*-5-(benzo[*d*]thiazol-6-ylmethylene)-2-thioxoimidazolidin-4-one (18)

2-thiohydantoin (0.213 g, 1.84 mmol), 1,3-benzothiazole-6-carbaldehyde (0.300 g, 1.84 mmol) and sodium acetate (0.452 g, 5.51 mmol) were used following the general procedure A described above. Yield: 22%. mp: >300°C. ^{1}H NMR (500 MHz, DMSO-d_6) δ ppm 6.63 - 6.65 (m, 1 H) 7.81 - 7.87 (m, 1 H) 8.07 - 8.12 (m, 1 H) 8.59 - 8.63 (m, 1 H) 9.47 (s, 1 H) 12.22 - 12.28 (m, 1 H) 12.40 - 12.46 (m, 1 H) ^{13}C NMR (126 MHz, DMSO-d_6) δ ppm 110.76 (s, 1 C) 123.03 (s, 1 C) 123.62 (s, 1 C) 128.36 (s, 1 C) 128.63 - 129.03 (m, 1 C) 134.30 (s, 1 C) 143.35 (s, 1 C) 152.87 - 153.40 (m, 1 C) 157.91 (s, 1 C) 165.75 (s, 1 C) 179.31 (s, 1 C). LC-MS (ESI): m/z MH^+= 262.

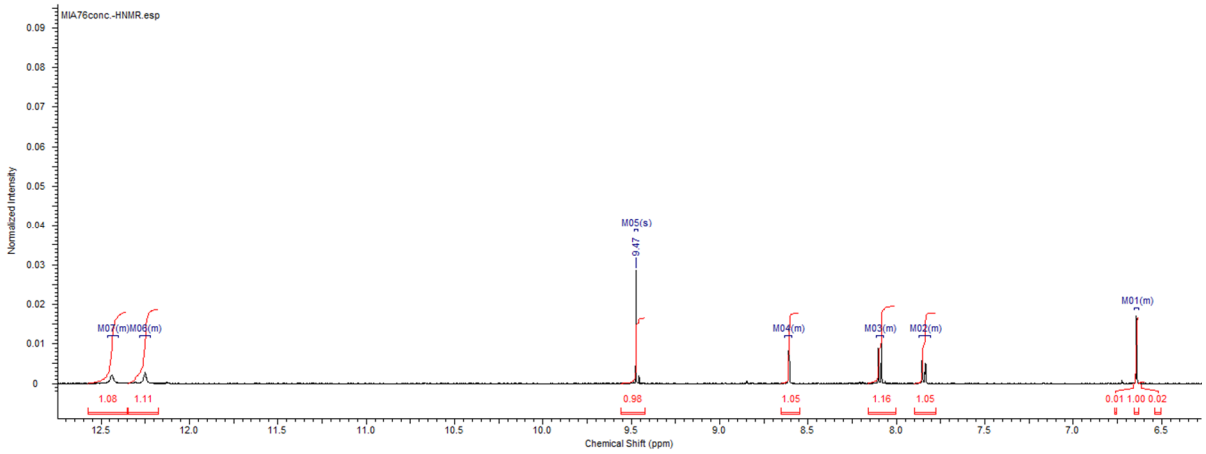

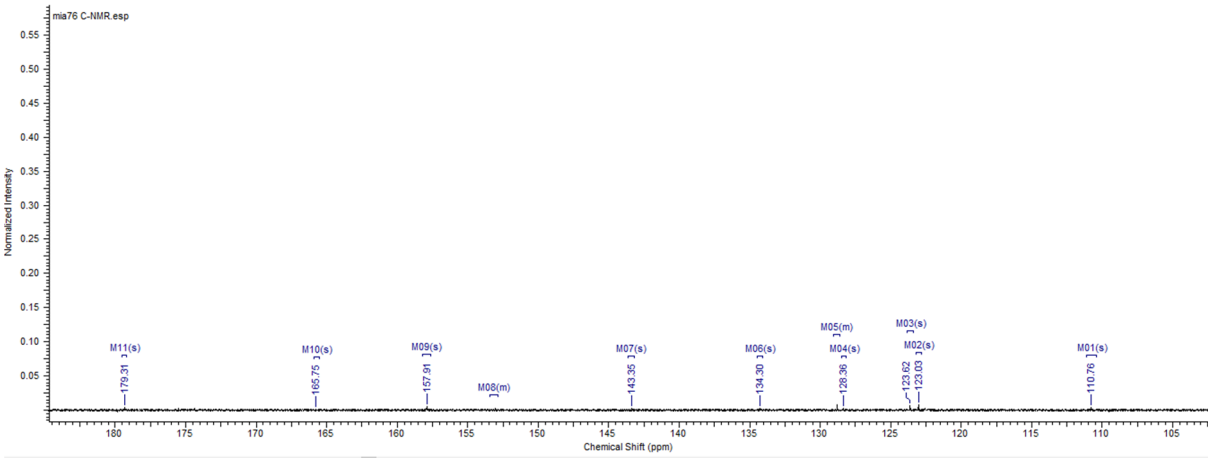

B2. Supplementary Tables

B2.1. Table S1. Selectivity of compounds 6 and 17 against a panel of selected protein kinases[a] covering all kinase families from the kinome tree.

Kinase family	Kinase	6	17
		% inhibition @ 5 µM (IC_{50} [nM])[b]	% inhibition @ 1 µM (IC_{50} [nM])[b]
CMGC	Clk2	65%	80%
	Clk3	44%	95% (86.6)
	Clk4	98% (31.8)	97% (17.8)
	CDK5/p25	n.i.	n.i.
	DYRK3	7%	84%
	DYRK4	n.i.	39%
	GSK3B (GSK3 beta)	8%	10%
	HIPK1 (Myak)	n.i.	33%
	MAPK14 (p38 alpha)	n.i.	6%
	MAPK8 (JNK1)	14%	7%
CAMK	PIM2	n.i.	31%
	CAMK2A (CaMKII alpha)	n.i.	7%
	MLCK (MLCK2)	12%	89% (157)
	MYLK (MLCK)	n.i.	48%
	MYLK2 (skMLCK)	n.i.	35%
	MKNK1 (MNK1)	-	44%
	MKNK2 (MNK2)	-	34%
TKL	MAP3K9 (MLK1)	n.i.	2%
	ACVR1 (ALK2)	-	37%
	RIPK2	-	83%
STE	MST4	n.i.	n.i.
AGC	PRKACA (PKA)	n.i.	n.i.
	PRKD2 (PKD2)	n.i.	19%
TK	ABL1	6%	14%
	NTRK2 (TRKB)	n.i.	3%
	EGFR	n.i.	n.i.
	ROS1	n.i.	5%
CK1	CSNK1D (CK1 delta)	n.i.	11%
	CSNK1E (CK1 epsilon)	n.i.	1%
	CSNK1G2 (CK1 gamma 2)	n.i.	43%
	CSNK1G3 (CK1 gamma 3)	n.i.	17%

[a]The screening list was especially composed to include all kinases that were frequently reported as off-targets for diverse chemical classes of Dyrk inhibitors [69,70,72,83,84] (complemented by Tables 1 and 2 in the main part). [b]Data represent mean values of duplicates that differed by less than 7%. IC_{50}s were only determined when the % inhibition was greater than 85%. Inhibition rates ≥ 80% are highlighted.

B2.2. Table S2. Involvement of the target kinases of compound 17 in the pathology of glioblastoma according to current literature.

Kinase	Involvement in glioblastoma pathology
STK17A	STK17A was found to be among the top 1–5% overexpressed genes in glioblastoma (along with EGFR) in several independent studies [85–87], [a–b] In addition, STK17A was among the top 1% of genes showing the highest gain of copy numbers in glioblastoma [88]. The overexpression in gliomas vs. healthy cells also correlated with the tumor grade [89]. Further recent studies provided evidence for a causal role of STK17A in the neoplastic transformation of glial cells [90,91].
CK2α	Particularly abundant in the brain and recently reported to be a promising target in glioblastoma [19].
Clk1	Clk1 mRNA is overexpressed in several types of brain cancer[b] and specifically upregulated in temozolomide–resistant glioblastoma [92,93]. These and other studies [94] pointed to a role of Clk1 in chemoresistance.

[a]Data were analyzed using the Oncomine web portal (http://www.oncomine.org).

[b]TCGA brain study, http://tcga-data.nci.nih.gov/tcga/ The Cancer Genome Atlas – Glioblastoma Multiforme Gene Expression Data (http://tcga-data.nci.nih.gov/tcga/)

B2.3. Table S3. Inhibition of U87MG cell growth by the multi-targeted inhibitors 14, 15, 16, 17 and AS605240.

compound	IC_{50} (µM)[a,b]
14	9.5
15	5.6
16	0.56
17	0.20
AS605240	0.32
harmine	7.2

[a]Values represent averages from three independent experiments with concentrations tested in triplicate; S.D. <15%. [b]measured in the presence of 1% fetal calf serum.

B3. Supplementary method

B3.1. MTT cell growth assay

U87MG glioma cells were seeded in a 96 well plate (5,000 cells per well) and allowed to adhere overnight in Dulbecco´s Modified Eagles Medium (DMEM, Sigma-Aldrich), supplemented with pen/strep (Invitrogen) and 10% fetal calf serum (FCS, Sigma-Aldrich). The following day, the medium was exchanged by DMEM with pen/strep mix and 1% FCS, also containing the test compounds in the desired concentrations (100 µl volume). The cells were grown for four days at 37 °C in a humidified incubator containing 5 % CO_2, without further change of medium. After that, 20 µL of a solution of 3-[4, 5-dimethylthiazol-2-yl]-2,5-diphenyltetrazolium bromide (MTT, Sigma) (5 mg/mL in PBS) was added to each well, the plate incubated again at 37°C for 30 – 40 min, followed by the addition of 100 µl of 10 % SDS/ 0.1 N HCl solution to solubilize the formazan dye. The plate was shaken for 3 h at 37°C, and the absorbance at 600 nm measured in a plate reader (BMG labtech, Germany). DMSO in the same total concentration as in the wells with compounds (≤ 0.2 %) was used as a reference for no inhibition, and medium without cells was treated with the same reagents to obtain the background.

4. Additional results not included in the papers

In our project we developed a new in vitro assay for testing the Dyrk1A inhibitory activity in cells. For this purpose we employed HEK293-tau-Dyrk1A cells, obtained by co-transfection of the HEK293-Dyrk1A cell line with an EGFP-tau plasmid using the DNA-complexing factor PEI in a specific ratio and the selecting agent geneticin G418 (Figure 4 and Scheme 1). The transcription of Dyrk1A was depending on tetracycline's concentration (Table 1) and the specific phosphorylation on the tyrosine residue T212 on the tau protein was followed using a specific antibody (Figure 5).

Conc. tetracycline (µg/ml)	GFP Fluorescence
-	3516
0,01	3335
0,02	4266
0,05	7516
0,07	9451
0,1	12880
0,2	34263
0,3	34739
0,5	34717
0,7	34738
1	34179

Table 1. Study on the variation of GFP fluorescence with increasing concentrations of tetracycline. For our experiments we used 0.3 µg/mL of tetracycline as it was the lowest concentration which gave an appreciably fluorescence level. Fluorescence was given by GFP-Dyrk1A, obtained using a plasmid containing the sequence for the GFP-tau fusion protein in the HEK 293 cells.

a) b)

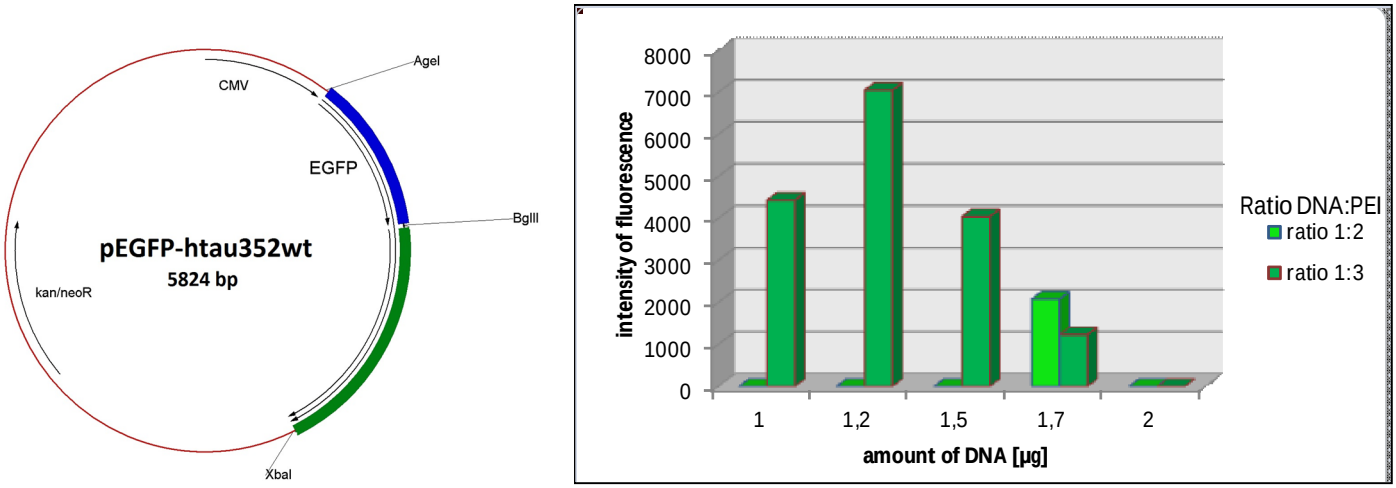

Figure 4. a) Representation of the pEGFP-htau plasmid. b) Graphical representation of the study of DNA/PEI ratio. We used the ratio 1:3 and 1.2 µg of DNA in our experiments as it gave the highest intensity of fluorescence. (EGFP = enhanced green fluorescent protein)

a) b)

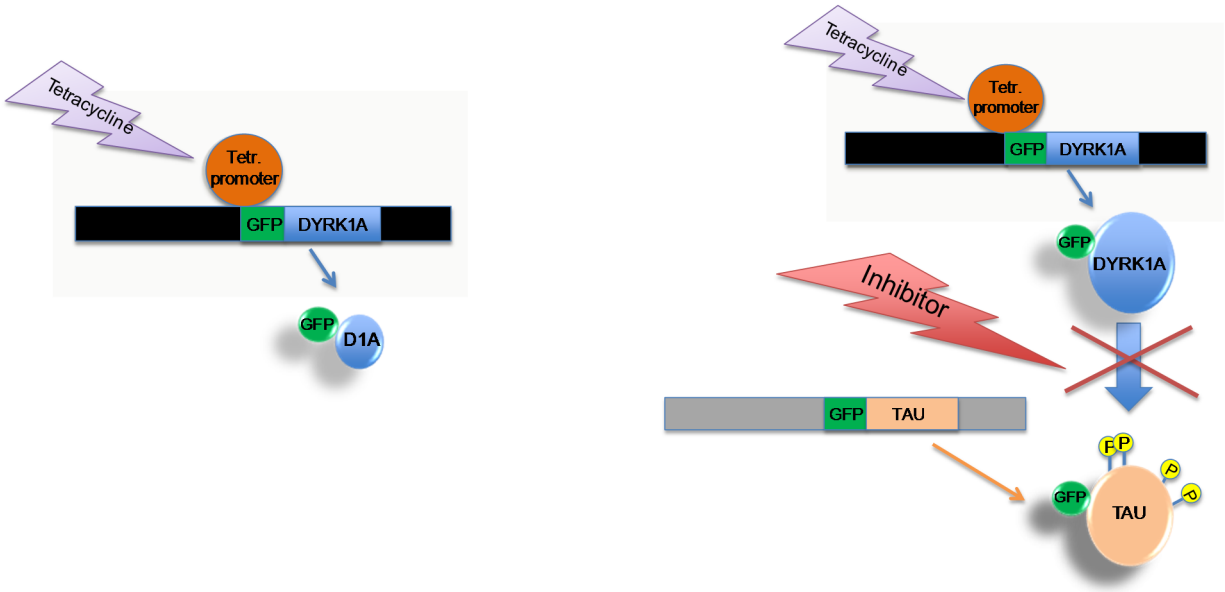

Scheme 1. a) Tetracycline activates a tetracycline promoter on the plasmid and the transcription of fluorescent-Dyrk1A is enabled. b) Dyrk1A phosphorylates the GFP-tau protein. The inhibitor blocks this process, thus reducing the signal detected by the phosphospecific antibody.

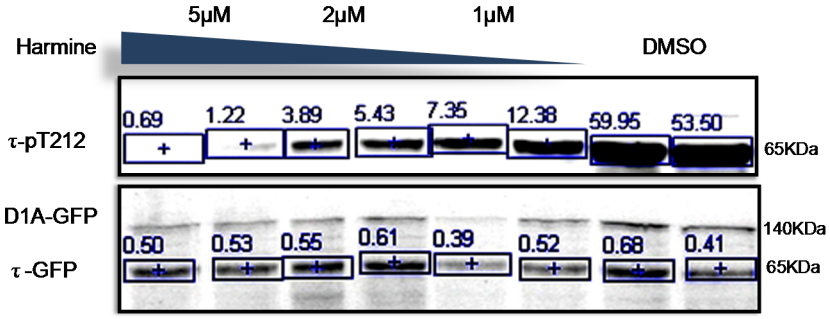

Figure 5. The tau protein phosphorylation at Threonine 212 in the HEK293-tau-Dyrk1A cells is dependent on Dyrk1A and can be fully suppressed by Harmine. Increasing concentrations of Harmine reduce progressively the signal of the bands in comparison with DMSO control. The tau-GFP signal due to the GFP-antibody is approximately the same in each well, therefore tau-pT212 signals don't need to be normalized except in one lane.

The activity towards beta-amyloid aggregation was checked using a $A\beta_{40}$ peptide aggregation assay mainly because of its slower kinetics. This assay, developed by Cellamare et al. [78], is based on the production of a fluorescent signal depending on the aggregation state using Thioflavin T and hexafluoroisopropanol as aggregation enhancer.

Dyrk1A activity was analyzed using a radioactive assay based on the phosphorylation of a woodtide peptide with γ^{32}-ATP. The phosphorylation state of the peptide was checked measuring the radioactivity level, in comparison with a DMSO control and a Harmine control. Different concentrations of our compounds were incubated in the reaction in order to obtain an IC_{50} value calculated using Origin Pro by OriginLabs (Figure 6).

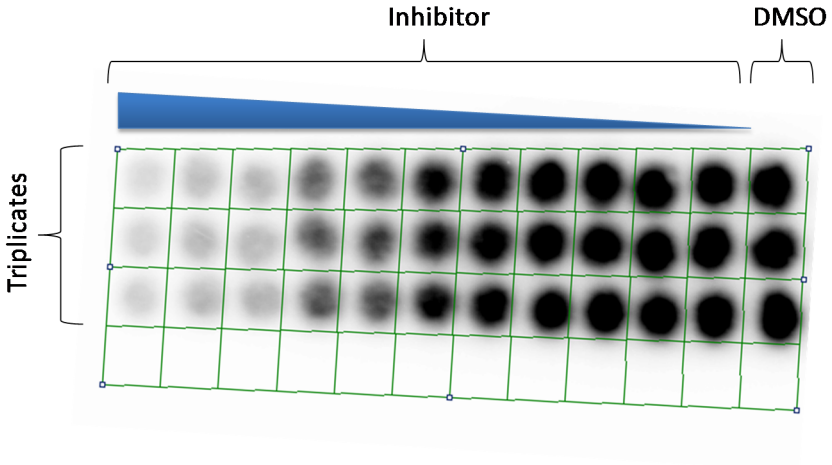

Figure 6. Example of determination of IC_{50} using the radioactivity test. Each spot represents a reaction performed at increasing concentrations in triplicates. Last column corresponds to DMSO control. Spot intensities decrease with the increasing of concentration of the kinase inhibitor.

5. Conclusions

It is currently believed that multi-factorial diseases such as cancer or neurodegenerative disorders cannot be treated with single molecular target drugs but with a combination of multiple-targets compounds that act simultaneously against such complex disease systems. This approach is fundamental to avoid drug resistance and it is becoming a common strategy in several important therapies.

This study was focused on the research of new drugs for the treatment of Alzheimer's disease (also in combination with Down Syndrome) and glioblastoma – both having in common that Dyrk1A plays a pathogenic role. These pathologies are very complex and they are known to be multi-factorial. It is therefore fundamental to use a multi-target strategy in order to attack the disease on different sides and better block its development.

Our panel of compounds successfully reached the goal of stopping some fundamental pathogenic processes *in vitro*, which are known to be relevant for the progression of the above mentioned diseases on different sides.

Publication A

In the first part of our project we were able to identify compounds from a panel of bis(hydroxyphenyl)thiophenes, that were able to interfere with the two major AD processes: beta-amyloid formation and tau phosphorylation through Dyrk1A. In particular, our best compound **8** showed a good inhibitory profile as it balances with success both inhibitory activities (Table 2) and it may represent an ideal dual selective compound for the treatment of the two major pathogenic mechanisms of Alzheimer's disease. The results obtained in the cell-free assays were confirmed in the cell-based assays, newly developed during this project (see "Additional results not included in the papers"). Using this assay, we were able to test compounds specifically inhibiting the tau phosphorylation by Dyrk1A in intact cells.

The design strategy was developed starting from the identification of a hit compound after screening an in-house library and considering the similarity of the hit compound to a reported binder of Aβ peptide aggregates. The optimization of compound **1** (Table 2) was focused on the purpose of reaching a good potency on both targets and on increasing selectivity towards all off-target kinases. Systematic variation of the position and nature of substituents on the two aromatic rings, generated a set of compounds which were tested against our two targets.

For Dyrk1A inhibition, none of the optimized compounds reached the inhibitory level of the hit compound. Nevertheless, a big improvement on the Aβ inhibition was observed introducing a methyl group in meta- and an hydroxyl group in para-position of both aromatic rings of the molecule (see Table 2).

A critical point for achieving good pharmacokinetic properties is the presence of a phenolic moiety in the structure of our inhibitors. Nevertheless, hydroxyl functions might be replaced bioisoterically in future optimizations or used to create ester prodrugs to allow the permeation through the blood brain barrier.

Name	**Structure**	**Dyrk1A IC_{50} (μM)[a),b)]**	**$Aβ_{40}$ % inhibition at 100μM (IC_{50}±SEM, μM)[c)]**	**Inhibition of tau phosphorylation in cells (IC_{50}, μM) [c)]**
1	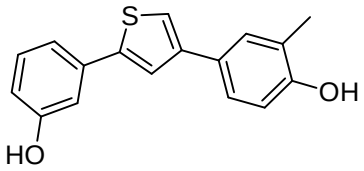	1.8	46±2	n.d.
8	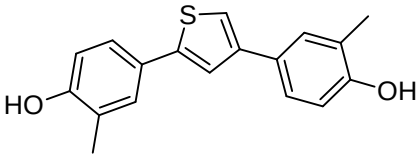	5.0	91±1 (11±3)	8.3

Table 2. Inhibitory activities of the hit compound **1** and the best compound **8** with a more balanced profile.

[a)] S.D.<10%; [b)] [ATP]= 100μM; [c)] S.D. < 15%; n.d. = not determined

Publication B

In the second part of our study we synthesized and tested a small library of benzylidene compounds which turned out to be potent and selective inhibitors of Dyrk1A, Clk1 and Ck2. Systematic variation of the heterocycles was important for modifying the mode of interaction with the enzyme and the physico-chemical properties of the molecules. Despite of the low molecular weight of our compounds, these modifications led to distinct kinase selectivities and potencies. The small size of the inhibitors as well as the presence of maximum one H-bond donor could be highly favorable also for the possible blood-brain barrier penetration.

Compound **6** was showing a high Dyrk1A inhibition (Table 3), but most importantly the best selectivity profile towards its closest homolog Dyrk1B (which differs from Dyrk1A for one amino acid in the ATP binding site) with a selectivity factor of 15.5 vs. 1.4 of the reference compound harmine. Therefore we were able to remarkably increase our selectivity towards other members of the Dyrk1A kinase family. Given the high homology between the two kinases, the degree of selectivity towards Dyrk1B was remarkable.

Our compound **7** displayed the most promising activity in our cell–based tau phosphorylation assay (Table 4). Furthermore it was not toxic toward HEK293 cells at concentrations up to 20 µM. Hence, it could be promising as co-inhibitor of Dyrk1A and Clk1/4 for the treatment of Alzheimer's disease.

Compounds **16** and **17** were not very selective towards several off-target kinases but they showed a very high potency especially against PI3K (Table 3), which is not surprising given their similarity with the previously reported thiazolidinedione AS605240[95]. Thus, we were able to identify the first compounds that inhibited oncogenic protein kinases along with the PI3 lipid kinases. The inhibition of this lipid kinase, together with the co-inhibition of Dyrk1A, blocks glioblastoma cell proliferation *via* two different pathways, thus increasing the potency for the treatment of this pathology (Figure 7).

Compound **17** might be an interesting agent against glioblastoma as it also inhibits STK17A, Ck2α and Clk1 (Table 3). These three kinases are highly expressed in glioblastoma cells (see Table S2 in the Supplementary Material of Publication B), so their simultaneous inhibition could be very effective for the regression of the pathology. Our goal to have a multi-target drug was successfully achieved with this compound. As shown in Figure 7, our inhibitor can block the tumors by blocking two kinases, hence two different pathways creating a synergistic action which could lead to an increased inhibitory efficacy.

Name	Structure	Dyrk1A	Clk1	Ck2α	STK17A	PI3K-p110-α	PI3K-p110-δ	PI3K-p110-γ
		IC_{50} (µM)[a]			(% inhibition / IC_{50}[b] [nM])			
6	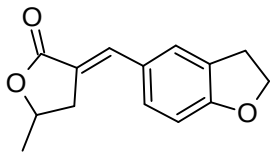	0.17 (**Dyrk1B:** 2.64)	0.43	>10	28%[c]	84%[c] (650)	73%[c]	75%[c]
7	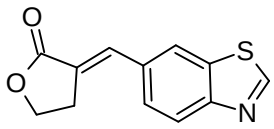	0.13	0.06	>10	n.d.	90%[c]	77%[c]	79%[c]
16	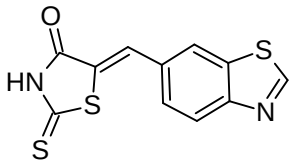	0.04	0.1	0.06	n.d.	98%[d] (2.2)	90%[d] (12.4)	97%[d] (2.3)
17	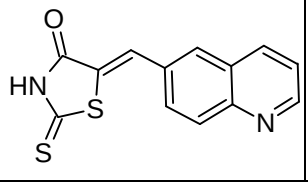	0.02	0.2	0.04	97%[d] (12.8)	100%[d] (2.6)	97%[d] (16.1)	97%[d] (2.3)

Table 3. Inhibitory activities of our best compounds **6**, **7**, **16** and **17**. n.d.= not determined; AS = AS605240

[a] S.D. ≤ 18%, [ATP]= 100µM; [b] data were calculated based on mean values of duplicates that differed by less than 7%; [c] % inhibition at 5 µM; [d] % inhibition at 1 µM; [c),d)] shown are mean values of two different measurements performed in duplicates (S.D. ≤ 2.5%).

Compound	6	7	16	17
IC_{50} (µM)[a]	2.1±0.06	0.2±0.01	2.1±0.25	1.4±0.43

Table 4. Inhibitory activities of our best compounds **6**, **7**, **16** and **17** of Dyrk1A-catalyzed tau Thr212 phosphorylation in stably transfected HEK293 cells; AS = AS605240

[a] IC_{50} values were calculated on triplicates, referring to the DMSO-treated cells signal (100%); ±S.D.

This study also included the analysis of the metabolic stability of our best compounds in rat plasma (see Table 4 of Publication B), which was successfully proved giving a long half-life profile for all compounds (more than 101 minutes for the less stable compound **16**), similar to the reference drug Diltiazem (half-life of 125 minutes) compared to the esterase-sensitive control compound N-acetyl-L-phenylalanine (less than five minutes). The stability in rat liver microsomes, however, requires optimization (half-life for **6** and **16**, 20 and 30 minutes respectively, data not shown).

The anti-proliferative activity of our best inhibitors has also been tested on U87MG glioma cell line giving an IC_{50} in the micromolar range (see Table S3 in Supplementary Material of Publication B) and, for some of them, we reached a nanomolar potency. This experiment was performed using MTT and the absorbance was measured in a plate reader, as described in the Supplementary Material §3.1 of Publication B.

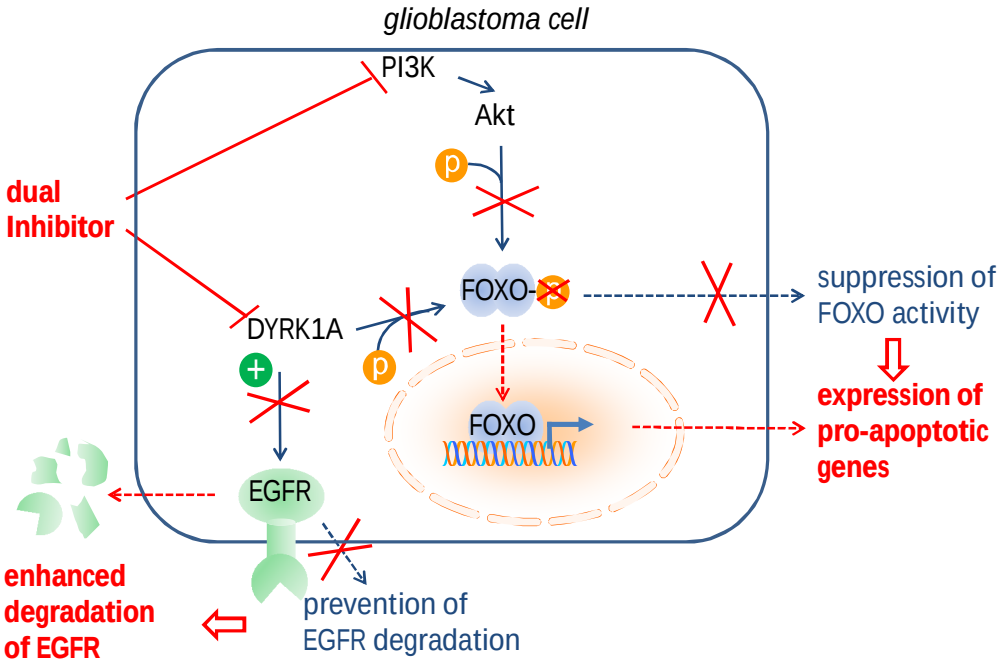

Figure 7. Anticipated synergistic anti-tumor effects (in red) based on dual PI3K/Dyrk1A inhibition in glioblastoma. The PI3K pathway is an established drug target in glioblastoma. Concomitant inhibition of Dyrk1A is expected to enhance the activation of FOXO, which leads to the induction of pro-apoptotic genes. Furthermore, the stabilizing effect on EGFR by Dyrk1A is abolished, thus decreasing the EGFR–mediated oncogenic signaling.

Overall, our compounds were shown to inhibit several targets involved in the development of some of the most malignant and invalidating neurological pathologies of the last decades: Alzheimer's disease and glioblastoma tumors.

6. Abbreviations

Aβ	Amyloid β
AchE	Acetylcholinesterase E
AD	Alzheimer's Disease
ALS	Amyotrophic Lateral Sclerosis
ApoE	Apolipoprotein E
APP	Amyloid Precursor Protein
CDK	Ciclin Dependent Kinase
CK	Casein Kinase
CLK	CDC-like kinase
CREB	cAMP response element-binding protein
DS	Down Syndrome
DSCR	Down Syndrome Critical Region
DYRK	Dual Specificity Tyrosine Kinase
FGFR	Fibroblast Growth Factor Receptor
FTD	Frontotemporal Dementia
GBM	Glioblastoma Multiforme
GFP	Green Fluorescent Protein
GPCR	G-protein Coupled Receptor
GSK	Glycogen Synthase Kinase
HBA	H-bond Acceptor
HD	Huntington's Disease
HFIP	Hexafluoroisopropanol
HGG	High-Grade Glioma
HRM	Harmine
LBD	Lewy Body Dementia
MAO	MonoAmino Oxidase
MAP	Mitogen-Activated Protein
n.d.	not determined
n.i.	no inhibition
NFAT	Nuclear Factor of Activated T-cells
NFT	Neurofibrillary tangle
NLS	Nuclear Localization Signal
PD	Parkinson Disease
PDGFR	Platelet-derived growth factor receptor
PEI	Poliethylenimine
PI/PIP	Phosphoinositol/Phosphoinositol phosphate
PIK	Phosfonotidil kinase
PK	Protein Kinase
PS	Presenilin
PSP	Progressive Supranuclear Palsy
ROS	Reactive Oxygen Species
SD	Standard Deviation
SR	Serine-arginine Rich
ThT	Thioflavin T

7. References

(1) Guimerá, J.; Casas, C.; Pucharcòs, C.; Solans, a; Domènech, a; Planas, a M.; Ashley, J.; Lovett, M.; Estivill, X.; Pritchard, M. a. A Human Homologue of Drosophila Minibrain (MNB) Is Expressed in the Neuronal Regions Affected in Down Syndrome and Maps to the Critical Region. *Hum. Mol. Genet.* **1996**, *5* (9), 1305–1310.

(2) Jin, K.; Park, S.; Ewton, D. Z.; Friedman, E. The Survival Kinase Mirk/Dyrk1B Is a Downstream Effector of Oncogenic K-Ras in Pancreatic Cancer. *Cancer Res.* **2007**, *67* (15), 7247–7255.

(3) Hu, J.; Nakhla, H.; Friedman, E. Transient Arrest in a Quiescent State Allows Ovarian Cancer Cells to Survive Suboptimal Growth Conditions and Is Mediated by Both Mirk/dyrk1b and p130/RB2. *Int. J. cancer* **2011**, *129* (2), 307–318.

(4) Deng, X.; Mercer, S. E.; Shah, S.; Ewton, D. Z.; Friedman, E. The Cyclin-Dependent Kinase Inhibitor p27Kip1 Is Stabilized in G(0) by Mirk/dyrk1B Kinase. *J. Biol. Chem.* **2004**, *279* (21), 22498–22504.

(5) Zou, Y.; Ewton, D. Z.; Deng, X.; Mercer, S. E.; Friedman, E. Mirk/dyrk1B Kinase Destabilizes Cyclin D1 by Phosphorylation at Threonine 288. *J. Biol. Chem.* **2004**, *279* (26), 27790–27798.

(6) Gao, J.; Zhao, Y.; Lv, Y.; Chen, Y.; Wei, B.; Tian, J.; Yang, Z.; Kong, F.; Pang, J.; Liu, J.; Shi, H. Mirk/Dyrk1B Mediates G0/G1 to S Phase Cell Cycle Progression and Cell Survival Involving MAPK/ERK Signaling in Human Cancer Cells. *Cancer Cell Int.* **2013**, *13* (1), 2.

(7) Deng, X.; Ewton, D. Z.; Friedman, E. Mirk/Dyrk1B Maintains the Viability of Quiescent Pancreatic Cancer Cells by Reducing Levels of Reactive Oxygen Species. *Cancer Res.* **2009**, *69* (8), 3317–3324.

(8) Taira, N.; Nihira, K.; Yamaguchi, T.; Miki, Y.; Yoshida, K. DYRK2 Is Targeted to the Nucleus and Controls p53 via Ser46 Phosphorylation in the Apoptotic Response to DNA Damage. *Mol. Cell* **2007**, *25* (5), 725–738.

(9) Taira, N.; Mimoto, R.; Kurata, M.; Yamaguchi, T.; Kitagawa, M.; Miki, Y.; Yoshida, K. DYRK2 Priming Phosphorylation of c-Jun and c-Myc Modulates Cell Cycle Progression in Human Cancer Cells. *J. Clin. Invest.* **2012**, *122* (3), 859–872.

(10) Geiger, J. N. mDYRK3 Kinase Is Expressed Selectively in Late Erythroid Progenitor Cells and Attenuates Colony-Forming Unit-Erythroid Development. *Blood* **2001**, *97* (4), 901–910.

(11) Papadopoulos, C.; Arato, K.; Lilienthal, E.; Zerweck, J.; Schutkowski, M.; Chatain, N.; Müller-Newen, G.; Becker, W.; de la Luna, S. Splice Variants of the Dual Specificity Tyrosine Phosphorylation-Regulated Kinase 4 (DYRK4) Differ in Their Subcellular Localization and Catalytic Activity. *J. Biol. Chem.* **2011**, *286* (7), 5494–5505.

(12) Colwill, K.; Pawson, T.; Andrews, B.; Prasad, J.; Manley, J. L.; Bell, J. C.; Duncan, P. I. The Clk/Sty Protein Kinase Phosphorylates SR Splicing Factors and Regulates Their Intranuclear Distribution. *EMBO J.* **1996**, *15* (2), 265–275.

(13) Duncan, P. I.; Stojdl, D. F.; Marius, R. M.; Bell, J. C. In Vivo Regulation of Alternative Pre-mRNA Splicing by the Clk1 Protein Kinase. *Mol. Cell. Biol.* **1997**, *17* (10), 5996–6001.

(14) Garcia-Blanco, M. A.; Baraniak, A. P.; Lasda, E. L. Alternative Splicing in Disease and Therapy. *Nat. Biotechnol.* **2004**, *22* (5), 535–546.

(15) Liu, F.; Gong, C.-X. Tau Exon 10 Alternative Splicing and Tauopathies. *Mol. Neurodegener.* **2008**, *3*, 8.

(16) Ward, A. J.; Cooper, T. A. The Pathobiology of Splicing. *J. Pathol.* **2010**, *220* (2), 152–163.

(17) Landesman-Bollag, E.; Romieu-Mourez, R.; Song, D. H.; Sonenshein, G. E.; Cardiff, R. D.; Seldin, D. C. Protein Kinase CK2 in Mammary Gland Tumorigenesis. *Oncogene* **2001**, *20* (25), 3247–3257.

(18) Perez, D. I.; Gil, C.; Martinez, A. Protein Kinases CK1 and CK2 as New Targets for Neurodegenerative Diseases. *Med. Res. Rev.* **2011**, *31* (6), 924–954.

(19) Nitta, R. T.; Gholamin, S.; Feroze, A. H.; Agarwal, M.; Cheshier, S. H.; Mitra, S. S.; Li, G. Casein Kinase 2α Regulates Glioblastoma Brain Tumor-Initiating Cell Growth through the β-Catenin Pathway. *Oncogene* **2014**.

(20) Pagano, M. A.; Cesaro, L.; Meggio, F.; Pinna, L. A. Protein Kinase CK2: A Newcomer in the "Druggable Kinome". *Biochem. Soc. Trans.* **2006**, *34* (Pt 6), 1303–1306.

(21) Katso, R.; Okkenhaug, K.; Ahmadi, K.; White, S.; Timms, J.; Waterfield, M. D. Cellular Function of Phosphoinositide 3-Kinases: Implications for Development, Homeostasis, and Cancer. *Annu. Rev. Cell Dev. Biol.* **2001**, *17*, 615–675.

(22) Vanhaesebroeck, B.; Leevers, S. J.; Panayotou, G.; Waterfield, M. D. Phosphoinositide 3-Kinases: A Conserved Family of Signal Transducers. *Trends Biochem. Sci.* **1997**, *22* (7), 267–272.

(23) Chantry, D.; Vojtek, A.; Kashishian, A.; Holtzman, D. A.; Wood, C.; Gray, P. W.; Cooper, J. A.; Hoekstra, M. F. p110 , a Novel Phosphatidylinositol 3-Kinase Catalytic Subunit That Associates with p85 and Is Expressed Predominantly in Leukocytes. *J. Biol. Chem.* **1997**, *272* (31), 19236–19241.

(24) Stephens, L. R.; Eguinoa, A.; Erdjument-Bromage, H.; Lui, M.; Cooke, F.; Coadwell, J.; Smrcka, A. S.; Thelen, M.; Cadwallader, K.; Tempst, P.; Hawkins, P. T. The G Beta Gamma Sensitivity of a PI3K Is Dependent upon a Tightly Associated Adaptor, p101. *Cell* **1997**, *89* (1), 105–114.

(25) Krugmann, S.; Hawkins, P. T.; Pryer, N.; Braselmann, S. Characterizing the Interactions between the Two Subunits of the p101/p110gamma Phosphoinositide 3-Kinase and Their Role in the Activation of This Enzyme by Gbeta Gamma Subunits. *J. Biol. Chem.* **1999**, *274* (24), 17152–17158.

(26) Arcaro, A.; Volinia, S.; Zvelebil, M. J.; Stein, R.; Watton, S. J.; Layton, M. J.; Gout, I.; Ahmadi, K.; Downward, J.; Waterfield, M. D. Human Phosphoinositide 3-Kinase C2beta, the Role of Calcium and the C2 Domain in Enzyme Activity. *J. Biol. Chem.* **1998**, *273* (49), 33082–33090.

(27) Domin, J.; Waterfield, M. D. Using Structure to Define the Function of Phosphoinositide 3-Kinase Family Members. *FEBS Lett.* **1997**, *410* (1), 91–95.

(28) Ursø, B.; Brown, R. A.; O'Rahilly, S.; Shepherd, P. R.; Siddle, K. The Alpha-Isoform of Class II Phosphoinositide 3-Kinase Is More Effectively Activated by Insulin Receptors than IGF Receptors, and Activation Requires Receptor NPEY Motifs. *FEBS Lett.* **1999**, *460* (3), 423–426.

(29) Brown, R. A.; Domin, J.; Arcaro, A.; Waterfield, M. D.; Shepherd, P. R. Insulin Activates the Alpha Isoform of Class II Phosphoinositide 3-Kinase. *J. Biol. Chem.* **1999**, *274* (21), 14529–14532.

(30) Arcaro, A.; Zvelebil, M. J.; Wallasch, C.; Ullrich, A.; Waterfield, M. D.; Domin, J. Class II Phosphoinositide 3-Kinases Are Downstream Targets of Activated Polypeptide Growth Factor Receptors. *Mol. Cell. Biol.* **2000**, *20* (11), 3817–3830.

(31) Turner, S. J.; Domin, J.; Waterfield, M. D.; Ward, S. G.; Westwick, J. The CC Chemokine Monocyte Chemotactic Peptide-1 Activates Both the Class I p85/p110 Phosphatidylinositol 3-Kinase and the Class II PI3K-C2alpha. *J. Biol. Chem.* **1998**, *273* (40), 25987–25995.

(32) Zhang, J.; Banfić, H.; Straforini, F.; Tosi, L.; Volinia, S.; Rittenhouse, S. E. A Type II Phosphoinositide 3-Kinase Is Stimulated via Activated Integrin in Platelets. A Source of Phosphatidylinositol 3-Phosphate. *J. Biol. Chem.* **1998**, *273* (23), 14081–14084.

(33) Yoshioka, K.; Yoshida, K.; Cui, H.; Wakayama, T.; Takuwa, N.; Okamoto, Y.; Du, W.; Qi, X.; Asanuma, K.; Sugihara, K.; Aki, S.; Miyazawa, H.; Biswas, K.; Nagakura, C.; Ueno, M.; Iseki, S.; Schwartz, R. J.; Okamoto, H.; Sasaki, T.; Matsui, O.; Asano, M.; Adams, R. H.; Takakura, N.; Takuwa, Y. Endothelial PI3K-C2α, a Class II PI3K, Has an Essential Role in Angiogenesis and Vascular Barrier Function. *Nat. Med.* **2012**, *18* (10), 1560–1569.

(34) Maehama, T.; Fukasawa, M.; Date, T.; Wakita, T.; Hanada, K. *A Class II Phosphoinositide 3-Kinase Plays an Indispensable Role in Hepatitis C Virus Replication*; 2013; Vol. 440.

(35) Meldrum, B.; Garthwaite, J. Excitatory Amino Acid Neurotoxicity and Neurodegenerative Disease. *Trends Pharmacol. Sci.* **1990**, *11* (9), 379–387.

(36) Lin, M. T.; Beal, M. F. Mitochondrial Dysfunction and Oxidative Stress in Neurodegenerative Diseases. *Nature* **2006**, *443* (7113), 787–795.

(37) Beal, M. F. Aging, Energy, and Oxidative Stress in Neurodegenerative Diseases. *Ann. Neurol.* **1995**, *38* (3), 357–366.

(38) Barnham, K. J.; Masters, C. L.; Bush, A. I. Neurodegenerative Diseases and Oxidative Stress. *Nat. Rev. Drug Discov.* **2004**, *3* (3), 205–214.

(39) Coyle, J. T.; Puttfarcken, P. Oxidative Stress, Glutamate, and Neurodegenerative Disorders. *Science* **1993**, *262* (5134), 689–695.

(40) Murphy, T. H.; Miyamoto, M.; Sastre, A.; Schnaar, R. L.; Coyle, J. T. Glutamate Toxicity in a Neuronal Cell Line Involves Inhibition of Cystine Transport Leading to Oxidative Stress. *Neuron* **1989**, *2* (6), 1547–1558.

(41) Murphy, S. L.; Xu, J.; Kochanek, K. D.; Statistics, V. National Vital Statistics Reports Deaths : Final Data for 2010. **2013**, *61* (4).

(42) Levy-Lahad, E.; Bird, T. D. Genetic Factors in Alzheimer's Disease: A Review of Recent Advances. *Ann. Neurol.* **1996**, *40* (6), 829–840.

(43) Levy-Lahad, E.; Wasco, W.; Poorkaj, P.; Romano, D. M.; Oshima, J.; Pettingell, W. H.; Yu, C. E.; Jondro, P. D.; Schmidt, S. D.; Wang, K. Candidate Gene for the Chromosome 1 Familial Alzheimer's Disease Locus. *Science* **1995**, *269* (5226), 973–977.

(44) Sherrington, R.; Rogaev, E. I.; Liang, Y.; Rogaeva, E. A.; Levesque, G.; Ikeda, M.; Chi, H.; Lin, C.; Li, G.; Holman, K.; Tsuda, T.; Mar, L.; Foncin, J. F.; Bruni, A. C.; Montesi, M. P.; Sorbi, S.; Rainero, I.; Pinessi, L.; Nee, L.; Chumakov, I.; Pollen, D.; Brookes, A.; Sanseau, P.; Polinsky, R. J.; Wasco, W.; Da Silva, H. A.; Haines, J. L.; Perkicak-Vance, M. A.; Tanzi, R. E.; Roses, A. D.; Fraser, P. E.; Rommens, J. M.; St George-Hyslop, P. H. Cloning of a Gene Bearing Missense Mutations in Early-Onset Familial Alzheimer's Disease. *Nature* **1995**, *375* (6534), 754–760.

(45) Corder, E. H.; Saunders, A. M.; Strittmatter, W. J.; Schmechel, D. E.; Gaskell, P. C.; Small, G. W.; Roses, A. D.; Haines, J. L.; Pericak-Vance, M. A. Gene Dose of Apolipoprotein E Type 4 Allele and the Risk of Alzheimer's Disease in Late Onset Families. *Science* **1993**, *261* (5123), 921–923.

(46) Strittmatter, W. J.; Saunders, A. M.; Schmechel, D.; Pericak-Vance, M.; Enghild, J.; Salvesen, G. S.; Roses, A. D. Apolipoprotein E: High-Avidity Binding to Beta-Amyloid and Increased Frequency of Type 4 Allele in Late-Onset Familial Alzheimer Disease. *Proc. Natl. Acad. Sci. U. S. A.* **1993**, *90* (5), 1977–1981.

(47) Goate, A.; Chartier-Harlin, M. C.; Mullan, M.; Brown, J.; Crawford, F.; Fidani, L.; Giuffra, L.; Haynes, A.; Irving, N.; James, L. Segregation of a Missense Mutation in the Amyloid Precursor Protein Gene with Familial Alzheimer's Disease. *Nature* **1991**, *349* (6311), 704–706.

(48) Tagawa, K.; Kunishita, T.; Maruyama, K.; Yoshikawa, K.; Kominami, E.; Tsuchiya, T.; Suzuki, K.; Tabira,

T.; Sugita, H.; Ishiura, S. Alzheimer's Disease Amyloid β-Clipping Enzyme (APP Secretase): Identification, Purification, and Characterization of the Enzyme. *Biochem. Biophys. Res. Commun.* **1991**, *177* (1), 377–387.

(49) Roher, A. E.; Lowenson, J. D.; Clarke, S.; Woods, A. S.; Cotter, R. J.; Gowing, E.; Ball, M. J. Beta-Amyloid-(1-42) Is a Major Component of Cerebrovascular Amyloid Deposits: Implications for the Pathology of Alzheimer Disease. *Proc. Natl. Acad. Sci.* **1993**, *90* (22), 10836–10840.

(50) Galdzicki, Z.; Siarey, R.; Pearce, R.; Stoll, J.; Rapoport, S. I. On the Cause of Mental Retardation in Down Syndrome: Extrapolation from Full and Segmental Trisomy 16 Mouse Models. *Brain Res. Rev.* **2001**, *35* (2), 115–145.

(51) Epstein, J.; Wiseman, C. V.; Sunday, S. R.; Klapper, F.; Alkalay, L.; Halmi, K. A. Neurocognitive Evidence Favors "top Down" over "bottom Up" Mechanisms in the Pathogenesis of Body Size Distortions in Anorexia Nervosa. *Eat. Weight Disord. - Stud. Anorexia, Bulim. Obes.* **2013**, *6* (3), 140–147.

(52) Rahmani, Z.; Blouin, J. L.; Creau-Goldberg, N.; Watkins, P. C.; Mattei, J. F.; Poissonnier, M.; Prieur, M.; Chettouh, Z.; Nicole, A.; Aurias, A. Critical Role of the D21S55 Region on Chromosome 21 in the Pathogenesis of Down Syndrome. *Proc. Natl. Acad. Sci. U. S. A.* **1989**, *86* (15), 5958–5962.

(53) Antonarakis, S. E.; Epstein, C. J. The Challenge of Down Syndrome. *Trends Mol. Med.* **2006**, *12* (10), 473–479.

(54) Davis, F. G.; Kupelian, V.; Freels, S.; McCarthy, B.; Surawicz, T. Prevalence Estimates for Primary Brain Tumors in the United States by Behavior and Major Histology Groups. *Neuro. Oncol.* **2001**, *3* (3), 152–158.

(55) Young, R. M.; Jamshidi, A.; Davis, G.; Sherman, J. H. Current Trends in the Surgical Management and Treatment of Adult Glioblastoma. *Ann. Transl. Med.* **2015**, *3* (9), 121.

(56) Bleeker, F. E.; Molenaar, R. J.; Leenstra, S. Recent Advances in the Molecular Understanding of Glioblastoma. *J. Neurooncol.* **2012**, *108* (1), 11–27.

(57) Van Meir, E. G.; Hadjipanayis, C. G.; Norden, A. D.; Shu, H.-K.; Wen, P. Y.; Olson, J. J. Exciting New Advances in Neuro-Oncology: The Avenue to a Cure for Malignant Glioma. *CA. Cancer J. Clin. 60* (3), 166–193.

(58) Kang, M.-K.; Kang, S.-K. Tumorigenesis of Chemotherapeutic Drug-Resistant Cancer Stem-like Cells in Brain Glioma. *Stem Cells Dev.* **2007**, *16* (5), 837–847.

(59) Ardon, H.; Van Gool, S.; Lopes, I. S.; Maes, W.; Sciot, R.; Wilms, G.; Demaerel, P.; Bijttebier, P.; Claes, L.; Goffin, J.; Van Calenbergh, F.; De Vleeschouwer, S. Integration of Autologous Dendritic Cell-Based Immunotherapy in the Primary Treatment for Patients with Newly Diagnosed Glioblastoma Multiforme: A Pilot Study. *J. Neurooncol.* **2010**, *99* (2), 261–272.

(60) De Vleeschouwer, S.; Fieuws, S.; Rutkowski, S.; Van Calenbergh, F.; Van Loon, J.; Goffin, J.; Sciot, R.; Wilms, G.; Demaerel, P.; Warmuth-Metz, M.; Soerensen, N.; Wolff, J. E. A.; Wagner, S.; Kaempgen, E.; Van Gool, S. W. Postoperative Adjuvant Dendritic Cell-Based Immunotherapy in Patients with Relapsed Glioblastoma Multiforme. *Clin. Cancer Res.* **2008**, *14* (10), 3098–3104.

(61) Udenfriend, S.; Witkop, B.; Redfield, B. G.; Weissbach, H. Studies with Reversible Inhibitors of Monoamine Oxidase: Harmaline and Related Compounds. *Biochem. Pharmacol.* **1958**, *1* (2), 160–165.

(62) Rizzo, S.; Rivière, C.; Piazzi, L.; Bisi, A.; Gobbi, S.; Bartolini, M.; Andrisano, V.; Morroni, F.; Tarozzi, A.; Monti, J.-P.; Rampa, A. Benzofuran-Based Hybrid Compounds for the Inhibition of Cholinesterase Activity, Beta Amyloid Aggregation, and Abeta Neurotoxicity. *J. Med. Chem.* **2008**, *51* (10), 2883–2886.

(63) Brogi, S.; Butini, S.; Maramai, S.; Colombo, R.; Verga, L.; Lanni, C.; De Lorenzi, E.; Lamponi, S.;

Andreassi, M.; Bartolini, M.; Andrisano, V.; Novellino, E.; Campiani, G.; Brindisi, M.; Gemma, S. Disease-Modifying Anti-Alzheimer's Drugs: Inhibitors of Human Cholinesterases Interfering with β-Amyloid Aggregation. *CNS Neurosci. Ther.* **2014**, *20* (7), 624–632.

(64) Catto, M.; Berezin, A. A.; Lo Re, D.; Loizou, G.; Demetriades, M.; De Stradis, A.; Campagna, F.; Koutentis, P. A.; Carotti, A. Design, Synthesis and Biological Evaluation of benzo[e][1,2,4]triazin-7(1H)-One and [1,2,4]-triazino[5,6,1-Jk]carbazol-6-One Derivatives as Dual Inhibitors of Beta-Amyloid Aggregation and Acetyl/butyryl Cholinesterase. *Eur. J. Med. Chem.* **2012**, *58*, 84–97.

(65) Rook, Y.; Schmidtke, K.-U.; Gaube, F.; Schepmann, D.; Wünsch, B.; Heilmann, J.; Lehmann, J.; Winckler, T. Bivalent Beta-Carbolines as Potential Multitarget Anti-Alzheimer Agents. *J. Med. Chem.* **2010**, *53* (9), 3611–3617.

(66) Apperley, J. F.; Gardembas, M.; Melo, J. V.; Russell-Jones, R.; Bain, B. J.; Baxter, E. J.; Chase, A.; Chessells, J. M.; Colombat, M.; Dearden, C. E.; Dimitrijevic, S.; Mahon, F.-X.; Marin, D.; Nikolova, Z.; Olavarria, E.; Silberman, S.; Schultheis, B.; Cross, N. C. P.; Goldman, J. M. Response to Imatinib Mesylate in Patients with Chronic Myeloproliferative Diseases with Rearrangements of the Platelet-Derived Growth Factor Receptor Beta. *N. Engl. J. Med.* **2002**, *347* (7), 481–487.

(67) Cluzeau, T.; Lippert, E.; Cayuela, J.-M.; Maarek, O.; Migeon, M.; Noguera, M.-E.; Dombret, H.; Rea, D. Novel Fusion between the Breakpoint Cluster Region and Platelet-Derived Growth Factor Receptor-Alpha Genes in a Patient with Chronic Myeloid Leukemia-like Neoplasm: Undetectable Residual Disease after Imatinib Therapy. *Eur. J. Haematol.* **2015**, *95* (5), 480–483.

(68) Trela, E.; Glowacki, S.; Błasiak, J.; Trela, E.; Glowacki, S.; Błasiak, J.; Bł asiak, J. Therapy of Chronic Myeloid Leukemia: Twilight of the Imatinib Era? *ISRN Oncol.* **2014**, *2014*, 596483.

(69) Tahtouh, T.; Elkins, J. M.; Filippakopoulos, P.; Soundararajan, M.; Burgy, G.; Durieu, E.; Cochet, C.; Schmid, R. S.; Lo, D. C.; Delhommel, F.; Oberholzer, A. E.; Pearl, L. H.; Carreaux, F.; Bazureau, J.-P.; Knapp, S.; Meijer, L. Selectivity, Cocrystal Structures, and Neuroprotective Properties of Leucettines, a Family of Protein Kinase Inhibitors Derived from the Marine Sponge Alkaloid Leucettamine B. *J. Med. Chem.* **2012**, *55* (21), 9312–9330.

(70) Bain, J.; McLauchlan, H.; Elliott, M.; Cohen, P. The Specificities of Protein Kinase Inhibitors: An Update. *Biochem. J.* **2003**, *371* (Pt 1), 199–204.

(71) Anastassiadis, T.; Deacon, S. W.; Devarajan, K.; Ma, H.; Peterson, J. R. Comprehensive Assay of Kinase Catalytic Activity Reveals Features of Kinase Inhibitor Selectivity. *Nat. Biotechnol.* **2011**, *29* (11), 1039–1045.

(72) M, P.; J, B.; Z, K.; S, S.; M, R.; G, D. M.; M, E.; A, O.; G, C.; F, M.; L, P. The Selectivity of Inhibitors of Protein Kinase CK2: An Update. **2008**.

(73) Cuny, G. D.; Robin, M.; Ulyanova, N. P.; Patnaik, D.; Pique, V.; Casano, G.; Liu, J.-F.; Lin, X.; Xian, J.; Glicksman, M. A.; Stein, R. L.; Higgins, J. M. G. Structure-Activity Relationship Study of Acridine Analogs as Haspin and DYRK2 Kinase Inhibitors. *Bioorg. Med. Chem. Lett.* **2010**, *20* (12), 3491–3494.

(74) Bey, E.; Marchais-Oberwinkler, S.; Negri, M.; Kruchten, P.; Oster, A.; Klein, T.; Spadaro, A.; Werth, R.; Frotscher, M.; Birk, B.; Hartmann, R. W. New Insights into the SAR and Binding Modes of Bis(hydroxyphenyl)thiophenes and -Benzenes: Influence of Additional Substituents on 17beta-Hydroxysteroid Dehydrogenase Type 1 (17beta-HSD1) Inhibitory Activity and Selectivity. *J. Med. Chem.* **2009**, *52* (21), 6724–6743.

(75) Bey, E.; Marchais-Oberwinkler, S.; Werth, R.; Negri, M.; Al-Soud, Y. A.; Kruchten, P.; Oster, A.; Frotscher, M.; Birk, B.; Hartmann, R. W. Design, Synthesis, Biological Evaluation and Pharmacokinetics of Bis(hydroxyphenyl) Substituted Azoles, Thiophenes, Benzenes, and Aza-Benzenes as Potent and Selective Nonsteroidal Inhibitors of 17beta-Hydroxysteroid Dehydrogenase Type 1 (17beta-HSD1). *J. Med. Chem.* **2008**, *51* (21), 6725–6739.

(76) Miralinaghi, P.; Schmitt, C.; Hartmann, R. W.; Frotscher, M.; Engel, M. 6-Hydroxybenzothiophene Ketones: Potent Inhibitors of 17β-Hydroxysteroid Dehydrogenase Type 1 (17β-HSD1) Owing to Favorable Molecule Geometry and Conformational Preorganization. *ChemMedChem* **2014**.

(77) Schmitt, C.; Kail, D.; Mariano, M.; Empting, M.; Weber, N.; Paul, T.; Hartmann, R. W.; Engel, M. Design and Synthesis of a Library of Lead-like 2,4-Bisheterocyclic Substituted Thiophenes as Selective Dyrk/Clk Inhibitors. *PLoS One* **2014**, *9* (3), e87851.

(78) Cellamare, S.; Stefanachi, A.; Stolfa, D. A.; Basile, T.; Catto, M.; Campagna, F.; Sotelo, E.; Acquafredda, P.; Carotti, A. Design, Synthesis, and Biological Evaluation of Glycine-Based Molecular Tongs as Inhibitors of Abeta1-40 Aggregation in Vitro. *Bioorg. Med. Chem.* **2008**, *16* (9), 4810–4822.

(79) Li, D.; Jackson, R. A.; Yusoff, P.; Guy, G. R. Direct Association of Sprouty-Related Protein with an EVH1 Domain (SPRED) 1 or SPRED2 with DYRK1A Modifies Substrate/kinase Interactions. *J. Biol. Chem.* **2010**, *285* (46), 35374–35385.

(80) Wegiel, J.; Dowjat, K.; Kaczmarski, W.; Kuchna, I.; Nowicki, K.; Frackowiak, J.; Mazur Kolecka, B.; Wegiel, J.; Silverman, W. P.; Reisberg, B.; Deleon, M.; Wisniewski, T.; Gong, C.-X.; Liu, F.; Adayev, T.; Chen-Hwang, M.-C.; Hwang, Y.-W. The Role of Overexpressed DYRK1A Protein in the Early Onset of Neurofibrillary Degeneration in Down Syndrome. *Acta Neuropathol.* **2008**, *116* (4), 391–407.

(81) Kimura, R.; Kamino, K.; Yamamoto, M.; Nuripa, A.; Kida, T.; Kazui, H.; Hashimoto, R.; Tanaka, T.; Kudo, T.; Yamagata, H.; Tabara, Y.; Miki, T.; Akatsu, H.; Kosaka, K.; Funakoshi, E.; Nishitomi, K.; Sakaguchi, G.; Kato, A.; Hattori, H.; Uema, T.; Takeda, M. The DYRK1A Gene, Encoded in Chromosome 21 Down Syndrome Critical Region, Bridges between Beta-Amyloid Production and Tau Phosphorylation in Alzheimer Disease. *Hum. Mol. Genet.* **2007**, *16* (1), 15–23.

(82) Mendgen, T.; Steuer, C.; Klein, C. D. Privileged Scaffolds or Promiscuous Binders: A Comparative Study on Rhodanines and Related Heterocycles in Medicinal Chemistry. *J. Med. Chem.* **2012**, *55* (2), 743–753.

(83) Anastassiadis, T.; Deacon, S. W.; Devarajan, K.; Ma, H.; Peterson, J. R. Comprehensive Assay of Kinase Catalytic Activity Reveals Features of Kinase Inhibitor Selectivity. *Nat Biotechnol* **2011**, *29* (11), 1039–1045.

(84) Cuny, G. D.; Robin, M.; Ulyanova, N. P.; Patnaik, D.; Pique, V.; Casano, G.; Liu, J. F.; Lin, X.; Xian, J.; Glicksman, M. A.; Stein, R. L.; Higgins, J. M. Structure-Activity Relationship Study of Acridine Analogs as Haspin and DYRK2 Kinase Inhibitors. *Bioorg Med Chem Lett* **2010**, *20* (12), 3491–3494.

(85) Sun, L.; Hui, A.-M.; Su, Q.; Vortmeyer, A.; Kotliarov, Y.; Pastorino, S.; Passaniti, A.; Menon, J.; Walling, J.; Bailey, R.; Rosenblum, M.; Mikkelsen, T.; Fine, H. A. Neuronal and Glioma-Derived Stem Cell Factor Induces Angiogenesis within the Brain. *Cancer Cell* **2006**, *9* (4), 287–300.

(86) Murat, A.; Migliavacca, E.; Gorlia, T.; Lambiv, W. L.; Shay, T.; Hamou, M.-F.; de Tribolet, N.; Regli, L.; Wick, W.; Kouwenhoven, M. C. M.; Hainfellner, J. A.; Heppner, F. L.; Dietrich, P.-Y.; Zimmer, Y.; Cairncross, J. G.; Janzer, R.-C.; Domany, E.; Delorenzi, M.; Stupp, R.; Hegi, M. E. Stem Cell-Related "self-Renewal" signature and High Epidermal Growth Factor Receptor Expression Associated with Resistance to Concomitant Chemoradiotherapy in Glioblastoma. *J. Clin. Oncol.* **2008**, *26* (18), 3015–3024.

(87) French, P. J.; Swagemakers, S. M. A.; Nagel, J. H. A.; Kouwenhoven, M. C. M.; Brouwer, E.; van der Spek, P.; Luider, T. M.; Kros, J. M.; van den Bent, M. J.; Sillevis Smitt, P. A. Gene Expression Profiles Associated with Treatment Response in Oligodendrogliomas. *Cancer Res.* **2005**, *65* (24), 11335–11344.

(88) Beroukhim, R.; Getz, G.; Nghiemphu, L.; Barretina, J.; Hsueh, T.; Linhart, D.; Vivanco, I.; Lee, J. C.; Huang, J. H.; Alexander, S.; Du, J.; Kau, T.; Thomas, R. K.; Shah, K.; Soto, H.; Perner, S.; Prensner, J.; Debiasi, R. M.; Demichelis, F.; Hatton, C.; Rubin, M. A.; Garraway, L. A.; Nelson, S. F.; Liau, L.; Mischel,

P. S.; Cloughesy, T. F.; Meyerson, M.; Golub, T. A.; Lander, E. S.; Mellinghoff, I. K.; Sellers, W. R. Assessing the Significance of Chromosomal Aberrations in Cancer: Methodology and Application to Glioma. *Proc. Natl. Acad. Sci. U. S. A.* **2007**, *104* (50), 20007–20012.

(89) Mao, P.; Hever-Jardine, M. P.; Rahme, G. J.; Yang, E.; Tam, J.; Kodali, A.; Biswal, B.; Fadul, C. E.; Gaur, A.; Israel, M. A.; Spinella, M. J. Serine/threonine Kinase 17A Is a Novel Candidate for Therapeutic Targeting in Glioblastoma. *PLoS One* **2013**, *8* (11), e81803.

(90) Mao, P.; Jardine, M. P.; Rahme, G. J.; Yang, E. C.; Tam, J.; Kodali, A.; Biswal, B.; Fadul, C. E.; Gaur, A. B.; Israel, M. A.; Pletnev, A.; Spinella, M. Abstract 4605: STK17A Is a Potential Therapeutic Target in Glioblastoma. *Cancer Res.* **2014**, *74* (19 Supplement).

(91) Read, R.; Marquez, J.; Mosley, C. CS-29 * A KINOME-WIDE RNAi-SCREEN IN DROSOPHILA GLIA AND HUMAN GBM CELLS REVEALS THAT Stk17A DRIVES NEOPLASTIC GLIAL CELL PROLIFERATION AND INVASION. *Neuro. Oncol.* **2014**, *16* (suppl 5), v57–v57.

(92) Auger, N.; Thillet, J.; Wanherdrick, K.; Idbaih, A.; Legrier, M.-E.; Dutrillaux, B.; Sanson, M.; Poupon, M.-F. Genetic Alterations Associated with Acquired Temozolomide Resistance in SNB-19, a Human Glioma Cell Line. *Mol. Cancer Ther.* **2006**, *5* (9), 2182–2192.

(93) Eblen, S. T. Regulation of Chemoresistance via Alternative Messenger RNA Splicing. *Biochem. Pharmacol.* **2012**, *83* (8), 1063–1072.

(94) Jain, P.; Karthikeyan, C.; Moorthy, N. S. H. N.; Waiker, D. K.; Jain, A. K.; Trivedi, P. Human CDC2-like Kinase 1 (CLK1): A Novel Target for Alzheimer's Disease. *Curr. Drug Targets* **2014**, *15* (5), 539–550.

(95) Camps, M.; Rückle, T.; Ji, H.; Ardissone, V.; Rintelen, F.; Shaw, J.; Ferrandi, C.; Chabert, C.; Gillieron, C.; Françon, B.; Martin, T.; Gretener, D.; Perrin, D.; Leroy, D.; Vitte, P.-A.; Hirsch, E.; Wymann, M. P.; Cirillo, R.; Schwarz, M. K.; Rommel, C. Blockade of PI3Kgamma Suppresses Joint Inflammation and Damage in Mouse Models of Rheumatoid Arthritis. *Nat. Med.* **2005**, *11* (9), 936–943.

8. Appendix

8.1. List of publications

1. First selective dual inhibitors of tau phosphorylation and beta-amyloid aggregation, two major pathogenic mechanisms in Alzheimer's disease
   Marica Mariano, Christian Schmitt, Parisa Miralinaghi, Marco Catto, Rolf W. Hartmann, Angelo Carotti, Matthias Engel
   ACS Chem. Neurosci. 2014, 5, 1198−1202; dx.doi.org/10.1021/cn5001815

2. Systematic diversification of benzylidene heterocycles yields novel inhibitor scaffolds selective for Dyrk1A, Clk1 and CK2
   Marica Mariano, Rolf W. Hartmann, Matthias Engel
   European Journal of Medicinal Chemistry 2016 vol: 112 pp: 209-216
   http://dx.doi.org/10.1016/j.ejmech.2016.02.017

3. Design and Synthesis of a Library of Lead-Like 2,4-Bisheterocyclic Substituted Thiophenes as Selective Dyrk/Clk Inhibitors
   Schmitt C, Kail D, **Mariano M**, Empting M, Weber N, Paul, T., Hartmann R. W., Engel, M.
   PLoS One 2014, 9 (3), e87851.

4. Hydroxybenzothiophene ketones are efficient pre-mRNA splicing modulators due to dual inhibition of Dyrk1A and Clk1/4
   Schmitt, Christian; Miralinaghi, Parisa Sadat; **Mariano, Marica**; Hartmann, Rolf; Engel, Matthias (2014) ACS Medicinal Chemistry Letters

9. Acknowledgements

I would like to thank all the people that were very important for realizing this work.

First of all, dr Matthias Engel and prof Hartmann for giving me the possibility to have such great experience in Germany and prof Carotti for his contribution to the co-tutelle between Italy and Germany.

In particular, thanks to Matthias for his big support and patience, for his wise advises and for sharing his deep knowledge and experience with me. His passion for scientific research was very inspiring for me. Thanks for giving me the opportunity to be part of your team.

Thanks to Christian, Tamara and Nadja for their big contribution to the experimental work. It was a great pleasure to co-operate with such competent co-workers. In particular, thanks to Tamara because, in spite of our first language problems, she was able to introduce me to the fantastic world of biology and thanks for being a nice friend and confident.

I want to thank all my colleagues and, in particular Marco, Enrico, Alessandro, Ahmed, Benoit, Antonio, Ivano, Giuseppe, Alberto. I could never forget our funny moments together…

Thanks to my flatmates Laura, Veronica, Mariona, Mayank and Hessam for sharing with me so many unforgettable moments in Dudweilerstrasse and for making me feel always at home even in a foreign country.

A big THANKS to my parents, my sister and my entire family for their support. Without you nothing could be possible!!! I have no words to describe how lucky I am of having you always by my side, even if at 1000 km distance.

Thanks to Tato, my sweet love, for being so motivating especially in the production of this thesis. Thanks for being always there for me and for loving and caring me.

Thanks to my homeland friend Valentina for being always so nice and for being one of the few people I can always count on.

Thanks to my new Calabrian family, to my Tairis Niko and to all the crazy people I have met in this wonderful region.